P52u

[redacted]

MARTIN MARIETTA ENERGY SYSTEMS LIBRARIES
3 4456 0353204 1

CENTRAL RESEARCH LIBRARY
DOCUMENT COLLECTION

ORNL-1482
Progress
4a

AEC RESEARCH AND DEVELOPMENT REPORT

DECLASSIFIED

CLASSIFICATION CHANGED TO:
BY AUTHORITY OF: E. J. Murphy 6-30-59
BY: R. C. Hansen 7-17-59

CHEMISTRY DIVISION

QUARTERLY PROGRESS REPORT

FOR PERIOD ENDING DECEMBER 31, 1952

LABORATORY RECORDS
1954

CENTRAL RESEARCH LIBRARY
DOCUMENT COLLECTION

LIBRARY LOAN COPY

DO NOT TRANSFER TO ANOTHER PERSON

If you wish someone else to see this document, send in name with document and the library will arrange a loan.

OAK RIDGE NATIONAL LABORATORY
OPERATED BY
CARBIDE AND CARBON CHEMICALS COMPANY
A DIVISION OF UNION CARBIDE AND CARBON CORPORATION

UCC

POST OFFICE BOX P
OAK RIDGE, TENNESSEE

RESTRICTED DATA
This document contains Restricted Data as defined in the Atomic Energy Act of 1954. Its transmittal or the disclosure of its contents in any manner to an unauthorized person is prohibited.

[redacted]

[redacted]

ORNL-1482

This document consists of 68 pages

Copy 4 of 135 copies Series A

Contract No W-7405-eng-26

CHEMISTRY DIVISION

QUARTERLY PROGRESS REPORT

for Period Ending December 31, 1952

S C Lind, Acting Director

G E Boyd, M A Bredig, Associate Directors

DATE ISSUED

FEB 27 1953

OAK RIDGE NATIONAL LABORATORY

Operated by

CARBIDE AND CARBON CHEMICALS COMPANY

A Division of Union Carbide and Carbon Corporation

Post Office Box P

Oak Ridge, Tennessee

[redacted]

MARTIN MARIETTA ENERGY SYSTEMS LIBRARIES

3 4456 0353204 1

[redacted]

ORNL-1482
Progress

INTERNAL DISTRIBUTION

1. C. E. Center
2. Biology Library
3. Health Physics Library
4-5. Central Research Library
6-13. Central Files
14. Reactor Experimental Engineering Library
15. C. E. Larson
16. W. B. Humes (K-25)
17. L. B. Emlet (Y-12)
18. A. M. Weinberg
19. E. H. Taylor
20. E. J. Murphy
21. E. D. Shipley
22. S. C. Lind
23. F. C. VonderLage
24. R. C. Briant
25. J. A. Swartout
26. F. L. Steahly
27. A. H. Snell
28. A. Hollaender
29. M. T. Kelley
30. G. H. Clewett
31. K. Z. Morgan
32. J. S. Felton
33. A. S. Householder
34. C. S. Harrill
35. C. E. Winters
36. D. W. Cardwell
37. E. M. King
38. J. A. Wethington
39. G. E. Boyd
40. M. A. Bredig
41. R. W. Stoughton
42. R. B. Briggs
43. G. W. Parker
44. C. J. Borkowski
45. G. H. Jenks
46. K. A. Kraus
47. H. A. Levy
48. R. S. Livingston
49. T. E. Willmarth
50. C. H. Secoy
51. C. J. Hochanadel
52. W. H. Baldwin
53. A. R. Brosi
54. R. N. Lyon
55. S. A. Reynolds
56. P. F. Thomason
57. E. G. Bohlmann
58. C. P. Keim
59. C. D. Susano
60. D. D. Cowen
61. P. M. Reyling
62. R. Livingston
63. G. H. Cartledge
64. E. R. VanArtsdalen
65. G. C. Williams
66. S. D. Schiffman (K-25)
67. E. P. Wigner (consultant)

EXTERNAL DISTRIBUTION

68-75. Argonne National Laboratory
76-83. Atomic Energy Commission, Washington
84-87. Brookhaven National Laboratory
88-91. Carbide and Carbon Chemicals Company (Y-12 Plant)
92-95. E. I. du Pont de Nemours and Company

[redacted]

[redacted]

[redacted]

96-97.	Knolls Atomic Power Laboratory
98-103.	General Electric Company, Richland
104.	Idaho Operations Office (Phillips Petroleum Co.)
105-108.	Los Alamos
109.	Mound Laboratory
110-112.	New York Operations Office
113.	Patent Branch, Washington
114.	Savannah River Operations Office, Wilmington
115-129.	Technical Information Service, Oak Ridge
130-133.	University of California Radiation Laboratory
134-135.	Westinghouse Electric Corporation

[redacted]

[redacted]

Chemistry Division quarterly progress reports previously issued in this series are as follows

ORNL-65	March, April, May, 1948
ORNL-176	June, July, August, 1948
ORNL-229	September, October, November, 1948
ORNL-336	December, 1948, January and February, 1949
ORNL-286	Period Ending June 30, 1949
ORNL-499	Period Ending September 30, 1949
ORNL-607	Period Ending December 31, 1949
ORNL-685	Period Ending March 31, 1950
ORNL-795	Period Ending June 30, 1950
ORNL-870	Period Ending September 30, 1950
ORNL-1036	Period Ending December 31, 1950
ORNL-1053	Period Ending March 31, 1951
ORNL-1116	Period Ending June 30, 1951
ORNL-1153	Period Ending September 30, 1951
ORNL-1260	Period Ending December 31, 1951
ORNL-1285	Period Ending March 31, 1952
ORNL-1344	Period Ending June 30, 1952
ORNL-1432	Period Ending September 30, 1952

[redacted]

[redacted]

CONTENTS

PAGE

SUMMARY 1

INORGANIC CHEMISTRY 4
- Thorium Hydrolysis Studies on Solid Thorium Salts 4
- Refractive Index of Uranyl Fluoride Solutions 7
- Chemistry of Fused Salts 8

NUCLEAR CHEMISTRY 9
- Capture Cross Section of Protactinium-233 9
- Characterization of Promethium-146 9
- Half-Life Measurements 11

RADIO-ORGANIC CHEMISTRY 12
- Radiation and Analytical Chemistry 12
- Carbon-14 Isotope Effect Studies 12
  - Formation of ketone derivatives 12
  - Effect of nuclear substituents in acetophenone-α-C^{14} on the isotope effect in the formation of the 2,4-dinitrophenylhydrazone at 25°C . 13
  - Isotope effect in the displacement reaction between acetophenone-α-C^{14} semicarbazone and 2,4-dinitrophenylhydrazine 13
  - Isotope effect in the catalytic reduction of acetophenone-α-C^{14} . . . 14
  - Isotope effect in the acid hydrolysis of hydrocyanic-C^{14} acid 15
  - Isotope effect during ozonization 15
  - Studies in solution scintillation counting of carbon-14 16
  - Preparation of standard comparison ionization chambers for carbon-14 assay 16
  - Organic reaction mechanism studies 17

CHEMISTRY OF SEPARATIONS PROCESSES 18
- Ion Exchange Studies 18
  - Pressure-volume relationships of cross-linked resins 18
  - Relationship of osmotic coefficients with ionic selectivity 21
- Organic Chemistry of Solvents 26

CHEMICAL PHYSICS 27
- Radio-Frequency Spectroscopy 27
  - Quadrupole spectroscopy 27
  - The iodine problem 27
- Neutron Diffraction Studies 29

[redacted]

[redacted]

CHEMISTRY OF THE SOLID STATE 30
Molten Metal-Metal Halide Systems 30
Structure of Molten Alkali Metal Halides 32
Crystal Structure of Sodium-Potassium Sulf 35
X-Ray Diffraction 35

RADIATION CHEMISTRY 35
Nucleation of Bubbles by Fission Recoils, Fast Neutrons, and X Rays . . 35
Some Fundamental Aspects of Bubble Growth 37
Radiation Chemistry of Ice 37
Uranyl-Sensitized Reaction of Hydrogen and Oxygen 38
Effects of Cobalt-60 Gamma Radiation on Aqueous Benzene Solutions . . . 39
Effects of Hydrogen and Oxygen on the Radiolysis and Photolysis of Dilute Aqueous Hydrogen Peroxide Solutions 40
Oxidation of Uranium(IV) by Gamma Rays 42
Gas-Phase Radiation Studies 42

INSTRUMENTATION 43
New Type of Multichannel Pulse Analyzer 43
Simple Count-Rate Meter as a Storage Element for Multichannel Analyzers 49
Circuit Changes in Scintillation Spectrometer, Model Q-1151 50
Regulated Negative High-Voltage Supply 51

REACTOR CHEMISTRY 52
Measurement of pH at High Temperatures 52
Chemistry of Corrosion 53
Studies on electrode potentials 53
Inhibition of corrosion by technetium compounds 54
Radiation of UO_2F_2 and UO_2SO_4 Solutions 56
Radiation Chemistry of Aqueous Reactor Solutions 57
Mechanism of the Hydrogen-Oxygen Recombination Reaction in Solutions . . 58
Catalytic Decomposition of Hydrogen Peroxide in Uranyl Sulfate Solutions 60
Solubility of UO_3 in Aqueous UO_2SO_4 and UO_2F_2 61
Oxidation States of Fission Products in Reactors 61

[redacted]

CHEMISTRY DIVISION QUARTERLY PROGRESS REPORT

SUMMARY

INORGANIC CHEMISTRY

Exploratory data on the stoichiometry of solid thorium chloride, bromide, and isocyanate hydrates are reported. An apparatus for the equilibration of a solid phase, deposited as a thin film, with an appropriate gas phase has been designed and tested.

The refractive index of uranyl fluoride solutions was measured. The value of 17.1 ± 0.1 cc for the mole refraction appears to be independent of concentration.

Measurements of the electric conductivity of molten lithium chloride in a fused-quartz cell at temperatures between 630 and 750 °C are in fair agreement with the equation $\log \kappa = 1.138 - 330/T$.

NUCLEAR CHEMISTRY

The thermal-neutron capture cross section of Pa^{233} has been measured as 125 ± 15 barns The existence of a 1-y half life prometheum isotope of mass 146 that gives 460- and 750-kev gamma rays has been definitely established.

An attempt is being made, by means of precision measurements, to determine the decay constants of several isotopes with half lives of the order of years with a standard deviation of 2% in a period of four months.

RADIO-ORGANIC CHEMISTRY

Aqueous solutions of acetic, propionic, succinic, and malonic acids and solid succinic acid have been irradiated with gamma rays from a Co^{60} source. Some products have been characterized. In general, the products were produced by decarboxylation and by coupling in the alpha position of the irradiated acids.

Six different examples of reactions in which isotope effects occur have been studied These include the formation of ketone derivatives, acid hydrolysis of a nitrile, oxidation, and reduction reactions. A previously constructed solution scintillation counter has been tested. The consistency of two standard ionization chambers has been studied over a one-year period.

The study of the Wagner rearrangement of 2-phenyl-1-acenaphthenol-1-C^{14} has been completed. During this rearrangement, phenyl migration occurs to the extent of 7.5%.

CHEMISTRY OF SEPARATION PROCESSES

The effects of cross linking on the pressure-volume relationships of cation exchangers have been determined. A reduced equation of state is proposed.

The "solution" concept of ion exchangers has been investigated. An attempt is made to correlate ion-exchange selectivities with osmotic coefficients calculated for various monovalent electrolytic systems.

De-esterification of tributyl phosphate with anhydrous sodium acetate produced no monobutyl phosphate, but only the dibutyl ester.

A third phase, formed when dibutyl phosphate in di-*n*-butyl ether was equilibrated with 5.0 *M* NaOH at 25°C contained 80% of the dibutyl phosphate employed as sodium dibutyl phosphate.

Preliminary tests indicate the solubility losses of phosphinic acid in aqueous solutions, from leaching uranium ores, to be less than 10 mg/liter.

CHEMICAL PHYSICS

The coherent and total scattering cross sections of scandium were determined as 17.5 and 24 barns, respectively. The crystal structure of PdO was confirmed by neutron-diffraction measurements.

A new high-radio-frequency spectrometer has been developed in which the frequency range is extended to over 300 megacycles. New quadrupole resonances were found in various bromine and iodine compounds. Measurements with SnI_4 yielded a very precise value for the nuclear quadrupole moment ratio, $Q(I^{129})\ Q(I^{127}) = 0.70121 \pm 0.00001$.

Progress has been made in the chemical purification of the iodide starting material as a preliminary step in synthesizing CH_3I^{131} for microwave studies.

CHEMISTRY OF THE SOLID STATE

Discrepancies in the strongly temperature-dependent solubilities of sodium and potassium in their molten chlorides, when determined by different methods of equilibration, or by thermal analysis, are believed to be due to difficulties in the mechanical separation of the liquid salt and metal phases. Efforts to eliminate these discrepancies are being continued.

The solubility of alkali metal, assumed to be mainly potassium, in melts of the approximate composition of the ternary eutectic LiF-NaF-KF was found to be 3.7 ± 0.5 mole % and is independent of temperature between 544 and 1040°C.

A review of the experimental data pertaining to the volume change on melting for most of the alkali metal halides suggests changes in structure, that is, the number of nearest neighboring ions of opposite charge, immediately below, at, or above the melting point. A change from eight- to six-fold coordination is definitely indicated in cesium bromide and iodide, either in the solids at an as yet undetermined transition temperature within 50°C below their melting points or on melting. Similar changes, sometimes only partial, from the six-fold coordination of the solids to five-fold or lower coordination in the liquid, probably occur in some of the other alkali metal halide melts, for example, the lithium metal halides.

RADIATION CHEMISTRY

Portions of a total of 4 g of deuterio-cuprene, prepared by α particle bombardment of deuterio acetylene, were examined by neutron diffraction, electron microscopy, and as a cyclotron target.

The study of nucleation of gas bubbles from superheated liquids by fission recoils, fast neutrons, and x rays was continued. It appears that the conditions for nucleation by fission recoils cannot be predicted by simple calculation based on a spherical nucleus Recoils from fast neutrons were found to be much more effective than x rays with a maximum energy of 50 kv.

A theoretical study of some fundamental aspects of gas-bubble growth yielded a numerical relationship that is in good agreement with some experimental data

Products of irradiation of ice at various temperatures are being studied The interpretation of the results is analogous to that for liquid water. A technique for determining small concentrations of hydrogen in oxygen gas has been developed in the course of this work.

The reaction of hydrogen and oxygen is shown to be photosensitized by uranyl sulfate in aqueous solution. It is first order in gas pressure for stoichiometric amounts of the gases. The yield of hydrogen in the decomposition of water by fission recoils is proportional to the square root of the uranium concentration for solution

in which at least 99.5% of the absorbed energy is fission energy.

The formation of hydrogen peroxide in oxygen-saturated 0.8 *N* sulfuric acid with benzene present is linear with time of irradiation with Co^{60} gamma rays, whereas in unbuffered benzene solutions, the rate decreases.

Hydrogen gas was found to enhance the quantum yield for hydrogen peroxide disappearance in photolysis with ultraviolet light at peroxide concentrations below 600 μmoles/l and reaches a value of 8.0 at about 20 μmoles/liter. The effect of oxygen on the radiolysis of hydrogen peroxide solutions by gamma rays has been demonstrated.

INSTRUMENTATION

A new type of multichannel pulse analyzer of greatly improved stability has been designed. Only one trigger is employed, irrespective of the number of channels. Use is made of a cathode-ray beam that is deflected across a metal grid and returned to its zero position, thus utilizing both the spaces and the webs of the grid as channels. The same principle of measuring deflecting voltage by means of a grid structure has been applied to a Hathaway high-speed galvanometer.

Improvements in the circuits of the ORNL model Q1151 amplifier-discriminator used with scintillation spectrometers have eliminated troublesome drifts in the instrument.

A well-regulated negative high-voltage supply and a triple-step generator for use in determining the resolving time of amplifiers, discriminators, scalers, etc. have been designed, built, and tested.

A simple count rate meter using a 5696, miniature gas tetrode has been designed for possible use as a storage element in multichannel analyzers.

REACTOR CHEMISTRY

Of five metal-metal oxide systems tested, a molybdenum-molybdenum oxide electrode appeared promising for pH measurements at high temperatures in an aqueous solution such as uranyl sulfate.

Effects of various factors such as thermal cycling, electropolishing, mechanical polishing, and temperature on the electrode potential of passivated stainless steels are described.

Experiments that demonstrate the passivating effect of pertechnetate ion on electrolytic iron, carbon, and stainless steels under various conditions are reported. A few tests with perrhenate indicate the effect to be absent with this ion.

Radiation studies in which the rate of corrosion of type 347 stainless steel is determined by measuring the rate of consumption of oxygen gas have been continued. A uranyl fluoride solution containing 40 g of uranium per liter gave an average rate of 3.5 mpy over a nine-week period compared with an out-of-reactor rate of 0.9 mpy over a six-day period. An amount of uranium equivalent to the amount of nickel oxidized is precipitated from the solution.

The rate of production of hydrogen has been found to be unaffected by acidity in the pH range from 1.4 to 3.5, but is lowered by about 3% at a pH of 0.6 for a 93.2%-enriched uranyl sulfate solution that contains 40 g of uranium per liter.

Introductory studies of the mechanism of the hydrogen-oxygen recombination reaction in solutions indicate that the reaction proceeds without the formation of a bonded activated complex. There are also indications that both sulfate and hydrogen ions may be involved in the reaction.

Further studies of the catalytic decomposition of hydrogen peroxide show that iron(III) is a better

catalyst than iron(II). A concentration of 6 to 10 ppm of copper(II) is sufficient for complete promoter action. Manganese(II) has been found to have negligible catalytic effect.

Work on the solubility of UO_3 in uranyl sulfate and uranyl fluoride solutions has been hampered by corrosion difficulties and problems in analysis. It appears that the corrosion problems have been solved, and useful data should be forthcoming.

Phase study of the two-liquid-phase region in the three-component system UO_3-SO_3-H_2O is in progress. Most of the past quarter has been devoted to the construction of apparatus by which a thermostatic method involving volume measurements can be employed. This technique, if successful, will yield information about the vapor phase, as well as each of the liquid phases.

A study of the oxidation states of specific fission products in homogeneous reactor environment has been started. The initial work will be with iodine.

Corrosion of type 347 stainless steel by UO_2F_2-NaF solutions is being investigated.

INORGANIC CHEMISTRY

THORIUM HYDROLYSIS STUDIES ON SOLID THORIUM SALTS

W. C. Waggener R. W. Stoughton

Studies that involve the stoichiometry of solid thorium salts prepared from aqueous solutions are continuing. During this period, work with the nitrate[1] and the perchlorate[1,2] has been extended to include the salts of several other monovalent anions of strong acids, namely, chloride, bromide, and thiocyanate. The respective interactions of these ions with thorium in aqueous solution were reported previously.[3]

The results given in Tables 1, 2, and 3 indicate that appreciable hydrolysis of the thorium ion can occur in the chloride, bromide, and thiocyanate when these salts are made by room-temperature evaporation of their acid solutions. The data obtained thus far have been exploratory and will not be further elaborated at this time.

(1) W. C. Waggener and R. W. Stoughton, *Chem. Quar. Prog. Rep. March 31, 1952*, ORNL-1285, p. 7.

(2) W. C. Waggener and R. W. Stoughton, *Chem. Quar. Prog. Rep. Dec. 31, 1951*, ORNL-1260, p. 1.

(3) W. C. Waggener and R. W. Stoughton, *Chem. Quar. Prog. Rep. Sept. 30, 1950*, ORNL-870, p. 16.

TABLE 1 STOICHIOMETRY OF THORIUM CHLORIDE HYDRATE

SAMPLE		QUANTITIES DETERMINED		
No.	Mmoles of Thorium	Molecular Weight per Mole of Thorium	Cationic* Charge	Mole Ratio of Cl to Th
10	0.1259	402.9	3.696	3.717
23	0.1444	399.1	3.698	3.713
25	0.1238	400.5	3.694	3.719
116	0.1131	402.2	3.710	3.750
		Avg. 401.2	3.700	3.725

*Determined by dissolving sample in standard $HClO_4$, placing on a cation-exchange resin column in the hydrogen form, eluting with water, and titrating the eluted hydrogen ion.

The thorium chloride hydrate of Table 1 had the average stoichiometric formula $Th(OH)_{0.288}Cl_{3.712} \cdot 1.81H_2O$. It was a white, hygroscopic powder that was prepared by fuming down $Th(NO_3)_4 \cdot 4.8H_2O$ to near dryness five or six times with fivefold to tenfold excess portions of concentrated HCl, dissolving in concentrated HCl, evaporating in a thin layer over a glass surface, and desiccating over Anhydrone at a pressure of 1 to 3 mm Hg and at room temperature for 790 hours. The x-ray powder pattern indicated that the material was crystalline with large cell dimensions.

The thorium bromide hydrate of Table 2 had the average stoichiometric formula $Th(OH)_{1.29}Br_{2.71} \cdot 0.70H_2O$. The material was a light-cream, hygroscopic powder that was prepared by fuming down $Th(NO_3)_4 \cdot 4.8H_2O$ to near dryness five or six times with five- to tenfold excess portions of concentrated HBr, dissolving in concentrated HBr, evaporating in a thin layer over a glass surface, and desiccating over Anhydrone at a pressure of 1 to 3 mm Hg and room temperature for 670 hours. The x-ray powder pattern was essentially noncrystalline.

The thorium thiocyanate hydrate of Table 3 had the average stoichiometric formula $Th(OH)_{0.47}(NCS)_{3.53} \cdot 6.1H_2O$. It was a very light-yellow, hygroscopic powder that was prepared by dissolving precipitated, washed $Th(OH)_4 \cdot XH_2O$ in cold (5 to 10°C) 0.67 *M* HCNS, and evaporating at room temperature to a a thin layer over a glass surface, then desiccating over Anhydrone at a pressure of 1 to 3 mm Hg and at room temperature for 624 hours. X-ray data have not yet been taken.

The principal effort has been the development of methods for the preparation and precise analysis (0.1%) of semimicro samples (about 50 mg). Small samples have practical advantages for this work in that the gas-solid equilibrium is obtained more rapidly with very thinly deposited films of salt, chemical transformations and manipulations are performed more

TABLE 2. STOICHIOMETRY OF THORIUM BROMIDE HYDRATE

SAMPLE		QUANTITIES DETERMINED		
No	Mmoles of Thorium	Molecular Weight per Mole of Thorium	Cationic Charge	Mole Ratio of Br to Th
45	0.1377	476.6	2.625	2.662
52	0.1477	489.6	2.757	2.778
		Avg. 483 1	2.691	2.720

TABLE 3 STOICHIOMETRY OF THORIUM THIOCYANATE HYDRATE

SAMPLE		QUANTITIES DETERMINED		
No	Mmoles of Thorium	Molecular Weight per Mole of Thorium	Cationic Charge	Mole Ratio of NCS to Th
4	0.1352	549.3	3.572	3.533
27	0.1411	561.3	3.522	3 493
		Avg. 555 3	3.547	3.513

rapidly, and samples of highly hygroscopic salts can be weighed and analyzed *in toto* without bulky or excessively elaborate apparatus.

Ten-milliliter calibrated pyrex centrifuge cones with standard-taper glass stoppers are used for sample containers and reactor vessels. These tubes and their contents (50- to 80-mg samples) are weighed on a semimicro balance against a similarly handled tube used as a tare. With proper care, weighings are made rapidly (2 to 4 min) to the nearest 0.01 milligram. The minimum reproducibility of the weight of a given tube after operations such as heating at 225°C, flaming, or wetting has been found to be ±0.05 milligram.

In achieving the stated precision in weighing these pyrex tubes, which have an outside surface of about 60 cm^2 and an over-all volume of 13 to 14 ml, it has been necessary to use a semimicro balance (Ainsworth, model TCX), control the balance-room humidity (40% ±2% RH) and temperature (better than ±1°C), acclimatize the tubes for 2 hr before weighing, routinely check the tubes for electrostatic charge with a simple gold-leaf electroscope before weighing, and dissipate any electrostatic charge on the tubes by means of a radioactive source.[4]

The choice of 40% RH for the weighing room was a compromise between electrostatic charge troubles, which were extremely aggravated at low humidities, and hygroscopic difficulties experienced in handling samples at higher humidities.

An apparatus for equilibrating a solid phase, deposited as a thin film upon the inner wall of the pyrex centrifuge tube, with an appropriate gas phase has been designed and tested satisfactorily. The apparatus consists of a vertical glass header connected to the center of a horizontal glass manifold. Six centrifuge tubes are connected to the manifold in a horizontal position by means of standard-taper joints.

Circulation of gas from the manifold to the tip of each centrifuge tube is accomplished by a 3-mm glass exhaust tube that enters the manifold by a ring seal and extends coaxially through the standard-taper joint. The tube is drawn out to a capillary point that is positioned near the tip of the centrifuge cone.

Humidity control of the gas phase in the range of 10 to 100% RH is provided by bubbling dry gas through a hygrostat (a suitable salt hydrate in contact with its saturated solution) and a glass-wool filter. Both the hygrostat and filter are suspended in a constant-temperature bath.

For experiments requiring very dry gas, a tube of desiccant and/or a cold-trap are employed.

The gas passes from the humidifying or the drying system through header and manifold, over the samples in the centrifuge cones, and then to the exhaust tubes. The effluent gas flows from the exhaust tubes through a fused KOH trap, a bubbler, and a Hoke needle valve (1/8 in.), and then to house vacuum.

The manifold pressure is measured by an open manometer and is adjusted to very slightly above atmospheric pressure in order to preclude any leakage through the ungreased ground-glass joints connecting the centrifuge cones.

The apparatus is being used at present for gas-solid phase equilibrations of $Th(NO_3)_4 \cdot 4.8H_2O$ at room temperature. A similar apparatus is being assembled for use in a thermostatically controlled oven.

(4) An electroplated Ru^{109} source at the bottom of a horizontally mounted cylindrical lead can of size to accept the centrifuge proper was effective in 20 to 200 sec, depending on the extent of surface charge

REFRACTIVE INDEX OF URANYL FLUORIDE SOLUTIONS

J. S. Johnson K. A. Kraus

The refractive index of uranyl fluoride solutions was measured with a Bausch and Lomb dipping refractometer (calibrated against known solutions) using sodium D light and the uranyl fluoride solutions previously described[5]. The reproducibility of the measurements is estimated to be ±.00004. The results are listed in Table 4.

[5] J S Johnson and K A Kraus, *Chem Quar Prog Rep Sept 30, 1952*, ORNL-1432 (in press)

The refractive indexes were fitted to the equation

$$n_D^t = n_D^{0\,t} + \alpha c + \beta c^{3/2} , \qquad (1)$$

where c is the concentration (molarity), α and β are constants, and where n_D^t and $n_D^{0\,t}$ are the measured refractive index of the solution and of water at temperature t respectively. Satisfactory fit of the data to Eq. 1 was obtained at 25°C using α = 0 02055 and β = -0 00185, and at 30°C using α = 0 02049 and β = -0 00183. The deviations between experimental and calculated values are shown in Table 4. It is believed that the scatter is due, to a large extent, to the inaccuracies in the analyses of the uranium solutions.

TABLE 4. REFRACTIVE INDEXES OF URANYL FLUORIDE SOLUTIONS

Wt %	REFRACTIVE INDEX				MOLE REFRACTION (cc) (25°C)
	25°C		30°C		
	n_D^{25}	Δn [a] x 10^5	n_D^{30}	Δn [a] x 10^5	
1.002	1.33319	-1	1.33266	-4	17
2.495	1.33417	0	1 33366	-5	17.0
4.985	1.33586	0	1.33531	-2	17.0
5.025	1.33597	-8			17.1
7.481	1.33764	-2	1.33705	-2	17.1
9.607	1.33925	-10	1.33864	-7	17.2
10.20	1.33963	-5	1.33907	-7	17.1
15.01	1.34333	-6	1.34275	-7	17.04
20.09	1.34756	-5	1.34692	-2	17.09
20.48	1.34788	-2	1.34721	+3	17.01
24 89	1.35188	-1	1 35114	+9	17.06
30 10	1 35705	0			17.09
30.18	1.35705	+6	1.35636	+11	17.21
33 39	1 36059	+1	1 35988	+5	17.09
40.27	1.36888	-5	1.36825	-9	17.14
46.36	1.37726	-1	1.37647	+6	17 15
50.27	1.38316	+14	1.38239	+18	17 13
50.90	1.38439	-5	1.38370	-11	17 15
56.90	1.39503	+1	1.39418	+10	17.13
57.10	1.39542	0	1.39457	+9	17 13
61.12	1.40392	-26	1.40303	-15	17 14
61.63	1 40475	+2	1.40407	-9	17 11

[a] Δn are the differences calculated values minus experimental values.

Values of the mole refraction (R) of UO_2F_2 were calculated according to the equation[6]

$$R = \frac{n^2 - 1}{n^2 + 2} \frac{1}{d} \left(\frac{1000}{m} + M \right) - \frac{(n^0)^2 - 1}{(n^0)^2 + 2} \frac{1}{d_0} \frac{1000}{m} , \quad (2)$$

where d is the density of the solution, m its molality, M the molecular weight of the solute, and d_0 the density of the solvent (water) The results of the calculations are also listed in Table 4. Within the accuracy of the data, R appears to be constant (R = 17 1 ± 0 1 cc) and hence does not reflect the considerable change in the degree of dimerization of uranyl fluoride which occurs in this concentration range. This insensitivity of R to dimerization is not unexpected.

CHEMISTRY OF FUSED SALTS

A. S. Dworkin I. S. Yaffe
D. J. Sasmor E. R. VanArtsdalen

During the past three months, various types of cells have been tested for determining electrical conductivity of fused salts, and considerable experience has been gained with several cells. At present, a capillary dip-cell fabricated of fused-quartz glass is preferred for general use. However, a capillary cell that incorporates the electrodes and crucible (for the melt) into a single unit has been tested and appears to be feasible for nonvolatile melts.

Further measurements of the electrical conductivity of fused lithium chloride have been made, and the specific conductances that have been determined are given in Table 5. There was considerable attack by the lithium chloride on the fused-quartz containers that became serious above about 700°C. For this reason, the last two conductance data of Table 5 are considered to be of doubtful accuracy. While the work was in progress, Edwards, Taylor, Russell, and Marenville[7] reported their determination of the specific conductance of lithium chloride at three temperatures. They have expressed their data in form of the equation

$$\log \kappa = 1\ 185 - 381/T,$$

where κ is the specific conductance and T the absolute temperature. The data of Table 5 are reproduced by the analogous equation

$$\log \kappa = 1.138 - 330/T,$$

and are seen to be in fair agreement. Edwards and coworkers reported considerable attack of fused quartz by molten lithium chloride, and they pointed out the difficulty in obtaining reliable data for this salt.

TABLE 5. SPECIFIC CONDUCTANCE OF LITHIUM CHLORIDE

TEMPERATURE (°C)	SPECIFIC CONDUCTANCE (mhos/cm)
630.6	5 813
642.3	5 926
655 0	6 013
674.4	6 097
678 8	6 125
716 6	6.347
747 1	6 518*
751.0	6 526*

*Accuracy doubtful.

The difficulty experienced in maintaining close temperature control at high temperatures was mentioned in the last report.[8] Further attention has been given to this problem. A controller assembly that contains a

(6) W Geffcken, *Z Phys Chem* **B5**, 81 (1929)

(7) J D Edwards, C S Taylor, A S Russell, and L F Marenville, *J Electrochem Soc* **99**, 527 (1952)

(8) A S Dworkin, D J Sasmor, I S Yaffe, and E R VanArtsdalen, *Chem Quar Prog Rep Sept 30, 1952*, ORNL-1432 (in press)

Speedomax recorder-controller, a DAT unit, and other lesser parts was obtained on temporary loan and found to maintain temperatures in the Marshall furnaces constant to better than 0.5 deg at 700°C. Accordingly, an order has been placed for a slightly modified form of this assembly which, it is hoped, will solve the temperature-control problems.

Thermodynamic studies of boron nitride have progressed. A sample of highly purified boron nitride with good microcrystalline structure has been obtained through the courtesy of the Norton Co. This material is being used in all the present studies. During preliminary attempts to determine the heat of combustion of an impure sample, corrosion of the calorimeter bomb was noted, but tests with Norton boron nitride showed no corrosion, and the indications are that combustion measurements can be carried out with good results. A calorimeter can has been constructed and calibrated in the low-temperature adiabatic calorimeter at the K-25 site. It has been filled with Norton boron nitride, and the determination of the low-temperature heat capacity of this material is in progress and should be completed within the next two or three weeks.

NUCLEAR CHEMISTRY

CAPTURE CROSS SECTION OF PROTACTINIUM-233

J. Halperin R. W. Stoughton

Work on this problem has been completed and will appear in ORNL-1462. the thermal neutron capture cross-section of Pa^{233} has been measured as 125 ± 15 barns.

CHARACTERIZATION OF PROMETHIUM-146

G. W. Parker W. J. Martin

A promethium isotope of mass 145 was first described by Butement[1] in 1951, when the present work was being initiated. Butement's conclusions in characterizing a *K*-capture decay in a 400-d Sm^{145} that gives rise to a longer-lived *K*-capture process in the resulting Pm^{145} have been fully verified and described in the previous quarterly report.[2]

Butement worked with material irradiated at a very low level, therefore it was likely that his observations should include products of only a first-order neutron absorption. This was indicated when he found that both Sm^{145} and Pm^{145} give off *K* and *L*, x radiation, apparently without gamma rays.

In contrast, it was noted by the authors that the initial separation of promethium from the irradiated, enriched Sm^{144} contained an appreciable amount of gamma activity to which energies of 80, 460 and 750 kev were assigned.[2] The obvious explanation was that the intensity of the irradiation and the duration (1 year at 3.6×10^{13} neutrons/cm^2·sec) converted a portion of the promethium to mass 146. Tentative identification of a 1-y promethium activity that has this mass number and possibly emits gamma rays has been proposed by Kistiakowsky.[3]

In order to support the conclusion that some of the extraneous gamma rays observed were certainly from Pm^{146}, a number of checks was made.

1. The promethium produced by the decay of the purified 400-d samarium

(1) F D S Butement, *Nature* **167**, 400 (1951)

(2) G W Parker and W J. Martin, *Chem Quar Prog Rep Sept 30, 1952*, ORNL-1432 (in press)

(3) V. Kistiakowsky, *Phys Rev* **87**, 859 (1952)

after it had been stripped of the promethium was compared with the original material, and it was found that the two harder gamma rays were totally absent in pure Pm^{145}.

2. A partial-decay curve of the mixed promethium isotopes clearly indicated an apparent half life of only 5 to 8 years. This is interpreted to indicate that about 2% of a 285-d activity is superimposed upon a pure 30-y activity.

3. A third method that involves the cyclotron production (the 86-in. cyclotron at the Y-12 site) of Pm^{146} by a preferred (p,n) reaction on enriched Nd^{146} has been carried almost to completion, however, impurities that arise from the Inconel (Ni, Cr) mounting in the cyclotron had to be removed by cation exchange, and time has not permitted completion of this check.

4. The enhancement of Pm^{146} by neutron irradiation of Pm^{145} has also been initiated in the LITR, however, it is believed that a neutron intensity such as is available only in the MTR will be required to accomplish a reasonable conversion. By this method, almost pure Pm^{146} should result, thereby serving to explain both the radiations and the relatively short half life.

5. Direct mass identification of a low concentration of Sm^{145} in the irradiated mixture lends considerable weight to the conclusions regarding the parent isotope. Mass spectrographic proof of the existence of two promethium isotopes is planned.

Using the results of the mass analyses by Sites and Baldock, Halperin of the ORNL Chemistry Division has assisted in analyzing the data for apparent neutron cross sections of the various samarium isotopes.

In Fig. 1, the results of the observed decay rate of two samples of Sm^{145} are shown, together with the standard Co^{60} that was used to illustrate the accuracy of counting. The slightly scattered points have been analyzed by the least-squares method to give essentially the same value of 360 days.

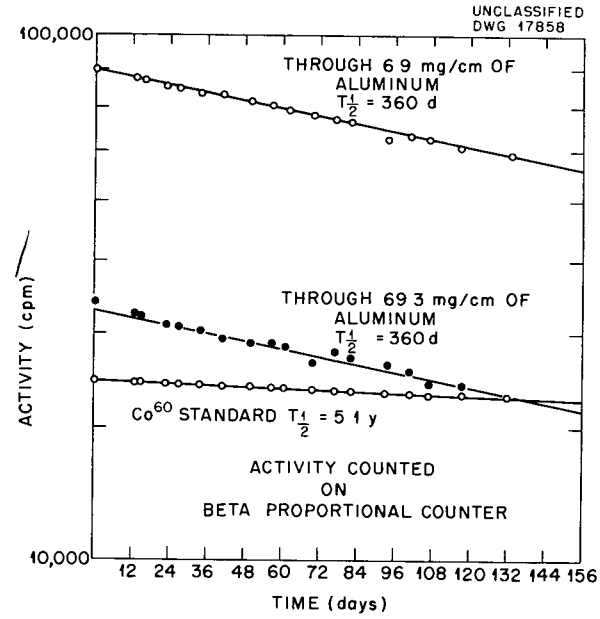

Fig. 1. Decay of Samarium-145.

The presumably pure Pm^{145} sample used in preparing the scintillation counter spectrograms shown in Fig. 2 was made by milking the once-stripped samarium of its promethium activity that had grown during a period of about 3 months. The presence of the K x ray and the 80-kev gamma ray is indicated in both the pure Pm^{145} and the mixed $Pm^{145-146}$ in Fig. 2. The inset in the same figure is the original spectrogram of the Pm^{145} that contains Pm^{146} and is compared with a pure Pm^{145} that is completely lacking in the 460- and 750-kev gammas.

A mass analysis was obtained on both the unirradiated and the irradiated samarium through the assistance of Baldock, Sites, and others at the Y-12 site. The results of the analyses are given in Table 6. The values listed are molecular ratios relative to the most abundant isotope (Sm^{144}), which is arbitrarily assigned a value of 100. The deduced cross-section values are included in the same table.

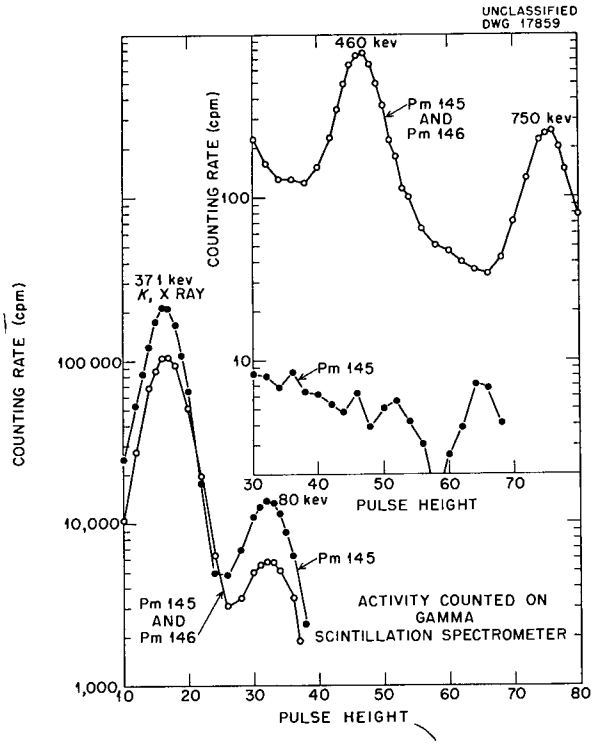

Fig 2. Spectrograms of Gamma Rays of Promethium-145 and Promethium-146.

HALF-LIFE MEASUREMENTS

A. R. Brosi B. H. Ketelle

It has recently become desirable to know, with greater precision, the decay constants of several isotopes with half lives of the order of years. An attempt is being made to determine these decay constants, by precision measurements of the ionization current produced by a given sample in an ionization chamber, as a function of time.

Care has been taken to minimize the constant sources of error that arise from chemical and isotopic impurities, instrumental drifts, and nonlinearity of the instrument response. Random fluctuations are being reduced by making repeated rate-of-drift measurements in order to obtain standard deviations of 0.1% or less for the mean reading. To attain this precision, reproducible positioning of the sample in the re-entrant-tube ion chamber

TABLE 6. MASS ANALYSES OF IRRADIATED SAMARIUM

SAMARIUM ISOTOPE	ABUNDANCE, RELATIVE TO SAMARIUM-144		CALCULATED CROSS SECTION (barns)
	Before Irradiation	After Irradiation	
144	100	100	1
145	0 00	0 073*	
146			
147	11 88	10 94	73
148	6 44	7 06	39
149	6 27	0 00	>>1100
150	2 77	8 03	116
151	0 00	0 07**	14,000
152	7 80	6 76	237
153			
154	5 64	5 58	9.4

* ~400-d Sm^{145}.
** ~500-y Sm^{151}

becomes quite important. Also, fluctuations in the frequency of the alternating current make it necessary to use good mechanical stop watches rather than electric timers when periods of the order of 200 sec or less are being timed.

At the present time, daily measurements are being made on samples of Ce^{144}, Co^{60}, Kr^{85}, A^{39}, and Ra^{226}. A least-squares analysis of data taken over a two-months period indicates a standard deviation in a 10-y half life of 6%.

The standard deviation should vary inversely as the number of mean lives over which decay is observed and also inversely as the square root of the number of measurements. In the present series of measurements, it should be possible, aside from any constant errors, to determine a 10-y half life with a standard deviation of 2% during a period of four months.

RADIO-ORGANIC CHEMISTRY

RADIATION AND ANALYTICAL CHEMISTRY

A. R. Jones W. J. Skraba

The study of the products formed by the action of gamma radiation from Co^{60} on dilute aqueous solutions of organic acids has continued.

In addition to succinic, tricarballylic, and alpha- and beta-butane-1,2,3,4 -tetracarboxylic acids, a fifth major product was formed from acetic acid in water. This substance, with partition coefficients similar to those of citric acid for several solvent pairs, has been isolated, as a colorless glass, from some large-scale experiments. Its solutions do not crystallize when seeded with citric acid. Since a likely identity for the material was carboxymethanetriacetic acid, the preparation of this compound was undertaken. A method found in early literature for the synthesis of the compound yielded a mixture of difficulty separable acids, none of which was the desired substance. A more elaborate synthesis is under way.

The nonvolatile acidic residue from the irradiation of aqueous propionic acid solutions was separated into five principal fractions by partitioning procedures. The identification of the largest fraction as dimethylsuccinic acid was easily made by the mixture-melting-point method. The other four fractions are being purified by further partitioning procedures.

Aqueous solutions of succinic acid, upon irradiation and subsequent evaporation, yielded the simplest mixture of products thus far obtained from these experiments. The residue consisted almost entirely of succinic acid and alpha- and beta-butane-1,2,3,4-tetracarboxylic acids.

Partition, between CB-35 and 0.5 *N* sulfuric acid, of the residue from the irradiation and evaporation of aqueous malonic acid solutions has demonstrated the complexity of radiation damage in this case, but no products have been identified.

Solid succinic acid was irradiated (2.2×10^8 r) in a lightly stoppered bottle, and the gaseous products were allowed to escape. The oily residue was steam distilled. The distillate contained acetic and propionic acids, the latter was in a larger amount. The material that is nonvolatile with steam is being separated by partition chromatography.

CARBON-14 ISOTOPE EFFECT STUDIES

Formation of Ketone Derivatives (V. F. Raaen, G. A. Ropp). Frequently, in the course of isotopic tracer studies involving organic and biological systems, the molar specific

activity of an organic compound can be measured most conveniently by assaying a crystalline, solid derivative of the compound. Since, in such a case, the derivative's molar specific activity must truly represent the molar specific activity of the original compound, there should be no isotopic fractionation during the preparation of the derivative. It was of interest therefore to determine to what extent isotopic fractionation occurred in the preparation of certain standard derivatives of C^{14}-labeled ketones under such conditions that the yields of the derivatives were not quantitative. The results listed in Table 7 were obtained by studies similar to those of Stevens and Attree,[1] who compared the specific activities of products of a reaction carried to completion and to 10 or 20% completion. From these specific activities, the ratio, k_{14}/k_{12}, was calculated[1] for the reactions involved.

Effect of Nuclear Substituents in Acetophenone-α-C^{14} on the Isotope Effect in the Formation of the 2,4-Dinitrophenylhydrazone at 25°C (V. F. Raaen, G. A. Ropp). As a continuation of a similar study[2] involving ester saponification, the isotope effect at 25°C has been determined for three acetophenones that were labeled with C^{14}. The data are presented in Table 8.

Isotope Effect in the Displacement Reaction Between Acetophenone-α-C^{14} Semicarbazone and 2,4-Dinitrophenylhydrazine (V. F. Raaen, G. A. Ropp). Isotope fractionation was studied in the reaction

$$C_6H_5C^{14}(CH_3)=NNHCONH_2 + (O_2N)_2C_6H_3NHNH_2 \longrightarrow (O_2N)_2C_6H_3C^{14}(CH_3)=NNHC_6H_5\downarrow + H_2NCONH_2 \quad .$$

(1) W. H. Stevens and R. Attree, *Can. J. Chem.* **B27**, 807 (1949).

(2) G. A. Ropp and V. F. Raaen, *Chem. Quar. Prog. Rep. Sept. 30, 1951*, ORNL-1432 (in press).

TABLE 7. RESULTS OF CARBON-14 ISOTOPE EFFECT STUDIES IN THE PREPARATION OF DERIVATIVES OF LABELED KETONES

KETONE	DERIVATIVE	TEMPERATURE (°C)	KETONE REACTED (%)	SPECIFIC ACTIVITY OF DERIVATIVE $\times 10^3$ (μc/mg)	APPROXIMATE VALUE OF k_{14}/k_{12}
Acetophenone-α-C^{14}	2,4-Dinitrophenylhydrazone	25	100	8.90	0.940
			10	8.37	
		25	100	8.99	0.934
			5	8.39	
		-75	100	9.09	0.910
			5	8.27	
	Semicarbazone	25	100	15.8	0.912
			10	14.4	
Benzophenone-α-C^{14}	2,4-Dinitrophenylhydrazone*	25	100	4.31	0.960
			20	4.15	

*This isotope effect has also been reported by F. Brown and D. Holland, *Can. J. Chem.* **30**, 438 (1952).

TABLE 8. ISOTOPE EFFECTS IN 2,4-DINITROPHENYLHYDRAZONE FORMATION FROM CARBON-14-LABELED ACETOPHENONES AT 25°C

KETONE	KETONE REACTED (%)	PRODUCT SPECIFIC ACTIVITY X 10^3 (μc/mg)	k_{14}/k_{12}	$100(k_{12}-k_{14})/k_{12}$
Acetophenone	100	8 94	0 949	5 1
	10	8 50		
m-Nitroacetophenone	100	6 95	0 960	4 0
	10	6 68		
p-Methoxyacetophenone	100	4 26	0 943	5 7
	10	4 03		

This reaction appears to be driven completely to the right by the insolubility of the 2,4-dinitrophenylhydrazone of acetophenone-α-C^{14}. Hence, it can be carried to any degree of completeness by adjusting the amount of 2,4-dinitrophenylhydrazine added. For the isotope fractionation study of the reaction, the specific activity of the precipitated acetophenone-2,4-dinitrophenylhydrazone was measured with sufficient 2,4-dinitrophenylhydrazine present to effect 10 and 100% reaction. The isotope effect, k_{14}/k_{12}, was found to have a value of 0.973 at 25°C.

As a part of this study, exchange was shown not to occur between acetophenone-α-C^{14}-unlabeled acetophenone semicarbazone under the conditions of the displacement reaction. This suggests that the displacement reaction may not go through a mechanism involving the dissociation of the semicarbazone to free acetophenone-α-C^{14}. A possible mechanism that would also permit the isotope fractionation found in this displacement reaction could involve an attack on the semicarbazone by 2,4-dinitrophenylhydrazine

$$C_6H_5C^{14}(CH_3){=}NNHCONH_2 + (O_2N)_2C_6H_3NHNH_2$$

$$\longrightarrow C_6H_5\overset{\overset{\displaystyle NHC_6H_3(NO_2)_2}{|}}{\underset{\underset{\displaystyle H_2N^{\oplus}}{|}}{C^{14}}}(CH_3)-N^{\ominus}-NHCONH_2.$$

This intermediate could then dissociate to give the reaction products observed. If the new bond to the labeled atom were formed in the same instant that the old bond to the labeled atom was broken, then the rather small isotope effect that was observed might be expected.

Isotope Effect in the Catalytic Reduction of Acetophenone-α-C^{14} (G. A. Ropp, V. F. Raaen). In the catalytic hydrogenation of C^{14}-labeled acetophenone, methylphenylcarbinol-C^{14} is formed

$$C_6H_5C^{14}OCH_3 + H_2O \xrightarrow[\text{25°C (ethyl alcohol)}]{\text{Pt}} C_6H_5C^{14}HOHCH_3.$$

In order to determine whether isotope fractionation occurred during the reaction, just sufficient hydrogen to cause 80% reduction of the labeled ketone was used in the manometric system, the reaction was stopped, and unreacted ketone was precipitated quantitatively by the addition of excess 2,4-dinitrophenylhydrazine

$$C_6H_5C^{14}OCH_3 + (O_2N)_2C_6H_3NHNH_2$$

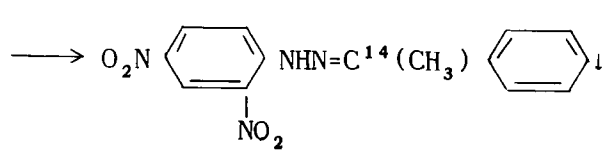

The specific activity of the 2,4-dinitrophenylhydrazone thus formed was compared with the same derivative

prepared from reaction of a sample of the original acetophenone-C^{14} with excess 2,4-dinitrophenylhydrazine

	SPECIFIC ACTIVITY x 10^3 (μc per mg)
Derivative of last 20% of acetophenone-α-C^{14}	9 88
Derivative of acetophenone-α-C^{14} before hydrogenation	9 05

These data correspond to a k_{14}/k_{12} value of approximately 0.95. This isotope effect is being checked by a second study of a different type.

Isotope Effect in the Acid Hydrolysis of Hydrocyanic-C^{14} Acid (G. A. Ropp, A. J. Weinberger). The acid hydrolysis of hydrocyanic acid to formic acid has been studied,[3] and the rate-controlling step has been suggested as the addition reaction

$$HCN + HX \longrightarrow HCX{=}NH ,$$

which is then followed by

$$HCX{=}NH + H_2O \longrightarrow HC(X)OHNH_2 \longrightarrow HCONH_2 + HX ,$$

and rapid hydrolysis of the amide,

$$HCONH_2 + H_2O \longrightarrow HCOONH_4 \xrightarrow{H^+} HCOOH .$$

A C^{14} isotope effect would therefore be of interest, since a bond to the labeled atom is broken and a new bond to the labeled atom is formed.

Preliminary experiments indicate that there is a normal isotope effect in the reaction that uses labeled hydrogen cyanide solution. Hydrogen cyanide-C^{14} was hydrolyzed approximately 30 to 40% in 7.84 *N* hydrochloric acid at 45°C in 25 minutes. In a second batch, the reaction was carried to approximately 50% completion in 45 minutes. In each case, unreacted hydrogen cyanide-C^{14} was precipitated and assayed as $CuC^{14}N$. The average assay for the original hydrogen cyanide-C^{14} was obtained in the same way. The resulting data were

REACTION (%)	SPECIFIC ACTIVITY OF UNREACTED $HC^{14}N$ x 10^4 (%)
0	292
30 to 40	303
about 50	309

Isotope Effect During Ozonization (W. A. Bonner, C. J. Collins). Experiments have been conducted to ascertain the presence of an isotope effect during the ozonization of an olefinic linkage, 1,2-diphenylethylene-1-C^{14} (singly labeled stilbene), that was ozonized fractionally in ethanolic 2,4-dinitrophenylhydrazine sulfate solution. This procedure produces benzaldehyde 2,4-dinitrophenylhydrazone directly, and 12 fractions of this derivative were collected during the course of the ozonization. The assays for each fraction are presented in Table 9. It will be noticed that the assays gradually increase as the ozonization goes toward completion. These results are in accord with a "normal" isotope effect during ozonization, and calculation shows the ratio k_{14}/k_{12} to be about 0.958.

TABLE 9. ASSAY OF FRACTIONS OF OZONIZED 1,2-DIPHENYLETHYLENE-1-C^{14}

FRACTION	PERCENTAGE OF TOTAL	ASSAY (μc/mmole)
1	8 26	0 4695 ± 0 0015
2	15 78	0 4700
3	23.56	0 4775 ± 0.0015
4	32 13	0 4765 ± 0 0005
5	39 91	0 4720
6	47 23	0 4800 ± 0 0010
7	54 58	0 4820 ± 0 0030
8	63 08	0 4835 ± 0 0000
9	72.62	0.4825 ± 0 0005
10	82 94	0 4925 ± 0 0005
11	91 41	0 4960 ± 0 0000
12	100 00	0 5060 ± 0 0000

(3) V K Krieble and J G McNally, *J Am Chem Soc* **51**, 3368 (1929)

Studies in Solution Scintillation Counting of Carbon-14 (A. J Weinberger, G. A. Ropp). By using the instrument previously described,[4] preliminary studies have been made with 0.5% terphenyl solutions (volume about 20 ml) in dioxane in quartz and glass cells with dimensions of about 2 in. by 2 in. by 1 cm. From these studies, four conclusions were drawn

1. The optimum operating voltage (the voltage is indicated on the instrument panel and is about 3/2 the voltage applied to the photocell) is 1400.

2. At 1400 volts, about 3% of the disintegration known to take place in a C^{14} compound that is added to the terphenyl-dioxane solution in the previously described cell is recorded by the register.

3. At 1400 volts, the background (count rate from a cell containing only 0.5% terphenyl in dioxane) is about 4 register cpm for a glass cell and about 2 register cpm for a quartz cell.

4. For a cell containing 0.4 μc of benzoic-α-C^{14} acid dissolved in 20 ml of 0.5% terphenyl solution in dioxane, the ratio of sample-cell register counts to background-cell register counts is about 8 1 to 10 1 at 1400 volts.

On the basis of these data, it has been decided that the instrument should be modified. The rebuilt instrument will have positions for three cells (sample, standard, and background cells) instead of two. The three cells will be automatically counted, in turn, for equal time intervals. Total counts from each cell will be indicated on one of three registers. Thus, the ratio of total sample counts to total standard counts can be calculated as

$$\frac{\text{Sample-cell counts} - \text{background-cell counts}}{\text{Standard-cell counts} - \text{background-cell counts}}$$

Thus, all activity measurements will be relative to the standard used. It is planned to count each of the three cells for a total of 10 to 60 min, depending on the precision desired. It is hoped that by the use of the newly designed instrument, C^{14}, S^{35}, and possibly other activities can be counted to a precision better than ±1% for samples that contain only a few tenths microcurie of activity.

Preparation of Standard Comparison Ionization Chambers for Carbon-14 Assay (A. J. Weinberger, O. K. Neville). Several types of ionization chambers for use as standard radioactive comparison samples have been prepared and tested. Carbon-14 determinations have been carried out through the measurement of the ionization currents produced by $C^{14}O_2$ in a Borkowski type of ionization chamber. It was found that the combination of a vibrating-reed electrometer and a Brown recorder was subject to fluctuations that made this method somewhat uncertain. In order to minimize these fluctuations, comparisons were made between standard ionization chambers and chambers containing the unknown samples.

The first standard comparison chamber used was a modified Borkowski type of ion chamber, inside of which was fastened a small piece of uranium metal in radioactive equilibrium with its decay products. The uranium was wrapped with sufficient aluminum foil to absorb all alpha particles. The chamber was not gas tight and the ionizable gas was air, which was essentially in equilibrium with the air in the counting room. It was possible that air-pressure changes could produce ionization-current variations in the chamber, also, escaping radon might produce alpha pulses. So far, these factors have not caused appreciable variations in ion currents. However, at the time the uranium chamber was placed in service, it was desirable to construct

[4] G A Ropp and J B Davidson, *Chem Quar Prog Rep Sept 30, 1952*, ORNL-1432 (in press)

and test sealed chambers in which there was no possibility of alpha contamination appearing. The first chamber was a gold-plated brass, Borkowski type of instrument that was filled with a known quantity of $C^{14}O_2$ from $Na_2C^{14}O_3$ that was prepared and standardized by NBS. This chamber was unsatisfactory, since the ion current decreased by about 1/2% per month, relative to that of the standard uranium chamber. The decrease was presumably the result of the diffusion of $C^{14}O_2$ through the rubber gaskets.

Polystyrene that contained C^{14} was available, and a second chamber containing this material as a source of weak beta activity was assembled. This was also a standard Borkowski type of chamber made of gold-plated brass. It contained two strips of polystyrene-C^{14}, each about 1/4 in. wide and about 3 in. long. These strips were bent in such a way that, when joined, they formed a boxed *X* ⊠. They were covered with gold leaf that was cemented with a dilute solution of DeKhotinsky wax in alcohol. The strips were pinned to the base of the chamber by means of a platinum pin through the gas inlet hole. The gold leaf furnished a low-resistance leak path for the electric charge that appeared in the polystyrene. Charge accumulations are known to produce erratic results when samples that have high specific resistance are counted with G-M tubes.

The assembled unit was evacuated for several hours to remove the alcohol from the wax. It was then filled with air, and the gas-inlet hole was sealed with DeKhotinsky wax.

The ionization currents from the uranium chamber and the polystyrene chamber were compared at intervals over a one-year period with the following results.

	AVERAGE DEVIATION FROM THE AVERAGE (%)
Ionization current	
Of uranium chamber (A)	1 1
Of polystyrene chamber (B)	1 0
Ratio of A to B	0 6

The results indicate that the polystyrene chamber is as good a comparison standard as the uranium chamber and that the major long-term fluctuations in the radioactivity-measuring combination of standard ionization chamber, vibrating-reed electrometer, and Brown recorder are caused mainly by the last two components. They also show that the changes in chamber ionization currents resulting from the air-pressure fluctuations encountered here are not serious.

Organic Reaction Mechanism Studies (W. A. Bonner, C. J. Collins). The study of the Wagner rearrangement of 2-phenyl-1-acenaphthenol-1-C^{14}, discussed initially in the previous quarterly report,[5] has now been completed. *Trans*-2-phenyl-1-acenaphthenol-1-C^{14}, when subjected to dehydration with phosphoric anhydride, produces 1-phenylacenaphthylene that contains C^{14} in both the 1- and 2-positions. Permanganate oxidation of this hydrocarbon led to polymeric materials, but degradation could be successfully accomplished by ozonization. Permanganate oxidation of the ozonide of 1-phenylacenaphthalene produced 8-benzoyl-1-naphthoic acid in good yield. Decarboxylation of this acid produced $C^{14}O_2$ and phenyl-1-naphthyl ketone-C^{14}. The latter ketone contained 7.5%, and the $C^{14}O_2$ contained 92.5% of the radioactivity originally present in the *trans*-2-phenyl-1-acenaphthenol-1-C^{14}. Thus, phenyl migration during dehydration occurred to the extent of 7.5%.

[5] W A Bonner and C J Collins, *Chem Quar Prog Rep Sept 30, 1952*, ORNL-1432 (in press)

Mechanistically, this dehydration may be explained in terms of (1) a classical carbonium-ion intermediate, (2) a concerted, or "push-pull" process, or (3) a symmetrical phenonium-ion intermediate. If mechanism (1) or (2) is operative, then 92.5% of the reaction may be considered to have occurred through *cis*-elimination of the elements of water from *trans*-2-phenyl-1-acenaphthenol-1-C^{14}, and 85% if mechanism (3) is operative.

CHEMISTRY OF SEPARATIONS PROCESSES

ION EXCHANGE STUDIES

Pressure-Volume Relationships of Cross-Linked Resins (Q. V. Larson, B. A. Soldano). Isopiestic studies have been made on a series of sulfonated styrene resins of varying degrees of cross linking. The primary purpose of the investigation was to determine the effects of cross linking on the activity of the water inside the exchanger. It was further hoped that some underlying equation could be found that would relate *P-V* effects for ion exchangers of all types of cross linking.

When water activities, $a_w = p/p_0$, are compared at constant normality (Fig. 3), it may be seen that the activity is increased by increasing cross linking. It appears that this effect is analogous to the imposition of a hydrostatic pressure on the interior of the exchanger.

The thermodynamics of this situation have been considered by Boyd and Soldano,[1] along with Gregor and Glueckauf.[2] A straightforward solution of this problem results in the equation

$$RT \ln \frac{a'_w}{a_w} = \bar{V}_w P \ , \qquad (1)$$

where

a'_w = activity of the water inside the exchanger,

a_w = activity of water outside the exchanger,

P = swelling pressure,

$\bar{V}_w$ = partial molar volume of the water.

A comparison of the water activities in the cross-linked and noncross-linked species is then made at constant molality. By assuming a value of 18.06 m^{-1} for $\bar{V}_w$, the values of P can then be calculated for different types of exchangers.

The experimental procedure used for these investigations has been described in detail.[2] Essentially, the procedure consists of equilibrating the hydrogen forms of varying degrees of cross-linked resins with weakly cross-linked resins, using saturated solutions of salts at different activities. The moisture uptake is measured, and a stoichiometric normality is determined that is based on the amount of water the resin contains, and the number of equivalents of H^+.

The *P-V* relationships were calculated for each degree of cross linking and are shown in Fig. 4. The first relationship that is apparent for all exchangers is the linearity of the *P-V* relationship. Interestingly, the extrapolated volume, V_0, does not reach the value found for the dry exchanger. The values of V_0 are shown in Table 10. According to the thesis, at V_0, no pressure is exerted on the exchanger. As would be expected, V_0 is the greatest for the weakly cross-linked resin. This preparation is so loosely knit that a considerable

(1) G. E. Boyd and B. A. Soldano, *Osmotic Free Energy of Ion Exchangers* (to be published).

(2) E. Glueckauf, *Proc. Roy. Soc. (London)* **214A**, 207 (1952).

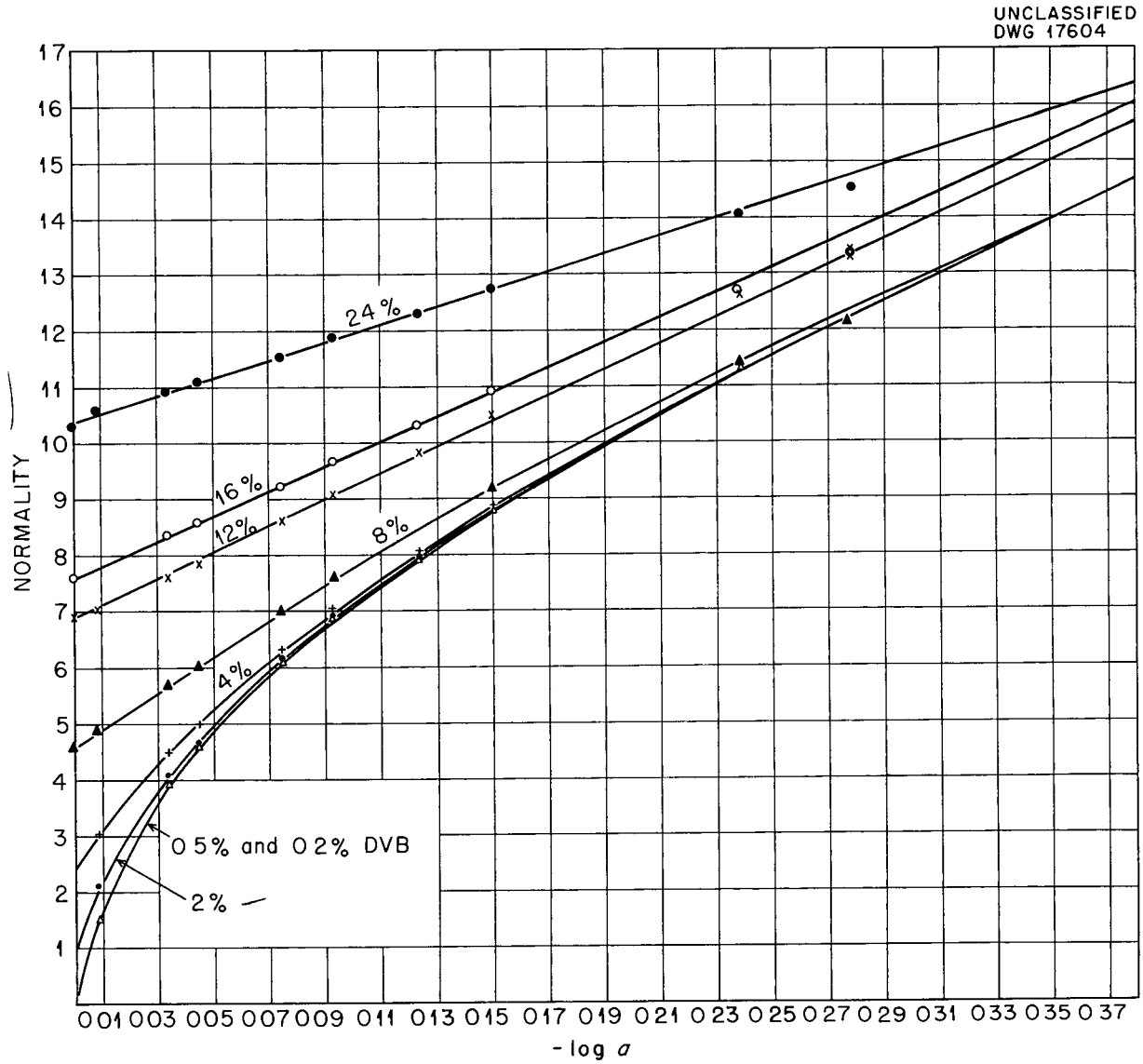

Fig. 3. Effect of Cross Linking on Moisture Adsorption of H^+ Resins.

amount of water must enter the resin before any extension takes place. It may be significant that the 16 and 12% preparations have the value of V_0 found. The difference between V_0 and the dry volumes approximately equals 18 cc. This would indicate that 1 eq of water goes into the resin before any extension takes place. This phenomenon could be related to the hydration of the sulfonate ion inside the exchanger.

The 24% preparation behaves differently. The amount of water at zero pressure is equal to 2 equivalents. There is a suggestion that the amount of moisture inside an exchanger is indeed a function of capacity and, the lower the capacity of the resin, the higher the amount of water per equivalent.

It would be of considerable interest if a reduced equation of state could be found for polystyrene exchangers of

different degrees of cross linkage. With this aim in mind, bulk moduli of the various preparations were calculated.

$$P = K \frac{(V - V_0)}{V_0} , \qquad (2)$$

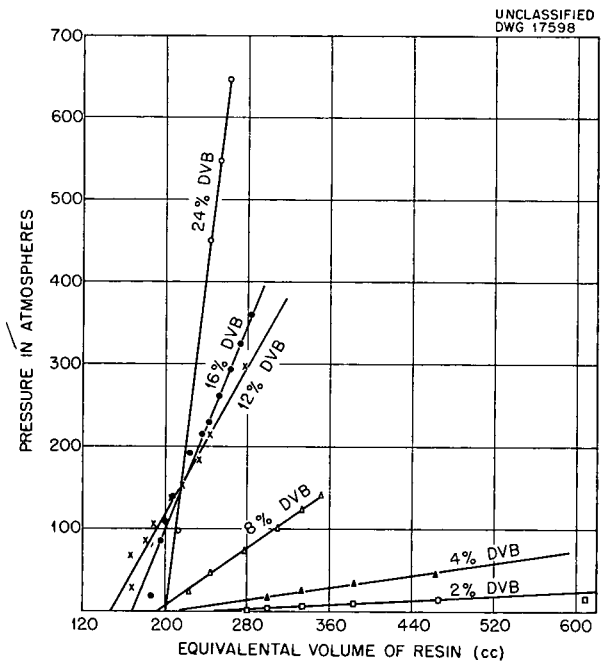

Fig. 4. PV Relationship of Cross-Linked Ion Exchangers.

where

P = swelling pressure,
K = bulk modulus,
V = the actual equivalental volume of the exchanger,
V_0 = extrapolated equivalental volume at zero pressure.

The values listed in Table 11 were obtained for the various cross linkings where $K = V_0$ times the slope of the P-V curves.

In Fig. 5, it is found that a plot of log K vs. the normality of the fully swollen H^+ resin is essentially a straight line, except for the 8% point. There appears to be no basis for eliminating that point, but for most cross linkings, a relationship does exist that relates the different structures. Therefore it can be stated that $K = e^{0.74(N)+2\ 3}$ where N = the normality of the fully swollen H^+ resin and K = the bulk modulus.

The reduced equation of state for all ion exchangers in the H^+ form then is

$$P = e^{0\ 74(N)+2\ 3} \frac{V - V_0}{V_0} \qquad (3)$$

This equation would also be useful for calculating P for any other salt-form of the exchanger. The value of K is

TABLE 10 P-V RELATIONSHIP OF CROSS-LINKED H^+ RESINS

CROSS LINKING (%)	CALCULATED SWELLING PRESSURE (atm/cc)	EXTRAPOLATED EQUIVALENTAL VOLUME (cc)	EQUIVALENTAL VOLUME OF FULLY HYDRATED H^+ RESIN (cc)	EQUIVALENTAL VOLUME OF OVEN-DRIED RESIN (cc)
0 5	0			133 6
2	25	250	1064 0	133 6
4	58	206	535	133 6
8	140 6	192	351 8	133 6
12	297	148	277 6	133 6
16	360	168	284	152 7
24	647	200	263 55	167 85
56	1170			
30	488			

TABLE 11 BULK MODULUS AS A FUNCTION OF CROSS LINKING

CROSS LINKINGS	K	NORMALITY OF THE FULLY SWOLLEN RESIN
2	16 88	1
4	39 1	2 56
8	168	4 58
12	333	6 9
16	522	7 6
24	2020	10 36

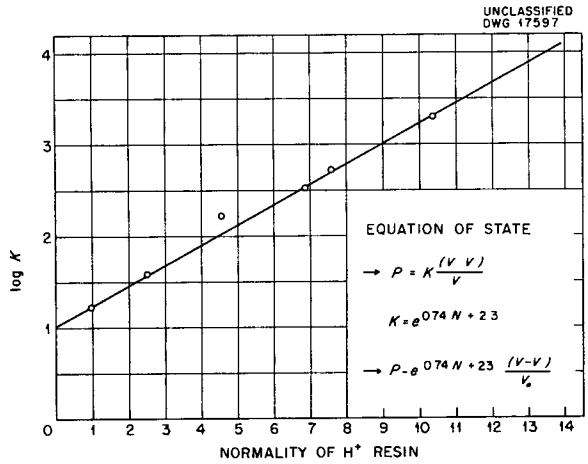

Fig. 5. Bulk Modulus vs. Normality of H^+ Resin.

first determined from the fully swollen H^+ form, then the value of K is inserted in the formula

$$P = K \frac{V - V_0}{V_0} . \qquad (4)$$

Since the slopes of P-V curves are independent of salt form and are only a function of the elastic properties of the exchanger, the pressure can be easily determined.

Moisture isotherms were also taken on colloidal 56- and 30%-DVB hydrogen forms. They showed a considerable deviation from the linearity found for the normal ion exchangers when log a is plotted against normality.

When these resins were equilibrated with H_2O of higher activity, a new process began to take place, namely, a surface condensation. At very high activities, the 56 and 30% colloidal resins actually contained more water per equivalent than the 2% preparation. It would appear that for the hydrogen form of a highly cross-linked resin, condensation takes place when the plot of log a vs. N ceases to be linear. In order to calculate the maximum swelling pressures for these two preparations, the initial linearity was extrapolated to $a = 1$.

Relationship of Osmotic Coefficients with Ionic Selectivity (Q. V. Larson, B. A. Solando). It is generally considered that the equilibrium behavior of ion exchangers can be explained by the hypothesis that a Gibbs-Donnan membrane equilibrium is involved. An exact thermodynamic analysis[1] applied to the reaction shows that the selectivity coefficient K_d, defined by

$$K_d = \frac{(B/A)_{resin}}{(B/A)_{water}} , \qquad (1)$$

is given by

$$RT \ln K_d = \pi(\overline{V}_A^0 - V_B^0) + RT \ln \left(\frac{\gamma_B}{\gamma_A}\right)_w - RT \ln \left(\frac{\gamma_B}{\gamma_A}\right)_r . \qquad (2)$$

For dilute external solutions, this simplifies to

$$\log K_d = \frac{\pi}{2.303\,RT} (\overline{V}_A^0 - V_B^0) - \log \left(\frac{\gamma_B}{\gamma_A}\right)_r \qquad (3)$$

where π = swelling pressure exerted by exchanger, $\overline{V}_A^0$ and $\overline{V}_B^0$ are stoichiometric partial molar volumes of ions A and B in the standard state at infinite dilution, and γ_A and γ_B are activity coefficients in the resin for the ions $A^{\pm}$ and $B^{\pm}$ or the salts A^+ resin and B^+ resin. At present, investigation is under way to test the validity of

the above equation by means of independent measurements of the selectivity coefficient, the swelling pressure, and the activity coefficients within the resin phase.

No direct method is available for determining the activity coefficients in the resin, but an attempt has been made to correlate these activity coefficients with measured osmotic coefficients of resins that have been completely converted to a cationic form. This treatment follows that originally proposed by Glueckauf.[2] Essentially, the osmotic coefficients are calculated from the adsorption isotherms of weakly cross-linked resins by using the equation

$$-\frac{\log a_w}{0.0078\ m_r} = \nu\theta\ , \qquad (4)$$

where

a_w = activity of the water,
m_r = calculated molality of the resin,
ν = number of ions formed per equivalent of resinate,
θ = osmotic coefficient.

According to Glueckauf[2] and Boyd and Soldano,[1] the values of ν tend toward unity, contrary to the value of 2 found for normal 1 1 electrolytes.

A plot (Fig. 6) of $(\theta - 1)$ against molality for all the monovalent salt forms indicates that the relationship

$$(\theta - 1) = -F(\overline{m}_r) + a_m m_r \qquad (5)$$

holds where $F(m_r)$ is identical for all salt forms and a is a specific constant for each form. Therefore the following equation can be written.

$$\log (a_w)m_r = 0.00782 \left[m_r - m_r F(m_r) + a_m m_r^2\right] . \qquad (6)$$

By using the Gibbs-Duhem equation, the following equation can be derived that gives the activity coefficients of the metal resinates

$$\log_e \gamma^0_{m_r} = -G(m_r) + 2a_m m_r\ . \qquad (7)$$

It now becomes apparent that if Eq. 5 is multiplied by 2, it is of the same form as Eq. 7. Therefore

$$[(\theta - 1)_1 - (\theta - 1)_2] = \log_e \gamma^0_1 - \log_e \gamma^0_2\ , \qquad (8)$$

since both $G(m_r)$ and $F(m_r)$ are constant functions for all salt forms and cancel. The activity coefficients calculated from osmotic data are for the pure salt forms of the resin, whereas those found in the exchanger by equilibrium measurements are for mixtures of two salt forms. In order to correlate these activity coefficients, recourse is made to Harned's rule for mixtures of strong electrolytes, where

$$\gamma_1(2) \equiv \log \gamma^0_1 - a_{12}m_2 \qquad (9)$$

$$\gamma_2(1) \equiv \log \gamma^0_2 - a_{21}m_1\ . \qquad (10)$$

γ^0_1, γ^0_2 are the activity coefficients of the solutions that contain only one salt at the fixed total molality, $\gamma_1(2)$ is the activity coefficient of salt 1 in a mixture of (2), and $\gamma_2(1)$ is the activity coefficient of salt 2 in a mixture of (1), a_{12} and a_{21} are specific constants for the systems involved. It must be pointed out that Harned's rule is empirical in nature and may not be universally valid. At present, however, it is the best

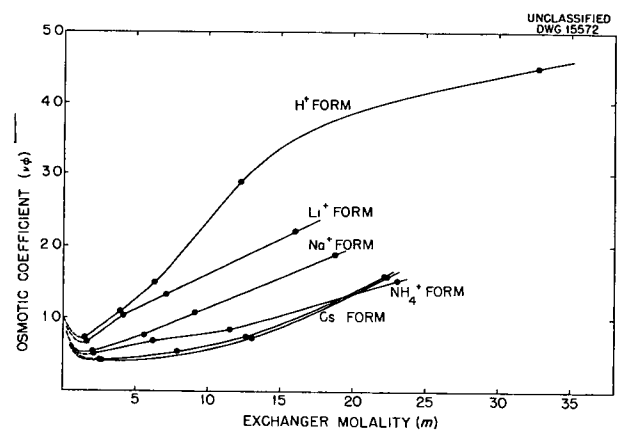

Fig. 6. Concentration Dependence of Osmotic Coefficients for Several Salt-Forms of 0.5% DVB-Dowex-50 Exchanger.

relationship available for treating mixtures of strong electrolytes. To simplify the use of Harned's rule, selectivities were measured with a trace of one component present. This procedure allows the equation

$$\gamma_1(2) \cong \log \gamma_1^0 \ .$$

A typical procedure for measuring selectivities is given for the Na*-H system where Na* is present in trace amounts. Pure hydrogen resin, 0.2 to 0.3 g, is equilibrated with 25 cc of a 0.1 *N* HCl solution containing a trace of another monovalent species, NaCl. The system is equilibrated for 24 hr, the phases separated, the resin washed with 100 cc of distilled water, and the washings collected. The sum of the activities of the washings and the initially separated solution gives an exact determination of the amount of trace species in the outside solution. The activity of the resin denotes the concentration of the trace inside the resin. Insertion of these values in Eq. 3 gives an experimentally determined K_d.

The experiments were conducted at an outside-solution concentration of 0.1 *N* because (1) the dilute solution would minimize the Donnan effects, (2) the activity coefficient of the trace substituent could be approximately equated to the activity coefficient of the 0.1 *N* salt and would allow the ln $(\gamma_B/\gamma_A)_w$ term in Eq. 2 to be dropped.

The values of π are calculated by the method outlined in the first section of this report.

Data were obtained on seven systems, but the results will be discussed in detail for only the Na-H system. The values needed to satisfy Eq. 3 are listed in Table 12.

In Fig. 7 is a plot of $(\log K_d - P\Delta V)$ vs. $\log (\gamma_H^0/\gamma_{Na}^0)$. Up to 20% cross linking, the curve is linear and the slope is 0.5. If the applicability of Harned's rule is assumed and if $a_{12} = -a_{21}$, then the value of $\log K_d - P\Delta V = \log \gamma_1^0/\gamma_2^0$. From Fig. 7 it is noted that this relationship is satisfied up to a normality of 9 except for the constant of 0.1. Indeed, the plot of $\log K_d$ vs. the activity coefficients calculated from osmotic data predicts a reversal of selectivity at low molality of hydrogen. This has been experimentally verified. Presumably, the constant factor 0.1 arises from the fact that $a_{12} \neq a_{21}$

It was considered of interest to determine the interaction coefficient

TABLE 12 RELATION OF OSMOTIC DATA TO K_d

DVB (%)	NORMALITY OF H^+ RESIN	$\log K_d$	$\log \frac{\gamma_H^0}{\gamma_{Na}^0}$	$P(\bar{V}_{H^+}^0 - \bar{V}_{Na}^0)$, $P = \pi$	$\log K_d - P\Delta V$
2	1 02	0	0 1	0	
4	2 4	0 053	0 226	0	0 053
8	4 58	0 13	0 426	0 0037	0 126
12	6 9	0 267	0 662	0 00784	0 26
16	7 6	0 318	0 768	0 0095	0.308
24	10 34	0 724	1 18	0 0171	0 707
20	9	0 455	1	0 0129	0 442
56	14 55	0 954	1 495	0 031	0 923

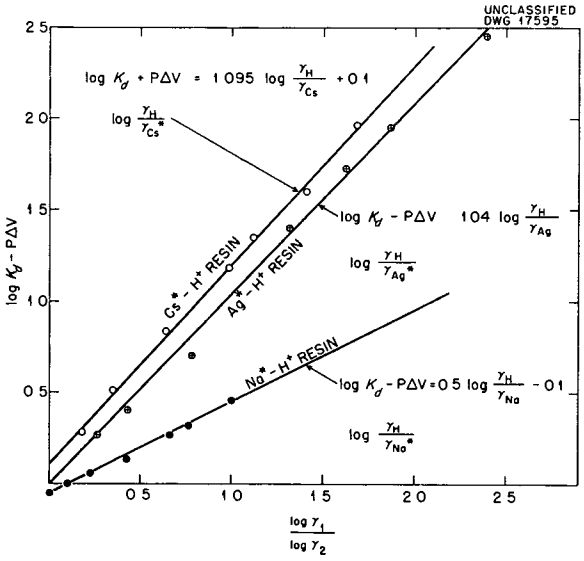

Fig. 7. Relationship Between Experimental K_d and Osmotic Coefficients Data.

a_{12} in the Na-H system as a function of molality. To do this, it must be assumed that the Akerloff's rule,

$$(a_{12} - a_{21})_m = \log \frac{\gamma_1^0}{\gamma_2^0} , \qquad (11)$$

applies to the systems. The validity of this assumption is demonstrated by the linear dependence of the log of the observed γ_1^0/γ_2^0 ratios on m, and the slopes, that is $(a_{12} - a_{21})$, that are in close agreement with those obtained by Akerloff for analogous mixtures of strong electrolytes. If Eq. 11 is substituted in 9 and 10, it is found that

$$\log K_d = a_{12}m \qquad (12)$$

for a trace of Na* in hydrogen resin. Table 13 gives a comparison of calculated a_{12} values with those found for the Na-H system by Harned and Owen. The calculated a_{12} values are approximately the right order of magnitude, thus indicating that the use of Harned's rule is a fair approximation of ion behavior in the resins.

The investigation was extended to a number of different systems that are

TABLE 13. COMPARISON OF a_{12} VALUES FOR RESIN-Na-H SYSTEM AND Na-H SYSTEM IN AQUEOUS SOLUTIONS

HARNED AND OWEN		CALCULATED FROM OSMOTIC DATA
Normality	a_{12}	a_{12}
2 4	0 031	0 0022
4 58	0 030	0 0275
6 9	0 029	0 0377
7 6		0 0405
9		0 0491

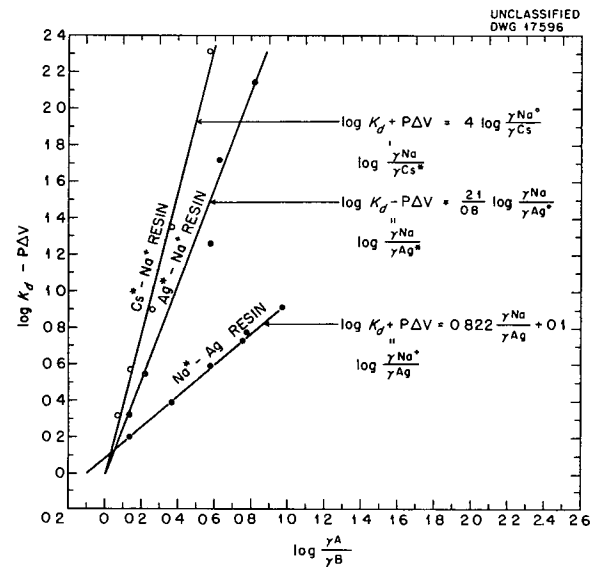

Fig. 8. K_d vs. Osmotic Coefficients

shown in Figs. 7 and 8. The one apparent relationship in all systems is the linearity of log K_d - $P\Delta V$ with molality and with log γ_1^0/γ_2^0. The experiments fall mainly into two categories (1) systems such as Na-H and Na-Li, the latter being satisfied by

$$\log K_d - P\Delta V = 0.87 \log \frac{\gamma_1^0}{\gamma_2^0} ,$$

and (2) systems involving trace Cs* and Ag* where the log γ_1^0/γ_2^0 must be multiplied by a constant greater than

1 and as large as 4. Systems in category 1 would have calculated values for a_{21} that are negative because the slope of the lines in Figs. 7 and 8 is less than 1. The negative values are in agreement with the a_{21} values calculated for most mixed aqueous salt solutions.

For the second category, a positive a_{21} must be postulated to satisfy Harned's rule, a condition found only for a few aqueous systems. In the case of the Ag*-H* system where $\log \gamma^0_H/\gamma^*_{Ag} \cong \gamma^0_H/\gamma^0_{Ag}$, the result would indicate that a trace of Ag* is not affected by the presence of hydrogen ion. However, the possibility has not been ruled out that an ion exchanger contains a very small percentage of groups that have an extremely high affinity for Ag* and Cs* ions.

The a_{12} values were calculated and are shown in Table 14. One fact that seems to be common to all the systems is that a_{12} appears to be constant over a considerable range of concentration. Furthermore, the a_{12} values for Ag* and Cs* in the trace are approximately identical for every system investigated.

One other factor should be mentioned, namely, the extent of the influence of osmotic pressure on the selectivity. One explanation attributes the change in selectivity to $P\Delta V$ changes and assumes that the difference between the logs of the resin activity coefficients is constant at all molalities. If this thesis were acceptable, then, according to Eq. 3, $\log K_d = P\Delta V + c$ In all the systems studied, log of K_d vs. $P\Delta V$ was linear for only the Na-H system, and in that case the slope of the line was 35 times greater than the theoretical slope. In most cases, the magnitude of the $P\Delta V$ effects is only a few per cent. The greatest correction comes in the Cs*-HR system at 56% cross linking where the correction is about 10%.

TABLE 14 CALCULATED INTERACTION COEFFICIENTS FOR EXCHANGE SYSTEMS

	NORMALITY	a_{12}
Na*-Ag^+ Resin	0 97	0 206
	4 7	0 083
	8 07	0 0732
	11 36	0 064
	12 05	0 0645
	16 48	0 0554
Na*-Li^+ Resin	0 528	0 13
	1 26	0 075
	2 62	0 0542
	5 09	0 0443
	7 74	0 0428
	8 42	0 0448
	12 43	0 0413
Na*-H^+ Resin	1 06	0 00
	2 4	0 0022
	4 58	0 0275
	6 9	0 0377
	7 6	0 0405
	10 34	
	9	0 0491
Ag-Na^+ Resin	0 54	
	1 17	0 291
	2 68	0 208
	5 56	0 16
	8 16	0 16
	8 94	0 2
	12 92	0 173
Cs*-Na^+ Resin	0 54	
	1 17	0 274
	2 68	0 213
	5 56	0 162
	8 16	0 166
	8 94	0 205
	12 92	0 18
Cs*-H^+ Resin	1	0 28
	2 4	0 214
	4 58	0 183
	6 9	0 171
	7 6	0 178
	10 36	0 189
	9	0 178
Ag*-H^+ Resin	1	0 277
	2 4	0 17
	4 58	0 154
	6 9	0 1435
	10 36	0 189
	9	0 193
	14 55	0 170

Several conclusions can be drawn from the data (1) The log of selectivity of a trace substituent present in a pure form of another resin is a linear function of the log of the ratio of the activity coefficients of the pure salt forms. Thus, the measurement of selectivities at only two concentrations enables the calculation of the selectivity for all other resin concentrations, that is, cross linkings. (2) Systems that do not involve trace Ag* or Cs* appear to give results in conformity with those found for aqueous solutions. (3) Trace Ag* and Cs* behave radically differently in exchangers. In fact, the activity coefficient of trace Ag* in H^+ resin appears to be the same as that of pure silver resinate. (4) The $P\Delta V$ contributions in most ion exchange systems have a minor effect on the selectivity of the system and rarely exceed 10%.

ORGANIC CHEMISTRY OF SOLVENTS

W. H. Baldwin C. E. Higgins

Reaction Between Sodium Acetate and Tributyl Phosphate. Dibutyl phosphate was readily prepared by the de-esterification of an excess of tributyl phosphate with anhydrous sodium acetate.[3] Further de-esterification would lead to monobutyl phosphate and orthophosphoric acid, consequently, 7 mmoles of tributyl phosphate and 14 mmoles of anhydrous sodium acetate in 5 ml of butyl carbitol were heated together at 200°C. The product isolated was shown by electrometric titration to be dibutyl phosphate (equivalent weight found, 215, calculated, 210). No evidence was found for monobutyl phosphate

[3] W H Baldwin and C E Higgins, *Chem Quar Prog Rep Sept 30, 1952*, ORNL-1432 (in press)

The System NaOH-H_2O-Dibutyl Phosphate and Dibutyl Ether. The third phase formed[3] when 50 ml of 0.05 *M* dibutyl phosphate in di-*n*-butyl ether was equilibrated with 50 ml of 5.0 *M* NaOH at 25°C amounted to 1.1 ml with a specific gravity of 1.11 at 25°C.

Two preparations of the third phase were analyzed for water with acetic anhydride, the sodium hydroxide was titrated with standard acid, the dibutyl phosphate was determined by the P^{32} in the molecule, and the dibutyl ether was determined refractometrically after extraction into 1-methylnaphthalene. The composition is shown in Table 15.

TABLE 15. COMPOSITION OF THIRD PHASE

SAMPLE NO	WATER (%)	NaOH (%)	SODIUM DIBUTYL PHOSPHATE (%)	DIBUTYL ETHER (%)
1	45 7	5 32	39 2	
2	45 3	5 28	39 4	9 3

The dibutyl phosphate in the third phase accounted for 80% of the amount employed in the equilibration.

Distribution of Di-(2-ethylhexyl)-Phosphinic Acid, P^{32}. The P^{32}-labeled phosphinic acid[3] has been used for the study of its distribution between organic solvents (decane or carbon tetrachloride) and aqueous solutions that represent the leaching of low grade uranium ores Preliminary findings[4] show that there were no solubility losses in aqueous solutions greater than 10 mg/l, and they were usually lower than this. Work is continuing on a second preparation of the phosphinic acid with a higher specific activity.

[4] W H Baldwin to K B Brown, *Solubility and Distribution of Di(2 Ethyl Hexyl) Phosphinic Acid*, ORNL CF-52-11-57 (Nov 5, 1952)

CHEMICAL PHYSICS

RADIO-FREQUENCY SPECTROSCOPY

Quadrupole Spectroscopy (R. Livingston, H. Zeldes). A high-frequency spectrometer was developed and used successfully on several problems. The new instrument, in its present form, is a simple triode regenerative oscillator using a transmission line tuned circuit. It extends the frequency range to over 300 Mc, thus making it possible to find many bromine and iodine quadrupole resonances. New resonances include those of PBr_3, CH_2Br_2, CF_2Br_2, $CFBr_3$, C_2H_5Br, C_2H_5I, CH_2BrCH_2Br, and C_3H_7Br. In many cases, comparisons of couplings can be made with the corresponding chlorine compounds, and these comparisons are consistent with the previously given[1] interpretations. An effort is being made to find resonances in a larger number of related bromine and iodine compounds, and the data will be treated in more detail later.

Quadrupole resonances were seen in a compound of I^{129}, and this has made possible a precise determination of the nuclear quadrupole moment ratio of I^{129} to stable I^{127}. The resonances were seen in SnI_4. About 40 mg of iodine, in solution as iodide and having an estimated isotopic composition of 80% I^{129} and 20% I^{127}, was obtained from G. Hebert. The iodine was extracted into carbon disulfide, tin metal added, and the reaction allowed to go to completion by warming to about 50°C. The resulting solution of SnI_4 in carbon disulfide was evaporated to dryness and the product sealed into a capillary of about 2-mm diameter. It is estimated that 30 mg of iodine, 24 mg of I^{129} and 6 mg of I^{127}, was in the tube as SnI_4. Resonances for both isotopes were seen at 77 and 20°K. The measurements are summarized in Table 16.

(1) R Livingston, *J Chem Phys* (in press)

There are two nonequivalent iodine lattice positions in SnI_4, and lines were observed for each, these are indicated in Table 16 as A and B. The calculations are summarized in Table 17.

The field gradient tensor asymmetry parameter,

$$\eta = \frac{q_{xx} - q_{yy}}{q_{zz}},$$

is calculated from the I^{129} frequency measurements using the perturbation theory developed by Bersohn.[2] Within the accuracy of the frequency measurements, $\eta = 0$ for iodine in the type-B lattice position. This also follows from the crystal structure[3] since it has one-fourth of the iodine atoms in the unit cell on a three-fold symmetry axis, which requires $\eta = 0$. The type-B lines are all appropriately weaker than the corresponding type-A lines. Dehmelt[4] had previously studied normal SnI_4 at room temperature, and, from the I^{127} transitions, found η values of 0 and 0.009, the same as the above lower-temperature values evaluated from I^{129}. His values of $eq_{zz}Q^{127}$ are appropriately lower because of the temperature difference. The final nuclear quadrupole moment ratio is

$$\frac{Q(I^{129})}{Q(I^{127})} = 0.701213 \pm 0.000015 .$$

This value is much more accurate than the earlier microwave value[5] of 0.7353.

The Iodine Problem (R. Livingston, B. Benjamin). The chemical purification of the iodide starting material

(2) R Bersohn, *J Chem Phys* **20**, 1505 (1952)

(3) R W G Wyckoff, *Crystal Structures*, Interscience Publishers, Inc , New York, 1951

(4) H G Dehmelt, *Naturwissenschaften* **130**, 356 (1951)

(5) R Livingston, O R Gilliam, and W Gordy, *Phys Rev* **76**, 149 (1949)

TABLE 16. OBSERVED FREQUENCIES IN SnI_4

TEMPERATURE (°K)	ASSIGNMENT			FREQUENCY (Mc)
	Lattice Type	Isotope	Transition	
77	A	I^{129}	3/2 → 5/2	138 6783
77	A	I^{129}	5/2 → 7/2	208 0254
77	A	I^{127}	1/2 → 3/2	207 6855
77	B	I^{129}	3/2 → 5/2	139 6604
77	B	I^{129}	5/2 → 7/2	209 4924
77	B	I^{127}	1/2 → 3/2	209.1324
20	A	I^{129}	3/2 → 5/2	139 2052
20	A	I^{129}	5/2 → 7/2	208 8157
20	A	I^{127}	1/2 → 3/2	208 4702
20	B	I^{129}	3/2 → 5/2	140 2356
20	B	I^{129}	5/2 → 7/2	210 3556
20	B	I^{127}	1/2 → 5/2	209 9923

TABLE 17. IODINE RESONANCES IN SnI_4

TEMPERATURE (°K)	LATTICE TYPE	η	$eq_{zz}Q^{129}$	$eq_{zz}Q^{127}$	$\frac{Q^{129}}{Q^{127}}$
77	A	0.00905	970.79	1384 45	0.701214
77	B	0	977.63	1394.22	0.701202
20	A	0.00900	974 48	1389.68	0.701228
20	B	0	981.65	1399.95	0 701207

has continued to be the main problem in synthesizing CH_3I^{131} for microwave studies. A solvent-extraction method, using cyclohexane as the extracting liquid for iodine, was tested but did not give a satisfactory product. Typical chemical yields for iodine were roughly 70%, but the iodine was not in a form that would readily allow CH_3I to be synthesized. Rather than spend time improving the extraction method, a much more direct approach has been devised. The iodine, as received in solution, is plated onto a silver electrode and then stripped into an appropriate solvent. Tracer-level tests show that the iodine can be plated essentially quantitatively from solutions containing large amounts of foreign salts (sodium sulfate and sulfite). The iodine can be electrolytically stripped into extremely dilute caustic or sodium sulfite, resulting in a product that weighed roughly 50 μg with a yield of 70 to 80%. The electrolytic stripping,

however, appears to oxidize the iodine to higher valence states, and trouble has been experienced in reducing it without adding greatly to the salt content of the sample. An alternate stripping operation that shows great promise is to place the silver electrode in a dilute H_2S solution containing a trace of caustic (about 30 μg). The iodine goes into solution quantitatively and very rapidly. Evaporating this solution to dryness removes the excess H_2S and gives a very-low-weight product, and preliminary tests indicate that it will be suitable for the needs of this work.

NEUTRON DIFFRACTION STUDIES

H. A. Levy S. W. Peterson

Errata in Previous Quarterly Reports. The following errors were introduced in earlier quarterly reports during editing.

In ORNL-1285 Page 59, column 2, line 8 should read "The value u = 0 53 was completely unsatisfactory, indicating that the displacement of Br is toward the approaching hydrogens". The direction of the displacement follows from the experimental determination of the parameter u, the reverse relation was wrongly implied in the report. Page 60, column 1, Table 21. The asterisk in the heading of the third column (indicating incompletely resolved maxima) is misplaced, and brackets grouping the entries were omitted. The correct arrangement shows that the first six values are derived from completely resolved maxima, and that following two zero values there are a group of three and a group of five entries derived from incompletely resolved maxima.

In ORNL-1344 Page 23, column 2. Errors appear in three sentences, which should read as follows. "A satisfactory balance of total aluminum indicated that the Al P was stoichiometric. The phosphide analysis was taken as establishing the percentage of Al P in the preparations. ..... Samples of the two preparations were ground and packed into thin-walled aluminum cylinders in a gloved box containing dry nitrogen".

Neutron Diffraction Studies on Scandium Orthovanadate and Scandium Oxide. The Neutron Scattering Properties of Scandium. (with W. O. Milligan and L. W. Vernon, Rice Institute, Houston, Texas). Examination of $ScVO_4$ and Sc_2O_3 by neutron diffraction has confirmed that these crystals possess previously assigned structures of the zircon and thallic oxide types, respectively. The following values for the neutron scattering properties of scandium were derived coherent scattering amplitude, f, (1 18 ± 0 05) × 10^{-12} cm., positive phase, coherent scattering cross-section, σ_{coh}, 17 5 ± 1 5 barns, mean total scattering cross-section, $\bar{\sigma}_s$, 24 ± 2 barns. The thermal neutron capture cross-section of Sc was measured by H. S. Pomerance (Physics Division, ORNL) during this work and the value 24 barns was obtained. A much lower value reported earlier is believed to be in error.

A detailed account of this work has been accepted for publication in the *Journal of Physical Chemistry* and is scheduled to appear in May or June, 1953.

The Structure of PdO (with J. Waser, Rice Institute, Houston, Texas) On the basis of neutron and x-ray diffraction data, the structure of PdO was confirmed to be based on the space-group D_{4h}^9 – $P4/mmc$ with two PdO per unit cell. The cell dimensions are a = 3 03 ± 0 01 Å, c = 5 33 ± 0 02 Å and the atomic positions are 2 Pd at 000, 1/2 1/2 1/2 and 2 O at 1/2 0 1/4, 1/2 0 3/4.

A detailed account has been submitted for publication to *Acta Crystallographica*

Work in Progress. Crystal structure studies are underway on the following materials KH_2PO_4, N-acetyl glycine (with V. Schomaker), P_4S_3 (with J. Waser), oxalic acid dihydrate (with B. S. Garrett), and urea. Measurement of the scattering amplitudes of Tl and its isotopes is also in progress.

CHEMISTRY OF THE SOLID STATE

MOLTEN METAL-METAL HALIDE SYSTEMS

M. A. Bredig H. R. Bronstein
J. W. Johnson W. T Smith[1]

Metal-Metal Chloride Systems. Experimental difficulties which do not seem to exist in the ternary fluoride systems described elsewhere are encountered in the chloride systems It appears that they may be connected with surface tension phenomena, that is, formation of emulsions of metals in the molten salts, which may prevent proper mechanical separation of the liquid metal and chloride phases after equilibration. The difficulties may also result from the much greater temperature dependence of the solubility of the metal in the salt

In two experiments in the sodium-sodium chloride system, the check-valve type of capsule that was successfully used with the fluorides[2] was employed Although equilibration over a period of 5 hr at 830 and 870°C was by diffusion rather than by mechanical stirring, the values of 11.3 mole % sodium at 830°C and 16.9 mole % at 870°C are not smaller, as expected, but far greater than the previous values[3] obtained with some mechanical stirring (3 and 7 mole %, respectively). One possible, though not entirely satisfactory explanation, may be the formation of an emulsion of metal in the molten salt after partial dissolution of the liquid sodium which, in this last experiment, must be assumed to have been rather finely dispersed throughout the pulverized solid chloride before the salt reached the temperature of its melting point

Another possible explanation is the assumption that the older values are too low because of rapid rejection of dissolved sodium metal into the vapor phase on cooling

Another approach to the determination of the solubility, particularly at the eutectic point of composition and temperature, was attempted by thermal analysis (cooling curves). Type 304 stainless steel capsules, 3/4 in OD and 6 in. long, were used, to which chromel-alumel thermocouples were welded. The tube contained 20 g of sodium chloride or potassium chloride and 7 g of sodium or 5.5 g of potassium metal, respectively, that is a considerable excess of metal over the amount soluble A tube containing only the salt, with a thermocouple also welded to it, was mounted alongside with each test tube and served as a reference. Eight different cooling curves, two with each of two different tubes for each of the two systems, starting from 30 deg above the melting point of the pure salts, gave rather well reproducible melting-point depressions of 6 5 ± 0 5°C for the Na-NaCl eutectic and 17 5 ± 0.5°C for the K-KCl system. When applied to the common formula

$$N_2 = \text{mole fraction of solute} = \frac{L(T_0 - T)}{RT_0 T} ,$$

(1) Consultant from the University of Tennessee

(2) M A Bredig, J W Johnson, H R Bronstein, and W T Smith, *Chem Quar Prog Rep Sept 30, 1952*, ORNL-1432 (in press)

(3) M A Bredig, J W Johnson, H R Bronstein, and W T Smith, *Chem Quar Prog Rep. June 30, 1952*, ORNL-1344, p 28

in which L is the heat of fusion of the pure solvent (salt), T_0 its melting point, and T the minimum eutectic temperature of the binary system, eutectic concentrations of 2.0 mole % Na and 5.0 mole % K, respectively, were obtained, assuming applicability of the Clausius-Clapeyron and Raoult laws.

The figure of 2 mole % for sodium in sodium chloride is in fair agreement with the solubility measurements reported previously.[4] Chemical analysis of the samples from the thermal analysis gave 2.7 and 3.3 mole %. One possible explanation for the somewhat higher values may be that they represent the solubility of sodium, not at the eutectic, but at the maximum temperature to which these samples were exposed, namely, 835°C, and that mechanical separation of the liquid sodium precipitating on cooling to the eutectic temperature did not take place. A similar explanation might hold for the corresponding discrepancy in the potassium-potassium chloride system where two of the analytical values of 6, 10, and 11 mole % for various sections of the samples are also larger, by a similar factor, than the thermodynamically calculated concentrations.

As long as these experimental uncertainties remain, it is not possible to attribute significance to the further possibility that the analytical values from the cooling curve samples are correct and that the low melting point depressions as observed are actually caused by low activity coefficients of the metals in the salt phase.

Potassium Metal in Ternary Alkali Fluoride Eutectic. The solubility of potassium metal in the ternary salt eutectic of lithium, sodium, and potassium fluorides was determined at various temperatures using the ball-check-valve capsule described in the previous quarterly report The results were as follows

TEMPERATURE (°C)	K (mole %)
544	3.8
668	3.8
672	3.8
686	3.5
1040	3.9

It appears that the solubility of potassium metal in the ternary alkali fluoride eutectic is not temperature dependent. However, the system is complex, with reduction equilibria of the type K + NaF = Na + KF.

Analysis of the liquid-metal alloy formed in the equilibration experiments was made in order to determine the extent of the reduction reaction at the various temperatures. The results are as follows

TEMPERATURE (°C)	MOLE PER CENT Of K	Of Na
544	87.7	12.3
668	79.5	20.5
920	85.1	14.9
	86.4	13.6

The result at the intermediate temperature of 668 °C differs from both the lower and the higher temperature tests. It will be checked with analyses of the runs at 672 and 686 °C. Disregarding the result at 668 °C, it appears that the reduction equilibrium, like the metal solubility, is practically temperature-independent. This is in agreement with the results of a study by Rink[5] and with thermodynamic data which, in addition, indicate that the reduction of lithium fluoride by potassium must be a minor reaction.

(4) *Ibid*, p 28, Fig 11

(5) E Rink, *Ann Chim (Paris)* **18**, 395-531 (1932)

STRUCTURE OF MOLTEN ALKALI METAL HALIDES

M. A. Bredig J. W. Johnson
W. T. Smith[1]

It was pointed out in an earlier report[6] that the theory by Harker and Cubicciotti of the solutions of metals in the melts of their halides required a modification in order to explain the high solubility found in alkali metal halide systems. Structural changes in the melt, that is, in coordination of the ions, were suggested as making "octahedral holes" available to solute atoms or molecules. It was thought that such changes ought to be accompanied and indicated by volume changes. Thus, the change in solid cesium chloride from the eightfold coordination of the simple, cubic, low-temperature form to the sixfold coordination of the face-centered, cubic, sodium chloride, high-temperature form, above 469°C, is accompanied by a volume increase of approximately 16% and is explained by simple geometrical considerations of the packing of spheres.

The results of a literature survey on volume changes on melting of the alkali metal halides are given in Table 18 and in Fig. 9. The most striking feature is the sudden increase in the volume change on melting for cesium bromide and iodide, when compared with the trends in these curves. The

$$\frac{V_1 - V_c}{V_c} 100$$

values are 26.4 and 25.6%, respectively, whereas for cesium fluoride and chloride they are 16.4 and 12.3%, respectively. If the transition in solid cesium chloride were disregarded and the

$$\frac{V_1 - V_c}{V_c} 100$$

value were obtained by a comparison of the volume of the liquid with the volume of the low temperature, simple, cubic phase, extrapolated to the melting temperature, this value would be 28.1%. Therefore it seems necessary to conclude that a structural transition similar to the one responsible for the change of 16% in the transition of solid cesium chloride has occurred in the bromide and iodide. X-ray measurements by Wagner and Tippert,[7] have shown that no such transition occurs up to temperatures 50°C below the melting points. Obviously, such a transition will have to occur either in the solid within the small temperature range below the melting point as yet not investigated, or on melting. X-ray diffraction measurements in the region directly below the melting point are planned in order to decide this question. The face-centered cubic structure has actually been observed in thin films of these compounds deposited on suitable supports from the vapor phase.[8] There remains, however, an appreciable chance that this face-centered cubic structure is metastable in the entire temperature range of the solid and that the structural change to lower coordination actually does take place on melting rather than in the solid.

(6) M A Bredig, J W Johnson, H R Bronstein, and W T Smith, *Chem Quar Prog Rep June 30, 1952*, ORNL-1344, p 27

(7) G Wagner and L Lippert, *Z physik Chem* **B31**, 263-74 (1936)

(8) L G Schulz, *J Chem Phys* **18**, 996 (1950)

TABLE 18. EXISTING DATA ON PERCENTAGE VOLUME CHANGES ON MELTING

METAL	FLUORIDE	CHLORIDE	BROMIDE	IODIDE
Lithium	30 9 (34 4)	27 8	26.1	
Sodium	29 6	27 9	25 6	21.8
Potassium	20 6	19.9	19 3	17 0
Rubidium	20.2*	13 3	14 8	14 6
Cesium	16 4*	12 3	26 4**	25 6**

*Estimated

**CsBr and CsI are in simple cubic structure, according to existing data.

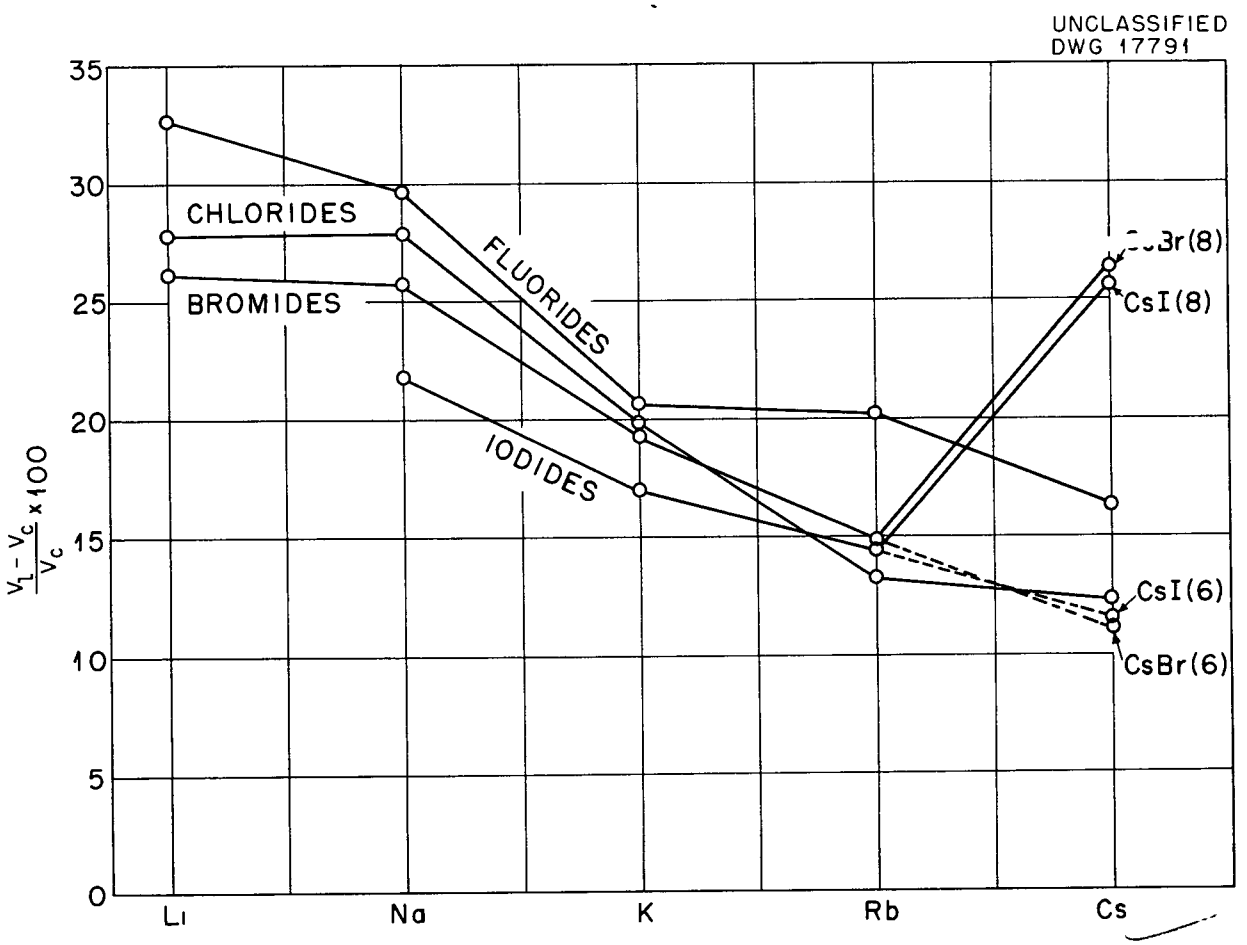

Fig. 9. Molecular Volume Change on Melting of Alkali Metal Halides.

Recent x-ray diffraction measurements in liquid aluminum chloride and indium iodide by Harris, Wood, and Ritter[9] have directly demonstrated for the first time in a chemical compound a change on melting from sixfold to fourfold and statistically 4.7-fold coordinations, respectively. These structural changes could be anticipated on the basis of the large volume changes on melting of the order of 45 to 100%, which were previously known for these compounds. Similar coordination changes have also been determined by diffraction methods for various elements such as lead, bismuth, and argon. In pursuance of the idea of a connection between volume change on melting and structure of the melt, it may further be suggested here that in the absence of structural discontinuities in the solids below the melting points, the comparatively large volume changes on melting in the lithium and most of the sodium metal halides (see Table 18 and Fig. 9) indicate considerable, if only partial, changes in coordination in their melts from those in their crystals. In particular, it is thought that coordinations involving the five nearest neighbors may occur much more frequently in liquids than in solids where the requirements of translatory repetition of a structural pattern effectively rule against this number. It should be pointed out,

(9) R L Harris, R E Wood, and H L Ritter, *J Am Chem Soc* **73**, 3151 (1951), R E Wood and H L Ritter, *J Am Chem Soc* **74**, 1760 (1952)

however, that a confirmation of this view by diffraction measurements in the liquid, difficult as they are, is needed. Indeed, while a large change in volume on melting is a definite indication of structural change, the reverse is not true, that is, it is impossible to postulate on the basis of absence of a large volume change on melting, the absence of such structural changes. Thus, in the case of lithium iodide with its small cations embedded in a lattice of large anions, transfer of lithium ions from sixfold to five- or fourfold coordination, or partial molecule formation, might not produce a considerable volume change. In view of the statistical nature of the ionic configurations in liquid salts, different from the conditions in phase transformations in solids, it must be kept in mind that the resulting volume change is a product of the volume change accompanying the change in coordination of one individual ion and a statistical weight factor determining the frequency, or number, or concentration of such lower coordinations. Even though this factor may be large, the change accompanying the individual process may be small and vice versa. The former case might be represented by the lithium halides (excepting the fluoride), in which the volume change is seen to decrease with increasing anion radius even though the probability of fourfold coordination may be assumed to increase for this very reason. Similarly, the coordination in molten potassium fluoride and sodium iodide may be different in spite of the similarity of the volume change on melting A smaller coordination number is naturally expected for sodium iodide with its large highly polarizable anion, and much smaller cation-to-anion radius ratio (0 45). In potassium fluoride with its large radius ratio of 1, the individual coordination change would produce a large volume change, but its frequency must be thought to be small because of unfavorable coulomb energy economy.

When applied to the theory of the solution of metals in their halides, these considerations may lead to an admittedly very tentative explanation of the temperature dependence of the solubility of sodium and potassium metals in their molten chlorides and of the temperature independence of the solubility of potassium metal in the lithium, sodium, and potassium fluoride eutectic.

The solubility of a volatile liquid or gas in another liquid, a relatively high-boiling solvent such as a salt phase, normally decreases rapidly with temperature because of a negative ΔH The vapor pressure of liquid sodium and potassium metals rapidly increases. The result of these two opposing influences might similarly, as in the cases of the alkaline earth metal halide systems, be a small change of solubility with temperature. While unbalance alone of the two opposing influences as a function of temperature might explain an increase of solubility with temperature, it seems also possible that a third factor might produce the unbalance, namely, structural change in the solvent. Thus, it may be a gradual increase in the frequency factor for lower than sixfold coordination around the cations in molten sodium and potassium chlorides with increasing temperature, that produces increasing opportunities for solute atoms or molecules to take their places in the sixfold, or higher, coordination within the anion "lattice."

On the other hand, in the ternary fluoride eutectic containing 45 mole % of lithium fluoride, a large part of the lithium ions may, as indicated in the behavior of the pure lithium fluoride, on melting, even near the ternary melting point, have shifted to lower than sixfold coordination, vacating the maximum number of "octahedral holes" that can be vacated in

this liquid in the whole temperature range under investigation (540 to 1040°C). No change in solubility with temperature should then be expected, in agreement with the actual observations.

CRYSTAL STRUCTURE OF SODIUM-POTASSIUM SULFATE

R. D. Ellison M. A. Bredig

A check of the accuracy of the structure reported by Gossner[10] for glaserite, approximate composition $K_3Na(SO_4)_2$, is being made. As mentioned in a previous quarterly report,[11] a Patterson projection of the interatomic distances on the basal plane of the hexagonal unit cell suggests that the sodium and potassium atoms are in positions with x and y coordinates (0,0), (0,0), (2/3, 1/3), (1/3, 2/3). The poor resolution characteristic of such projections prevents the direct determination of which position is occupied by the sodium atoms and which is occupied by the potassium atoms. The inherent multiplicities in the projection allow the determination of the position of the sulfur atoms, but suggest several orientations as equally likely for the sulfate tetrahedra. Calculations of the structure factors for the $hk0$ reflections considering the tetrahedra in each of the suggested orientations and the sodium atom in each of the suggested positions leads to the tentative conclusion different from Gossner's structure proposal, that the sodium and potassium atoms are not entirely ordered, but that the sodium atom is equally likely to be found in any of the four positions mentioned as possible for it. The z components of all atomic positions and the exact extent of the disorder remain to be found.

[10] B Gossner, *Neues Jahrb Mineral* **57A**, 89-116 (1928)

[11] R D Ellison and M A Bredig, *Chem Quar Prog Rep March 31, 1952*, ORNL-1285, p 76

X-RAY DIFFRACTION

R. D. Ellison M. A. Bredig

Assistance was given to various groups, particularly in connection with the HRP, by examination and identification of numerous solid specimens.

RADIATION CHEMISTRY

NUCLEATION OF BUBBLES BY FISSION RECOILS, FAST NEUTRONS, AND X RAYS

J. A. Ghormley

In a previous report,[1] data were given for bubble nucleation by fission recoils in a limited temperature range. Similar experiments have now been conducted at higher temperatures by heating the solution in the upper part of one of the ampoules (No. 4) to give the desired total pressure. Data obtained at higher temperatures, as well as those reported previously, are shown in Fig. 10. The line that has been drawn for ΔT corresponding with ΔP = 110 cm Hg fits the data within experimental error. However, the line has no theoretical significance because the degree of superheating necessary before fission can nucleate bubbles at any particular total pressure is a function not only of vapor pressure but also of vapor density, heat of vaporization, and surface tension, all of which vary with temperature. At the higher temperatures, an estimation of the rate of vapor-phase growth was possible

[1] J A Ghormley, C J Hochanadel, and A C Stewart, *Chem Quar Prog Rep Sept 30, 1952*, ORNL-1432 (in press)

from visual observations. With the normal boiling temperature of 234°C, the vapor phase nucleated by fission was estimated to expand at a rate of 3 cm/sec in the capillary (0.6 mm ID, 2.5 mm OD).

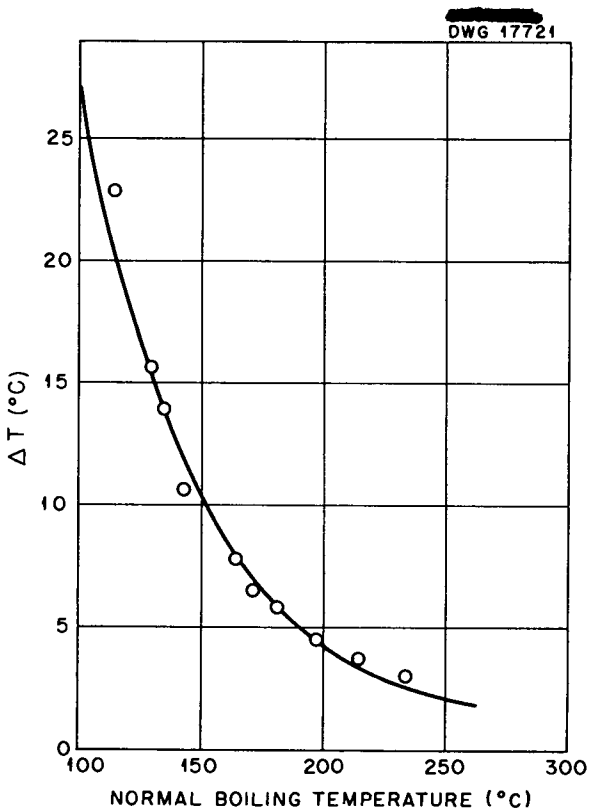

Fig. 10. Maximum Superheat Possible in UO_2SO_4 Solutions in Which Fission Is Occurring. Line drawn is for ΔT corresponding to ΔP = 110 cm of Hg.

A calculation made from the observed ΔT, by assuming a spherical nucleus, shows that at 200°C the nucleus diameter is about 10^{-4} cm and the energy required to evaporate sufficient water to form a bubble of this size is 60 Mev (surface energy is negligible). The length of the fission track, in which about 160-Mev energy is available, is about 4×10^{-3} cm or about 40 times the calculated diameter of a bubble of critical size. The maximum density of energy release along the fission track is only about 8 Mev in 10^{-4} cm, considerably less than the 60 Mev needed to form a bubble of this diameter. It appears that the conditions under which fission recoils can nucleate bubbles cannot be predicted by simple calculations based on a spherical nucleus.

Bubble nucleation by fast neutrons has also been observed in superheated water. In a capillary U tube open to the atmosphere, with the top at room temperature, water was maintained at 208°C for 30 min or more before a fast-neutron source was brought near the ampoule, producing nucleation in 17, 20, and 75 sec in three successive observations.

Further observations have been made on bubble nucleation in ether by x rays and fast neutrons. The temperature of the upper part of an ampoule of ether was controlled to give a normal boiling temperature of 121.6°C, and the lower capillary end of the ampoule was slowly heated in a glycerin bath. At temperatures ranging from 133 to 137°C and averaging 134.8°C (eight observations) in the absence of radiation, nucleation occurred at the tip of the ampoule, and the meniscus rose in the capillary (0.7 mm ID, 2 0 mm OD) at a velocity of about 1 cm/sec. During exposure to 50-kv x rays, nucleation was observed at different points in the superheated ether (leaving varying amounts of liquid in the capillary) at temperatures from 132.3 to 135°C and averaging 133.2°C (four observations). With a fast-neutron source near the ampoule, nucleation occurred reproducibly at 125.0°C (five observations). These data show that recoils from fast neutrons are much more effective in producing bubble nuclei than are the photoelectrons produced by 50-kv x rays.

SOME FUNDAMENTAL ASPECTS OF BUBBLE GROWTH

H. M. Rosenstock

The following approximate equation has been derived for the rate of growth of a vapor bubble in a superheated liquid

$$\frac{dN}{dt} = \frac{2\sigma\left(\frac{1}{r^*} - \frac{1}{r}\right)\alpha}{\sqrt{2\pi mkT}} \text{ molecules sec}^{-1}\text{ cm}^{-2} \text{ vaporizing into the bubble,}$$

where

σ = surface tension of the liquid,

r = instantaneous radius of the growing bubble,

r^* = radius of a bubble in thermodynamic equilibrium with the liquid exerting vapor pressure P_a and subjected to an external pressure P_e, according to the equation $P_a - P_e = 2\sigma/r^*$,[2]

α = condensation coefficient, that fraction of vapor molecules bombarding a liquid that condenses,[3]

T = temperature of the liquid at the bubble boundary,

k = Boltzmann constant.

The equation was derived in order to discuss the upper limits on the rate of bubble growth that are demanded by the kinetic theory. The time-varying temperature gradient behind the bubble boundary has been completely neglected. The equation has been applied to the experimentally measured growth rates of water vapor bubbles extrapolated to zero time with the following results for water at 1 atm pressure and superheated 1°C.

Growth rate, molecules sec^{-1} cm^{-2}	
Calculated	3.5×10^{12}
Extrapolated experimental[4]	$\sim 3.0 \times 10^{12}$

This startling agreement is not to be taken too literally, in view of the experimental difficulties attending accurate temperature measurements in a boiling system and some undefined complications arising from boundary-layer effects. Further refinements of the equation are under way.

The reasonable agreement obtained above has opened up an interesting possibility regarding the mechanisms that may cause relaxation phenomena in boiling liquids. For example, a liquid boiling under steady-state conditions has a well-defined bulk-density distribution. This bulk density is a function of the power input. A discontinuous power surge is accompanied by a measurable relaxation time in the density change. A possible mechanism for this relaxation phenomenon, based on the high initial growth rate of vapor bubbles, is under investigation.

RADIATION CHEMISTRY OF ICE

A. C. Stewart J. A. Ghormley

In order to permit study of initial yields for hydrogen production in ice prepared from oxygen saturated water, a technique has been developed for the determination of small concentrations of hydrogen in oxygen gas. One gram of coconut charcoal, previously outgassed at about 500°C and then cooled to −78°C, has been found to remove all the 0.2 cc of oxygen from an oxygen-hydrogen mixture without removing any appreciable fraction of the 0.002 cc of hydrogen in the mixture.

Hydrogen and hydrogen peroxide concentrations observed after melting ice that was prepared by rapid freezing of oxygen-saturated water and irradiated at various temperatures are shown in Fig. 11. Hydrogen peroxide is found in excess over the hydrogen. This is thought to indicate that some of the hydrogen peroxide is formed from the oxygen present. The hydrogen and

(2) J Frenkel, *Kinetic Theory of Liquids*, p 371, Clarendon Press, Oxford, 1946

(3) G Wyllie, *Proc Roy Soc (London)* **A197**, 383 (1949)

(4) W Fritz and W Ende, *Physik Z* **37**, 391 (1936)

an approximately equivalent amount of hydrogen peroxide are believed to be formed from ice in regions of dense energy release, an interpretation analogous to that for liquid water.

It has been shown[5] that radiation-induced reaction occurs between hydrogen and hydrogen peroxide at -78°C and presumably also at somewhat lower temperatures, but such reaction occurs with a much lower yield, if at all, at -196°C. These conclusions were based on the results obtained from samples given relatively large doses, and it is possible that during short irradiation at low temperatures an appreciable fraction of the energy is stored in the form of trapped charges or frozen-in free radicals that may react with the stable H_2 and H_2O_2 molecules when the irradiated ice is warmed. Thus, the products found, after melting, in samples irradiated for short periods at -196°C or lower temperatures may not represent the concentrations of these stable products formed during irradiation.

(5) A C Stewart and J A Ghormley, *Chem Quar Prog Rep March 31, 1952*, ORNL-1285, p 65

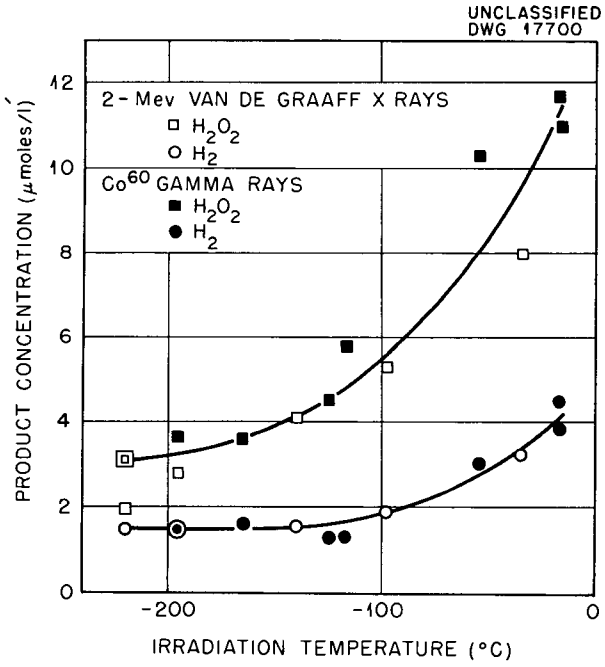

Fig. 11. Hydrogen and Hydrogen Peroxide Found After Melting Irradiated Ice. Ice was prepared by rapid freezing of oxygen-saturated water and was irradiated at 1.9×10^{17} w/g/min with 2-Mev Van de Graaff x rays or Co^{60} gamma rays.

URANYL-SENSITIZED REACTION OF HYDROGEN AND OXYGEN

T. J. Sworski

The reaction between hydrogen and oxygen is catalyzed[6] by uranyl sulfate at elevated temperatures. As shown in Fig. 12, this reaction is also photosensitized by uranyl sulfate. The photolyses were carried out with a low-pressure mercury lamp (Hanovia SC 2537) at constant light intensity in the same sealed silica ampoules that had been previously employed in a study of gas production in water by

(6) H F McDuffie *et al*, *Chem Quar Prog Rep Sept 30, 1951*, ORNL-1153, p 93

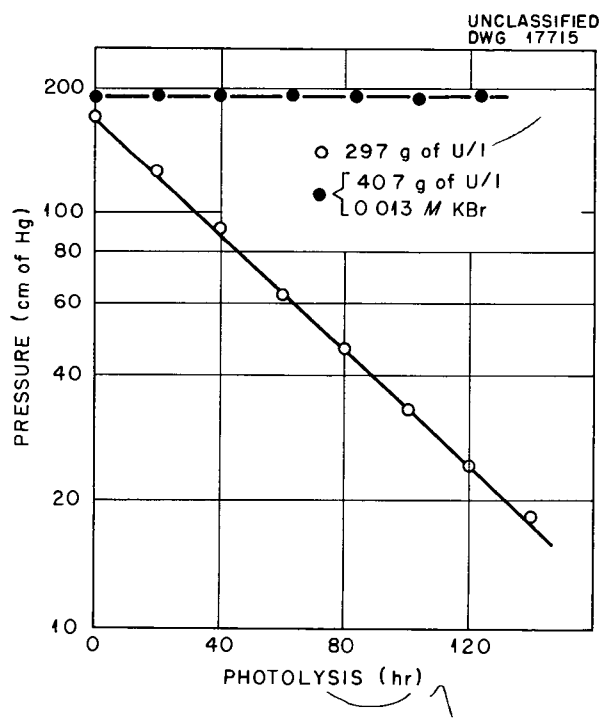

Fig. 12. Reaction of Hydrogen and Oxygen Photosensitized by Uranyl Sulfate.

fission recoils.[7] The reaction is first order in total gas pressure for those ampoules that contain hydrogen and oxygen in stoichiometric amounts. At present, it is assumed that the photosensitized reaction is first order in hydrogen concentration, just as in the thermal reaction. Potassium bromide inhibits the photosensitized reaction.

The yield of hydrogen in the decomposition of water by fission recoils is dependent upon the uranium concentration.[7] Replot of the data, as given in Fig. 13, shows that the yield of hydrogen is proportional to the square root of the uranium concentration for solutions in which at least 99.5% of the absorbed energy is fission energy. Straight lines that have a common intercept at $G_{H_2} = 1.83$ fit the data for UO_2F_2, UO_2SO_4, and $U(SO_4)_2$ solutions. This intercept value is interpreted as the hydrogen yield for the decomposition of water by fission recoils. The differences in slope of the three lines are an effect of pH.

(7) J W Boyle et al, *Reactor Science and Technology* 3, No 1, April 1953 (in press)

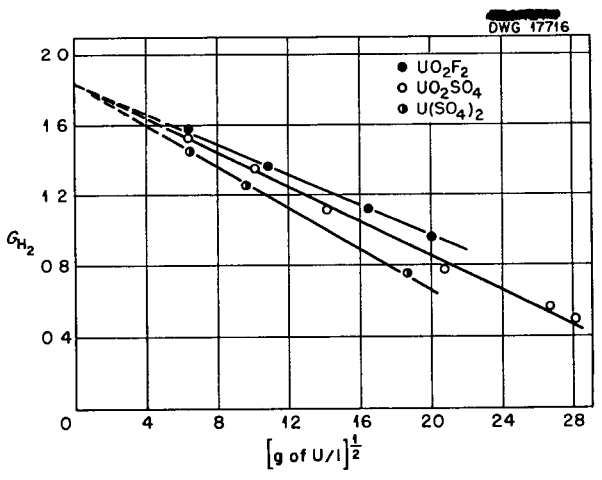

Fig. 13. Initial Yields of Hydrogen From Pile-Irradiated Solutions. Fission energy/total energy >99.5%.

Because an effect of pH is superimposed upon that of uranium concentration, it would be a mistake to read too much significance into the linearity of the square root relationship. Nevertheless, the uranium effect is consistent with at least two alternative forms of mechanism (1) hydrogen (probably not in its ultimate molecular form) reacts with oxygen to give water in a zero-order process catalyzed by UO_2^{++} (or U^{4+}) ion, (2) the UO_2^{++} (or U^{4+}) ion removes energy from the system and makes it unavailable for hydrogen production.

EFFECTS OF COBALT-60 GAMMA RADIATION ON AQUEOUS BENZENE SOLUTIONS

T. J. Sworski

The initial yield of hydrogen peroxide in oxygen-saturated aqueous benzene solutions increases with increasing acid concentration.[8] Another effect of acid concentration is shown in Fig. 14. The formation of hydrogen peroxide

(8) T J Sworski, *Chem Quar Prog Rep June 30, 1952*, ORNL-1344, p 30

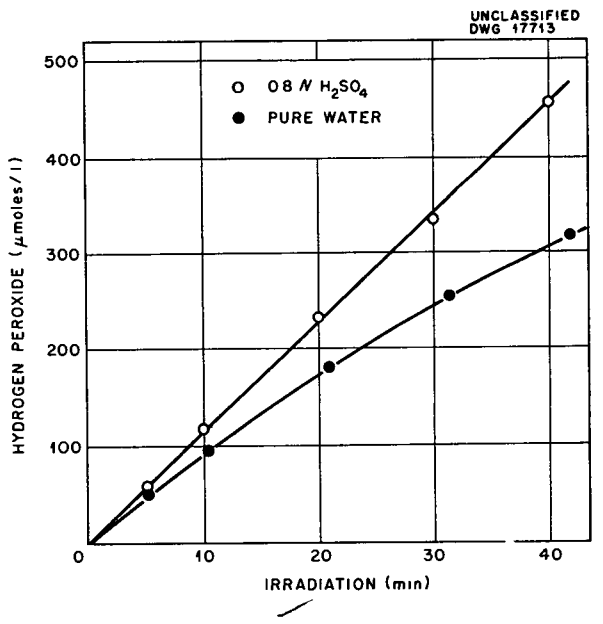

Fig. 14. Hydrogen Peroxide Formation in Oxygen-Saturated Aqueous Benzene Solutions.

in oxygen-saturated 0.8*N* sulfuric acid with benzene present is linear with time of irradiation, whereas in unbuffered benzene solutions, the rate of formation decreases with increasing time of irradiation. This effect of acid has been reported for hydrogen peroxide formation in oxygen-saturated pure water.[9]

Phenol cannot be determined in highly acid solutions in the presence of hydrogen peroxide by the alkaline method[10] because the alkaline-induced change in optical density of the alkaline phenol solution takes place too rapidly to be observed. The method of Carr[11] is a quantitative measure of phenol formation in oxygen-saturated aqueous benzene solutions as is shown in Fig. 15 by comparison with the alkaline method. The phenol yield, as determined by the method of Carr, is dependent upon acid concentration in the same manner as the hydrogen peroxide yield, that is, a higher yield results at high acid concentration. This is in agreement with the results of Weiss.[12]

(9) M Ebert and J W Boag, paper presented before the Faraday Society, Leeds, England, April 1952, T J Sworski, *J Chem Phys* **21** (to be published)

(10) T J Sworski, *J Chem Phys* **20**, 1817 (1952)

(11) M E J Carr, *Nature* **167**, 363 (1951)

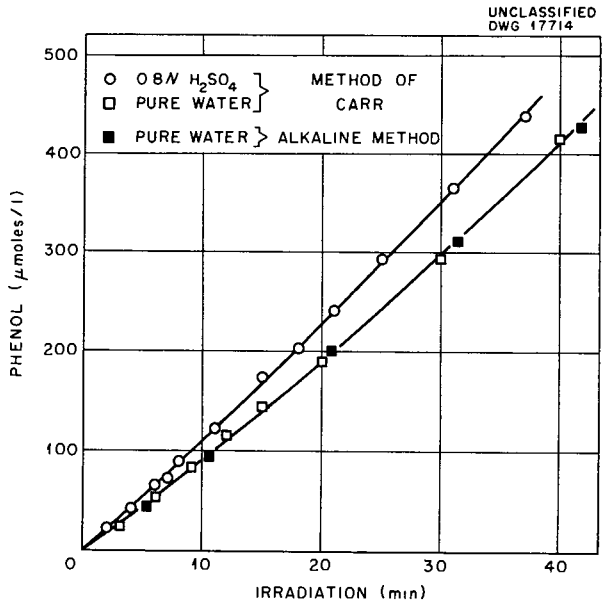

Fig. 15. Phenol Formation in Oxygen-Saturated Aqueous Benzene Solutions.

EFFECTS OF HYDROGEN AND OXYGEN ON THE RADIOLYSIS AND PHOTOLYSIS OF DILUTE AQUEOUS HYDROGEN PEROXIDE SOLUTIONS

C. Hochanadel

The effect of dissolved hydrogen on the gamma-ray-induced decomposition of dilute hydrogen peroxide solutions has been reported previously.[13] The results were explained in terms of reactions involving the free radicals H and OH, which are generally considered to be formed in the radiolysis of water according to the reaction

$$H_2O \rightsquigarrow H + OH \ . \qquad (1)$$

The effect of dissolved hydrogen presumably occurs through the reaction

$$H_2 + OH \longrightarrow H_2O + H \ . \qquad (2)$$

According to Urey, Dawsey, and Rice,[14] the primary process occurring on absorption of ultraviolet light (λ <3100 Å) by hydrogen peroxide is represented by

$$H_2O_2 \xrightarrow{h\nu} 2OH \ . \qquad (3)$$

Dissolved hydrogen would therefore be expected to exert some influence on the photolysis of dilute hydrogen peroxide solutions, and results are reported that show this effect.

There is considerable evidence to indicate that the reaction

$$H + O_2 \longrightarrow HO_2 \qquad (4)$$

occurs very readily. Therefore dissolved oxygen should influence any reaction in which hydrogen atoms are intermediates, such as the radiolysis of hydrogen peroxide with or without added hydrogen or the photolysis of

(12) G Stein and J Weiss, *J Chem Soc*, 3245 (1949)

(13) C J Hochanadel, *J Phys Chem* **56**, 587 (1952)

(14) H C Urey, L H Dawsey, and F O Rice, *J Am Chem Soc* **51**, 1374 (1929)

hydrogen peroxide with added hydrogen. The role of dissolved oxygen in the mechanism for the radiolysis of hydrogen peroxide has been neglected or minimized by several authors.[15,16] Results obtained here by sweeping the oxygen out of solution with helium during irradiation show that oxygen has a pronounced effect on peroxide decomposition in these systems.

Effect of Hydrogen on the Photolysis of Hydrogen Peroxide Solutions. Hydrogen peroxide solutions were photolyzed by means of the full, unfiltered output of a G-E, 4-watt, germicidal lamp that radiates most of its energy at 2537 Å. The lamp output was continuously monitored by an RCA 935 photocell, the output of which was measured with a low-drift electrometer and recorded. Solutions were made up with 90% inhibitor-free hydrogen peroxide and pure water. Irradiations were made in a clear-silica, cylindrical vessel that contained about 60 ml of solution. Samples were removed periodically during irradiation and analyzed by the triiodide optical-absorption method. Solutions with initial peroxide concentrations of 70, 230, 415, 600, and 1850 μmoles/l were photolyzed either with helium sweeping or with hydrogen sweeping through the solution during irradiation. Also, solutions that were initially saturated with air or with hydrogen were photolyzed with no gas sweeping during irradiation.

The rate of decomposition of peroxide was the same for air-saturated or helium-swept solutions and was proportional to the peroxide concentration. As shown by Lea,[17] this relationship obtains at low peroxide concentrations and high light intensities, where the decomposition is no longer a chain reaction, under these conditions, he obtained a limiting quantum yield of 1.39. The presence of oxygen should have no effect, since there are no H atoms with which it could react.

The effect of hydrogen sweeping (hydrogen concentration about 780 μmoles/l) on the yield of peroxide disappearance is shown in Fig. 16, where the quantum yield is plotted against the peroxide concentration. Quantum yields for hydrogen-swept solutions were obtained by comparing rates (determined from slopes of concentration-irradiation time curves) with rates for air-saturated solutions (or helium-swept solutions) and assuming Lea's value for the quantum yield (ϕ = 1.4) for the latter. Hydrogen is seen to enhance the quantum yield for peroxide disappearance at peroxide concentrations below about 600 μmoles/l, the quantum yield reaches a value of 8.0 at about 20 μmoles/liter. Assuming a quantum yield of unity for reaction 3, this value corresponds to a chain length of 4. In the concentration range from 600 to 1850 μmoles/l, the added hydrogen caused a slight decrease in yield, the value at 1850 μmoles/l being 1.1. The concentration range

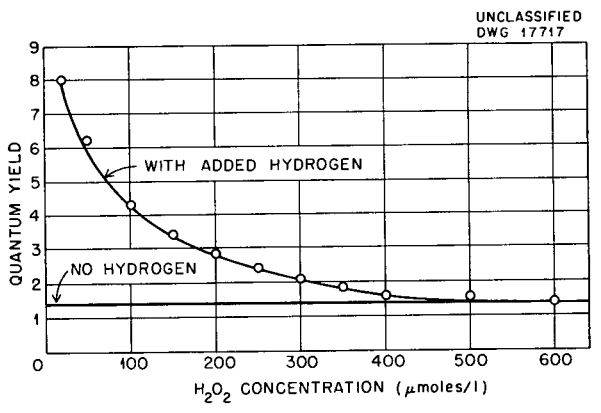

Fig. 16. Effect of Added Hydrogen on Decomposition of Hydrogen Peroxide by Ultraviolet Light.

(15) E J Hart and M S Matheson, *Trans Faraday Soc* No 12, 169 (1952)

(16) J Weiss, *Trans Faraday Soc* No 12, 161 (1952)

(17) D E Lea, *Trans Faraday Soc* **45**, 81 (1949)

will be extended, and the effect of pH will also be investigated. In solutions initially saturated with hydrogen, but with no sweeping during irradiation, the initial rate of peroxide disappearance was the same as that for hydrogen-swept solutions. However, the rate soon became less than that for hydrogen-swept solutions, and eventually the peroxide reached what appeared to be a steady-state concentration. This effect is being investigated further.

Effect of Oxygen on the Radiolysis of Hydrogen Peroxide Solutions. Some experiments were carried out to determine the effect of dissolved oxygen on the decomposition of hydrogen peroxide by gamma rays Several authors[16,17] have reported yields for gamma-ray decomposition as dependent on $[H_2O_2]^{1/2}$, and the role of oxygen was neglected in the mechanisms proposed. Previously, the author had reported the same yields for the decomposition of peroxide by gamma rays in solutions that contained 100 and 4000 μmoles/liter. Experiments by Ebert and Boag,[18] in which nitrogen was swept through solution during irradiation, support the observation that the yield is independent of peroxide concentration in this range. Some additional experiments were carried out in which helium was swept through the solution during irradiation. The results, shown in Fig 17, indicate a small variation in yield from 3.8 molecules/100 ev at a concentration of 100 μmoles/l to 5.1 molecules/100 ev at 1850 μmoles/liter. The yield is definitely not dependent on the $[H_2O_2]^{1/2}$, and the variation obtained here might indicate inefficient oxygen removal during irradiation. Curves for air-saturated and oxygen-swept solutions are also shown. The starting peroxide concentration of 415 μmoles/l was actually below the steady-state level that would obtain at an oxygen concentration corresponding to saturation at 1 atm pressure (about 1260 μmoles/l).

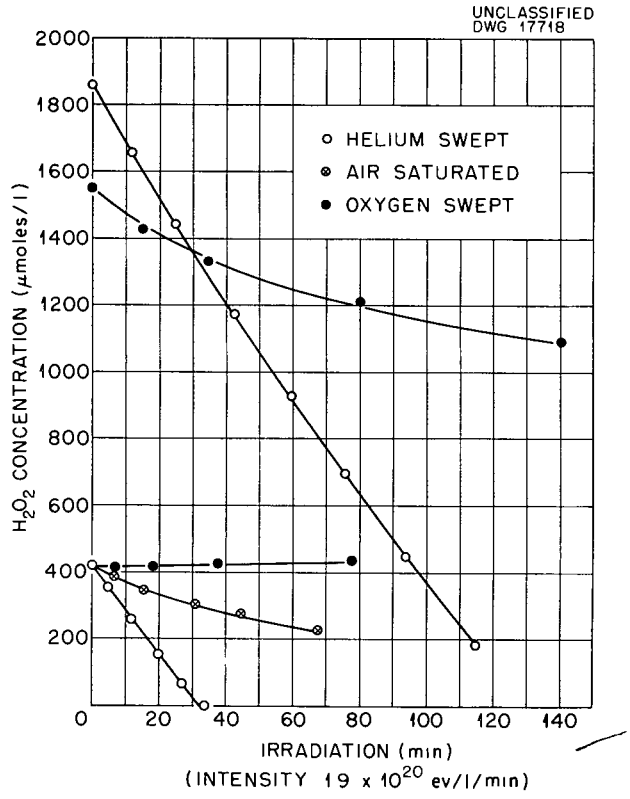

Fig. 17. Effect of Oxygen on Decomposition of Hydrogen Peroxide by Gamma Rays.

OXIDATION OF URANIUM(IV) BY GAMMA RAYS

C. Hochanadel

Additional experiments are being carried out to determine the effects of pH, concentration, and added solutes on the oxidation of uranium(IV) by gamma rays.

GAS-PHASE RADIATION STUDIES

S. C. Lind P. S. Rudolph

Studies on Alpha-Ray Deuterio-Cuprene Approximately 4 g of alpha-ray deuterio-cuprene[19] has been

(18) M Ebert and J W Boag, *Trans Faraday Soc* No 12, 189 (1952)

(19) S C Lind and P S Rudolph, *Chem Quar Prog Rep March 31, 1952*, ORNL-1285, p 70

prepared, and portions have been utilized in various ways. H. A. Levy used about 1 g for neutron-diffraction studies, and preliminary calculations indicate that no information on the structure on this polymer will be forthcoming from these studies.

W. W. Harris of the Works Laboratory at K-25 made electron-microscope photographs on a 0.1-g sample. These photographs show a spherical structure with diameters of 8,000 to 11,000 Å, which is in agreement with the work of Watson.[20] However, contrary to Watson's findings, the photographs indicate that the polymer is a solid rather than a liquid. The electron microscopy will be further exploited if deemed advisable.

Two samples (about 0.1 g each) were given to A. Zucker, of the Cyclotron group at Y-12, for use as a special target. This target was bombarded with 25-Mev nitrogen ions (N^{3+}). The radium-D (Pb^{210}) activity occluded with the polymer interfered with this work, however, the results were so satisfactory that the group will make deuterio-cuprene by the electrical-discharge method for future use.

Radon-Collecting System. A radon-collecting system to be used in gas-phase radiation studies has been designed, and the components have been fabricated. Two 100-mg $RaSO_4$ sources are being converted to $RaCl_2$ ~~that~~ will be employed as the radon source. This conversion is being done in Building 3014 and is near completion. The collecting station will be located in a special hood in a hot laboratory (room 221) of Building 4501.

In conjunction with the $RaSO_4$ conversion, three sources of radium compounds that are free of mesothorium (about 4 mc of radium) will be converted to $RaCl_2$ and put into solution. Portions of the resulting solution will be available to those workers requiring fractional millicurie sources of mesothorium-free radium.

Ion-Yield Studies. The electrical instrumentation to be used in conjunction with the gas-phase radiation studies in the presence of electric fields has been designed, and the fabrication by the Instrument Department has been completed This instrumentation will be tested in the near future

(20) J L Watson and K Kaufmann, *J Applied Phys* **17**, 996 (1946), J L Watson, *J Phys Chem* **51**, 654 (1947)

INSTRUMENTATION

NEW TYPE OF MULTICHANNEL PULSE ANALYZER

C. J. Borkowski F. Porter
J. K. East

An ideal system for determining the voltage-pulse distributions from scintillation spectrometers, proportional-counter spectrometers, or pulse-ion-chamber spectrometers would measure the amplitude of every pulse from the detector with the required precision and sort these pulses into as many channels as may be required. In almost all applications, a multichannel analyzer with 50 to 100 stable channels would be a most useful instrument. To obtain this many channels, using conventional triggers and anticoincidence circuits to define each channel edge, imposes a rather difficult problem in keeping the channel widths constant and in keeping the equipment properly calibrated, aligned, and cooled.

In the new system described here, only one trigger is used regardless of whether there are 10 or 100 channels. Variations in the trigger sensitivity with time have a negligible effect on the channel widths. The principle of

the system is as follows: A cathode-ray beam is deflected vertically across a metal grid as shown in Fig. 18. The grid has 25 blank spaces and 25 webs that are the same width as the spaces. Behind the grid is a Ag-Mg metal signal plate that is negative with respect to the grid and has a secondary emission ratio of about 4. A pulse is obtained from the signal plate each time the beam passes an opening in the grid.

To utilize the spaces, as well as the webs, as channels, it is necessary for the beam to return to the zero position. Thus, for full deflection, the beam would pass through 25 spaces on the rise of the pulse and 25 spaces on the fall, as a result, 50 pulses would be obtained from the signal plate, thus indicating that the pulse fell into the 50th channel. With this type of grid construction there are no gaps or overlapping of channels, and a maximum output signal is obtained. If the pulse fed to the deflection plates has a linear rise of 25 μsec and a linear fall of 25 μsec, the 50 pulses from the signal plate would each be separated by 1 μsecond. The dead time of the system would be 50 μseconds. Pulses from the signal plate pass to a trigger and a ring type of scaler that serves as the discriminator. The operation of the scaler-discriminator is described below. If a scaler pulse sorter with a dead time of 0.1 μsec were used,

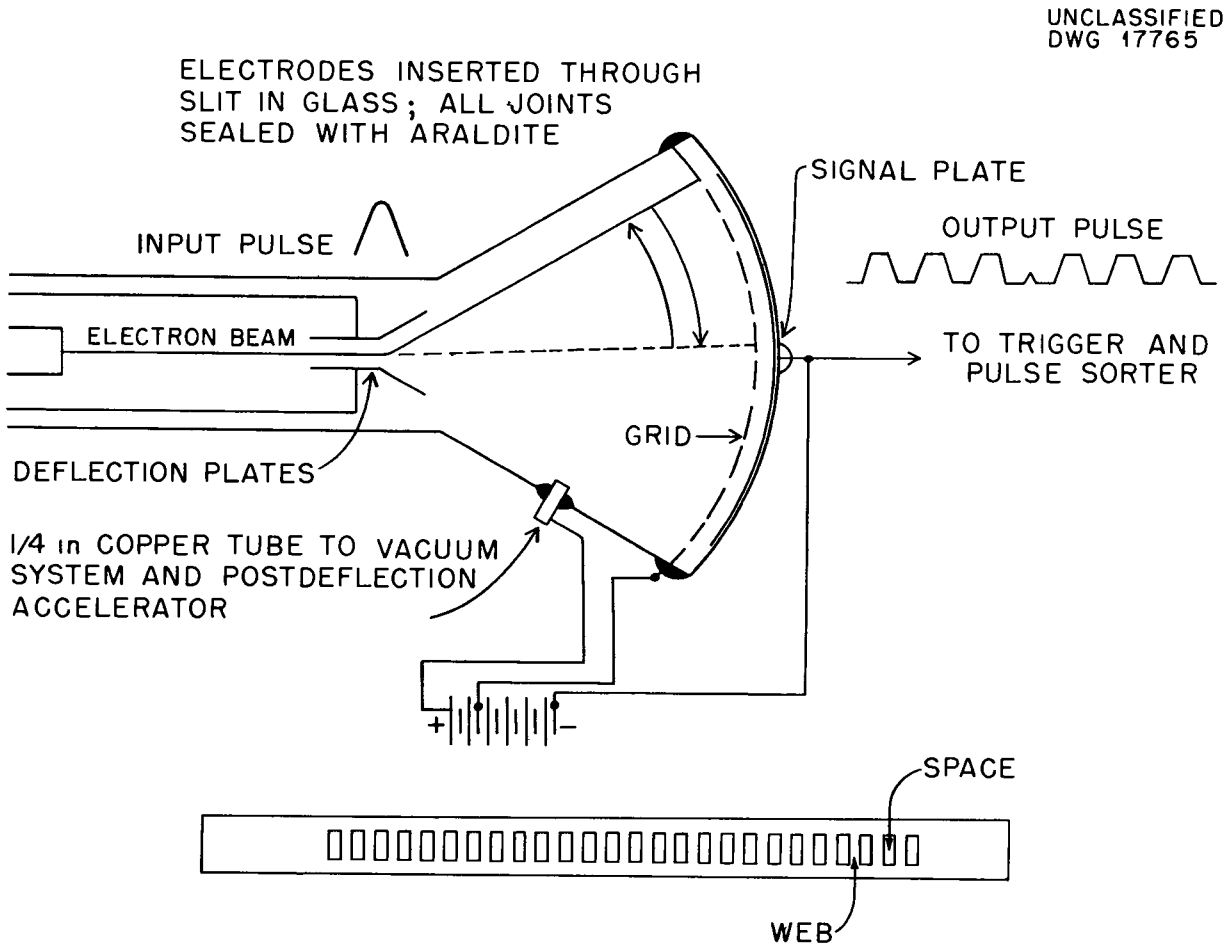

Fig. 18. Cathode-Ray Tube Multichannel Analyzer.

the over-all dead time of the 50-channel analyzer would be about 5 μseconds.

A grid and a signal plate were inserted into a 5CP1 cathode-ray tube through slots as shown in Fig. 18. The signal-plate connection was made through a small hole drilled in the center of the face of the cathode-ray tube. When the vacuum was broken, the tube was filled with argon in order to prevent the deterioration of the cathode. Connection to the vacuum-pumping system was made through a 1/4-in. copper tube that was threaded into the postaccelerator Kovar-metal connector. All joints were sealed with Araldite. Since the tube could not be outgassed by heating, it was permanently attached to a diffusion pump system, and a pressure below 10^{-5} mm was maintained. At a beam current of 1 μa, 20-mv pulses were obtained from the signal plate. The electron-beam spot size at this current was about 0.3 mm, which gave 6 spots per channel. A driver amplifier and pulse-shaping circuit designed by E. Fairstein allowed a 4-in. deflection to be used, thus giving 50 channels. Figure 18 shows a representation of the undifferentiated pulses from the signal plate as they appeared on an oscilloscope. The filament of the tube opened after about 100 hr of operation. Sufficient information was obtained on the stability of this type of tube to consider the manufacture of two such tubes by Dumont as soon as suitable grids are made.

The basic idea of measuring a beam deflection by means of a grid, as described, can be applied to the measurement of the energy of neutrons in a time-of-flight system. The synchronizing pulse from a neutron shutter, for example, would turn on the cathode-ray beam that is driven by a linear-rising triangular pulse. The pulse from the neutron detector would turn off the beam. The number of pulses obtained from the signal plate would determine the time of flight of the neutron, that is, its energy. By this method, stable time channels 0.1-μsec wide could be used.

Oscillograph Galvanometer Pulse Analyzer. The same principle of measuring a deflection voltage by means of a grid structure has been applied to a Hathaway, high-speed galvanometer (Fig. 19). The undamped natural resonant frequency of this galvanometer is 10,000 cycles per second. Electromagnetic damping of such a galvanometer is small; so viscous fluid damping is employed. Thus the galvanometer is always correctly damped, regardless of the circuit in which it is used. The damped resonant frequency is 4000 cycles per second.

The galvanometer is a bifilar type with a small mirror that normally is

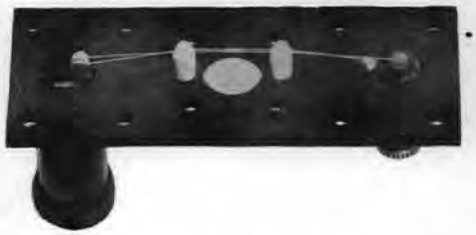

Front plate and moving element.

Fig. 19. Hathaway Oscillograph Galvanometer.

used to reflect a beam of light onto a moving chart of photosensitive paper or film in an oscillograph. In the present application, the beam of light is allowed to sweep across a grid similar to the one shown in Fig. 18 except that it was made by photographic reproduction Behind the grid is a photomultiplier. The number of light pulses obtained determines the channel into which the pulse will fall.

When the galvanometer is driven with a square pulse of 20-μsec duration, the galvanometer will rise in 30 μsec and fall in 50 μseconds. With this pulse duration, the galvanometer does not reach the peak d-c level of the square pulse, but its deflection is linearly proportional to the amplitude of the driving pulse. A pulse about 90-μsec wide is required for the galvanometer to reach full d-c amplitude. Under the fastest operating conditions, the galvanometer pulse analyzer may measure and sort the amplitude of 10,000 pulses during 1 second.

The resistance of the galvanometer is 0.7 ohm, and the deflection sensitivity is 1 mm/50 ma for a 20-cm optical-beam length. At this distance, the smallest effective spot diameter is 0.25 mm. With four spots per channel, more than satisfactory stability of operation is obtained A 20% change in trigger sensitivity produces less than a 1% change in channel width A total of fifty 1-mm channels can be obtained with a 10-deg deflection of the mirror. It is of interest to know that the saving in time amounts to only a factor of 2 when an analyzer with an infinitely short resolving time is used in place of an analyzer that has a resolving time of 100 μsec, when the integral counting rate in the main amplifier is 10,000 counts per second. Since the new system is capable of having many more channels with fewer tubes, less components, and smaller power requirements than the conventional types, a net saving in time is possible at these counting rates. At lower counting rates, the saving in time is even greater.

Since the dead time of the present galvanometer analyzer is 150 μsec, a storage system that also has this dead time can be used without the necessity of corrections for coincidence loss. The longer dead time allows other types of storage systems to be considered, for example, the single-tube thyratron rate-meter circuit that consumes a total of 1 watt of filament and plate power per storage channel and has no zero drift. Its resolving time is 80 μseconds.

An interesting application of this type of analyzer is that the average energy of a spectrum can be obtained by using two scalers. One scaler records the total number of events accumulated and the other scaler, which is connected to the photomultiplier, records the total energy in the accumulated events. Dividing one by the other gives the average energy per pulse.

Description of Circuitry. A number of analyzer systems have been constructed that use the Hathaway galvanometer as the deflection device. The system shown in Fig. 20 is the result of considerable refinement of previous systems. It is especially designed for the fast-response galvanometer Impedance-matching devices such as the cathode follower are omitted in an attempt to simplify the system diagram. Since it is desired that the analyzer operate at 100% duty cycle without distortion of the pulse amplitude spectrum, it is necessary to use direct coupling in most cases. In order that the biased diode may charge the pulse-shaping network to the peak amplitude of the applied pulse, it is necessary to lengthen the A-1 amplifier pulse by changing the delay line in the A-1 from 1.0 to 1.2 μseconds. This change is necessary because the high-frequency

response of the system is decreased by the insertion of the amplifier-gating circuit. Since the response time of the galvanometer for large pulses is approximately 50 μsec, it is necessary to lengthen the 1.2-μsec A-1 amplifier pulse. The first pulse-forming network in conjunction with the biased diode develops a pulse with a pulse rise that is the same as the A-1 pulse, and the fall is that of a parallel RC circuit with slightly less than critical inductance in series with the resistance. The pulse returns to the base line in approximately 50 μseconds. The amplitude of the pulse is that portion of the A-1 amplifier pulse that exceeds the bias level of the diode. The biased diode enables a choice to be made of the portion of the pulse spectrum to be analyzed.

Since it is desirable to control the fraction of the pulse spectrum that falls into each channel, a channel-width amplifier is used, following the first pulse-shaping network. A second pulse-shaping network, which clips off the top 20% of the pulse, is placed in the output of the channel-width amplifier. This results in an output pulse that approaches a square pulse, which gives the most rapid response for a given peak current and pulse width when applied to the galvanometer coil. The shaped pulse gives one channel deflection for 50 ma of peak current.

Because of the low galvanometer resistance (approximately 0.7 Ω) and high peak current requirements, considerable difficulty was experienced in finding an efficient system for driving the fast-response galvanometer. A push-pull audio transformer was used, although it did not furnish an efficient match and resulted in an impractical driver amplifier. Because of the good low-frequency response of the transformer, only a short-duty cycle could be used without distortion of the pulse-amplitude spectrum. To

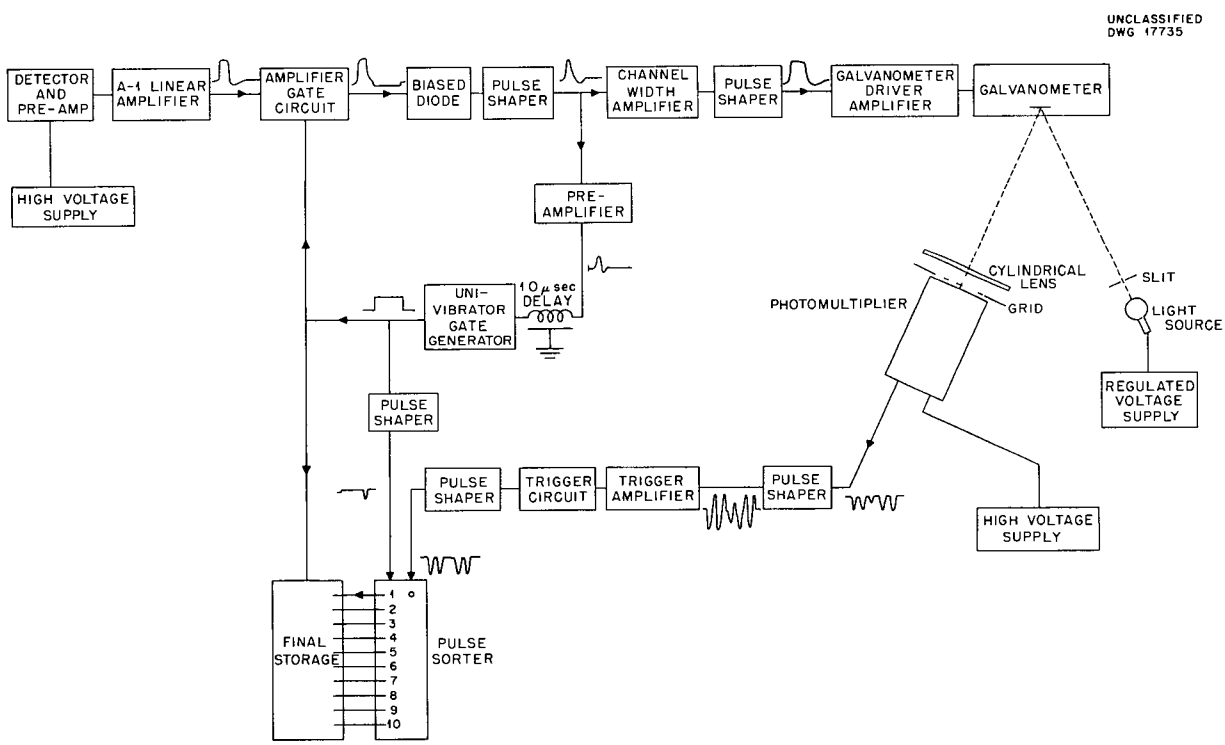

Fig. 20. Block Diagram of Galvanometer Pulse Analyzer.

achieve a high-duty cycle, a direct-coupled current amplifier with sufficient feedback to give approximately unity gain is used in the present system.

In order that the pulse spectrum may not be distorted, it is necessary that a second pulse be prevented from entering the analyzer within its recovery time, which is 150 μseconds. This is accomplished as follows Any pulse that exceeds the bias level of the diode by a few tenths of a volt is amplified by the preamplifier, delayed 1 sec to allow the A-1 amplifier pulse to reach its peak height, and then applied to the univibrator that generates a gating signal that closes the gate between the A-1 amplifier and the biased diode. This pulse is also used to turn off the final storage while the A-1 amplifier pulse amplitude is being determined. The trailing edge of the gating pulse is used to reset the pulse sorter, thus transferring information from the sorter to the final storage.

In this system where the number of pulses obtained from the photomultiplier is proportional to the pulse height being measured, it is necessary that the circuitry following the photomultiplier be capable of handling a large number of pulses spaced approximately 1 μsec apart. This spacing varies with the amplitude of the measured pulse.

Two methods were used to convert the current pulse obtained from the photomultiplier into a voltage pulse. One method was to pass the current through a resistor, a second method was to pass the current through an inductance with slightly less than critical damping. In each case, it is desired to minimize the shunt capacity in order to obtain maximum-amplitude voltage pulse. It is also desirable to present a positive pulse to the trigger circuit. Therefore a plate amplifier with a feedback gain of 4 is used to transfer the voltage pulse to the trigger circuit. The trigger circuit is a level-setting device that determines into which of two channels a pulse will fall if it is on an edge of a channel. A pulse-shaping network that is capable of driving the pulse sorter is placed in the output of the trigger circuit.

The pulse sorter used in this system is a ring scaler that is normally conducting at the zero position. When a pulse is applied to the pulse sorter, the conducting state advances one position or channel. For example, a pulse from the A-1 amplifier produces a number of pulses proportional to its amplitude, and, in turn, the sorter is advanced an equal number of channels. When the reset pulse is applied, the sorter is returned to the zero position, and a pulse is transferred from its temporary storage in the sorter to the final storage unit. Each channel of the final storage is connected to its appropriate channel in the sorter. It should be recalled that the final storage gate was opened at the instant the reset pulse was applied. At this time, the amplitude of the pulse from the A-1 amplifier has been recorded, and the system is ready to receive a second pulse. The recovery time of this system is 150 μseconds. The final storage used in this system was 10 scales of 8 with a Veeder-Root recorder.

The results of a series of measurements of the Cs^{137} gamma-ray distribution with this analyzer are shown in Table 19. Although the analyzer has not been in operation sufficiently long to obtain long-time stability data, the drift in 24 hr is a small fraction of 1% in the energy axis, and no drift was observed in the channel width.

TABLE 19. EFFECT OF GATING THE AMPLIFIER ON PERFORMANCE OF GALVANOMETER MULTICHANNEL ANALYZER WITH A 661-kev GAMMA-RAY SOURCE IN A SCINTILLATION SPECTROMETER

TYPE OF ANALYZER	CONDITION OF GATE CIRCUIT	INTEGRAL COUNTS PER SECOND	FULL-WIDTH HALF-HEIGHT (%)	PEAK-TO-VALLEY RATIO
Fast single channel	None	400	8.0 ± 0 3	42
		2500	8.0 ± 0 3	42
Galvanometer multichannel	In	400	8 0 ± 0 3	44
	In	2500	8 0 ± 0 3	44
	Out	400	9 5 ± 0 3	24
	Out	2500	12.0 ± 0.3	10

SIMPLE COUNT-RATE METER AS A STORAGE ELEMENT FOR MULTICHANNEL ANALYZERS

J. Eddlemon C. J. Borkowski

The counting-rate meter described (Fig. 21) is being considered as a possible storage element for a 50-channel galvanometer pulse analyzer. Only one tube per storage channel is used, and the total power consumption is 1 watt. The resolving time of the rate meter is 80 μseconds. The information from each storage channel will be plotted on a Brown recorder. Consideration is being given to an oscilloscope display of the 50-channel spectrum by use of a telemetering commutator that will sweep the information from the 50-channel storage.

The problem of utilizing electrical pulses to indicate counting rate resolves itself into transferring a fixed amount of energy per pulse to the indicating element. This requirement necessitates the use of pulse-shaping and pulse-limiting stages in order that a fixed charge will be transferred to the indicating circuit with each input pulse. The gas-tetrode, with associated elements, meets the requirement and obviates the necessity of special stages for pulse shaping and limiting.

A 5696 miniature gas-tetrode is used in the present circuit, this

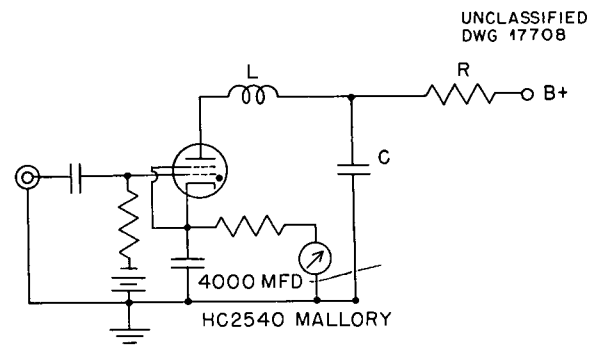

Fig. 21. Simple Count-Rate Meter.

tube was chosen because of its low filament drain (150 ma) and fast deionization time (approximately 25 μsec). Essentially, the basic circuit is a simple relaxation-oscillator type of circuit with the thyratron biased beyond cutoff, it is quite similar to the 2050 rate meter.[1]

The capacitance C in the plate circuit and the plate-supply voltage minus the tube drop determine the amount of charge to be transferred with each incoming pulse, thus the range of the count-rate meter can conveniently be changed by switching the amount of capacitance in the plate circuit. When the tube fires, the charge from plate capacitor C is

[1] C J Borkowski and C R Marsh, *"Poppy" - Pulse-Type Detector for Alphas, Betas, Gammas, and Neutrons*, CP-3316 (June 30, 1945), Sketch Q-299F

transferred to the damping capacitor, 4000 μf, in the cathode return. This charge, in turn, flows through the meter, thus giving an indication of rate. During the time of conduction, plate resistor *R* serves to isolate the circuit from the *B* supply, and after deionization, it provides a charging path for the plate capacitor

In order to use a long time constant in the meter circuit and still realize good linearity, it is desirable to use a high supply voltage. For the present, 300 volts is used in the supply. To quench the tube without using a plate resistor of prohibitive value when applying this potential, it is necessary to include a small inductor in the plate circuit, this also serves to limit peak plate current to a safe value. The value of inductance should be such that the time of one cycle at the resonant frequency of the inductor *L* and capacitor *C* is greater than the deionization time of the tube. Thus, the tube is allowed to conduct for no more than one-half cycle of the resonant frequency before the plate is driven negative. One disadvantage of this method is that the tube can conduct continuously if plate voltage is applied before grid bias is present.

The tube drop apparently varies with change in filament voltage, with a regulated plate supply of 300 volts, a 5% change in line voltage results in a 2% change in output. Operation from a regulated line precludes this source of error. Between shield grid and cathode, there exists a convection current of approximately 10 μa during the quiescent state, thereby making it desirable to tie this grid to the cathode rather than to ground or to some other bias point.

An obvious and highly important advantage of this type of circuit, when working at low counting rates, is that there is no zero drift in the output circuit. There is a small drift in plate-voltage drop during the first week of operation of a new tube, however, after this aging, the tube apparently stabilizes.

In testing for variation with different 5696's, the maximum change in output was 4% for eight tubes tried.

CIRCUIT CHANGES IN SCINTILLATION SPECTROMETER, MODEL Q-1151

E Fairstein

The scintillation spectrometers used in the Chemistry Division have the ORNL model Q-1151 amplifier-discriminator as one of the components Drifts in the discriminator that result from grid current in the 404 A tubes have proved to be a continuing source of trouble

A circuit change in the output stage of the amplifier that greatly reduces the effects of grid current is shown in Fig 22 This change is simple to make and should be incorporated in all instruments of this type presently in use

As is shown in the diagram, the pulse-height selector control circuit is transferred from the 404 A input to the input of a cathode follower The 404 A grids are then directly connected to the cathode follower output. This change does not eliminate the grid current, but it greatly reduces its effect The cathode

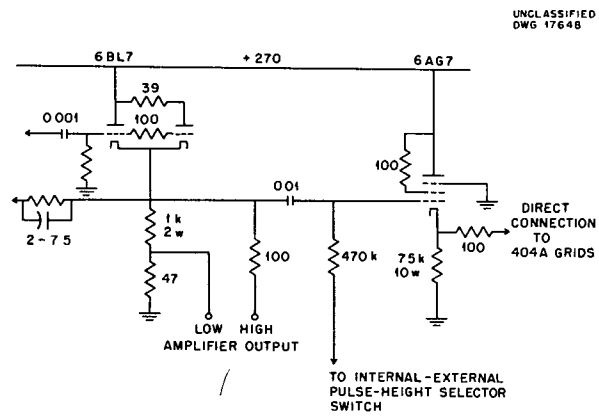

Fig 22. A1 Amplifier-Output Circuit Modifications.

follower has an impedance more than 200 times lower than that of the pulse-height selector circuit and can therefore prevent shifts in 404 A grid bias

REGULATED NEGATIVE HIGH-VOLTAGE SUPPLY

E Fairstein H J Hurst

A regulated negative high-voltage supply was designed, built, and tested The voltage range is 0 5 to 4 5 kv at a maximum load current of 3 ma Noise and ripple vary from 0 25 volt at 500-volts output to 1 5 volts at 4 5 kv The regulation is such that line-voltage changes are reduced by a factor of about 100 The drift in voltage is approximately 0 1% per 24 hours, short time drifts are about 0 5%

The circuit is shown in Fig 23 The added complexity that results from the use of a constant current tube in

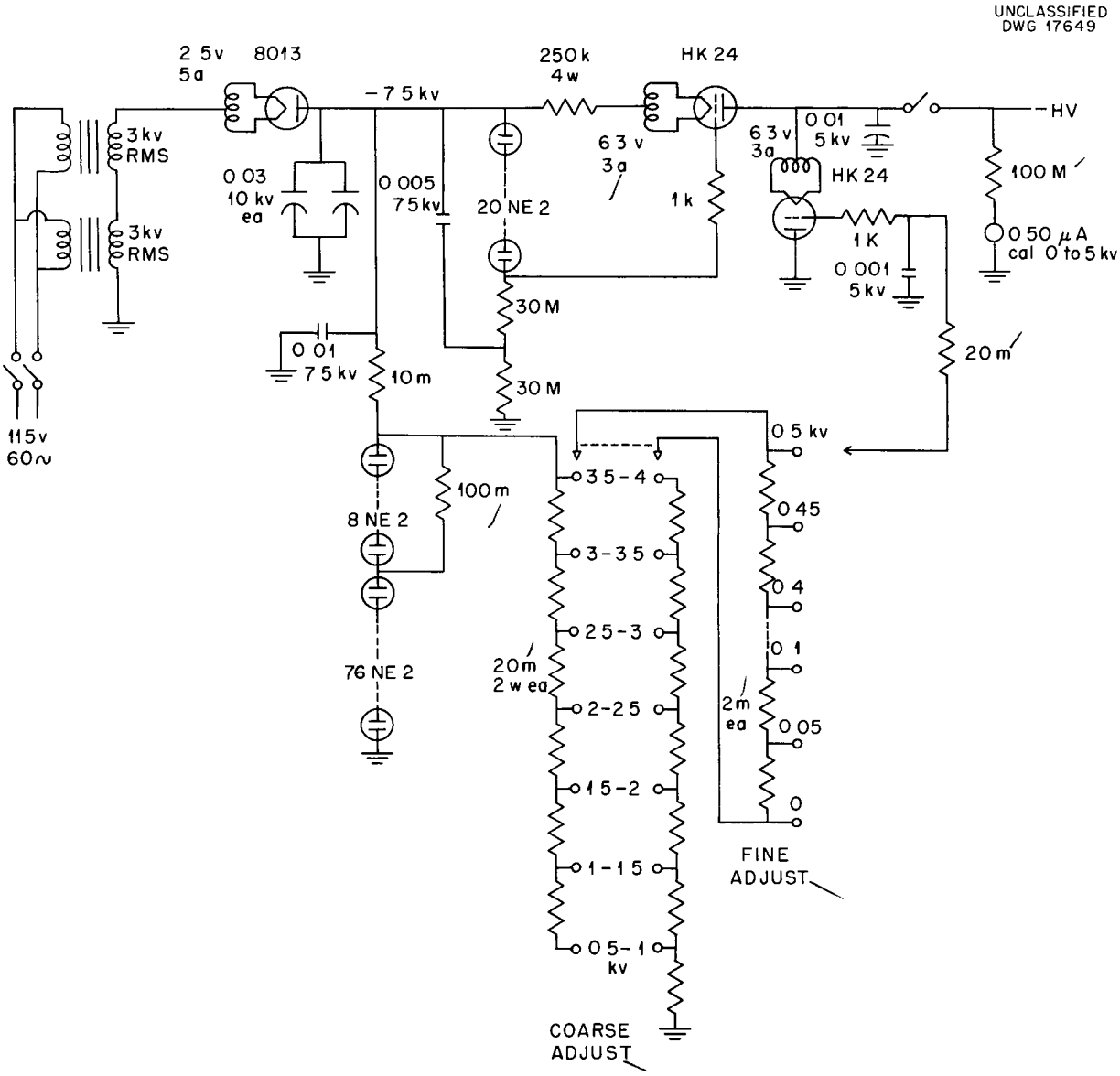

Fig. 23. Regulated Negative High-Voltage Power Supply.

place of the usual load resistor for the shunt regulator more than pays for itself in improved performance, and is an innovation that can be used to advantage in lower voltage supplies, as well

A triple-step generator was designed, built, and tested It will be used for determining the resolving time of amplifiers, discriminators, scalers, etc A block diagram appears in Fig 24

The main signal output consists of a negative going staircase wave Each of the steps has a rise of 0 04 μsec and a fall of 2000 μsec, which simulates the signals obtained from a radiation detector The leading edge of two of the steps can each be continuously delayed with respect to the first step The range is 0 to 1 msec in three decade ranges The amplitude of each of the steps is adjustable from 0 to 1 volt The output is designed to operate into a 100-ohm load

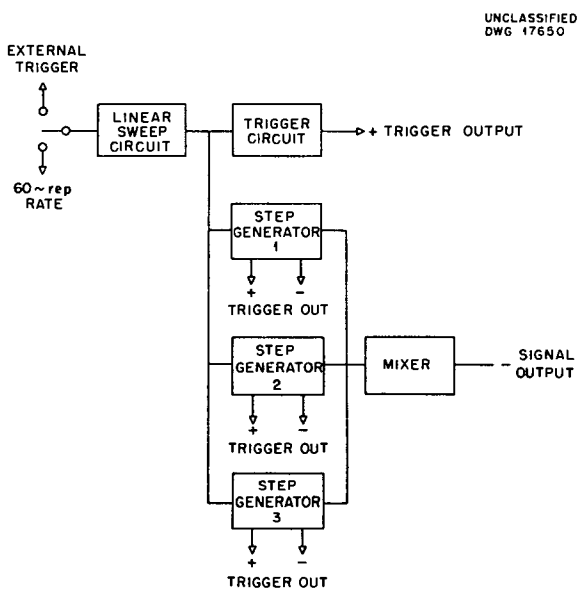

Fig. 24. Triple-Step Generator.

The auxiliary signal outputs consist of pulses One output is provided to trigger an oscilloscope sweep It can be delayed or advanced with respect to the first step of the main output The remaining outputs are from each of the three step generators and are in time coincidence with their respective steps

The operation of the instrument is as follows A linear sweep is generated from the power line or from an external triggering source The sweep voltage is applied to four Schmitt triggers that can be biased for different triggering levels. The adjustment of these bias levels is the means for determining the time separation between pulses Three of the triggers are used for generating main signal steps The individual steps are combined in a linear mixer to give the output signal The fourth trigger is used for initiating the sweep in the oscilloscope that will usually be used in association with the generator

REACTOR CHEMISTRY

MEASUREMENT OF pH AT HIGH TEMPERATURES

M. H. Lietzke

It is often desirable to know the hydrogen-ion concentration of solutions at high temperatures. For example, in the case of aqueous homogeneous reactors, the pH of the solution gives a measure of the solution stability. Failure of the solution is always accompanied by a decrease in pH. Moreover, precipitation of the uranium is forewarned by an initial slow decrease in pH before actual failure of the solution occurs. Thus it would be useful to develop an electrode that could be used to give a continuous record of the pH of the solution.

Five metal-metal oxide systems have been reported in the literature as showing satisfactory response to changes in hydrogen-ion concentration so as to be suitable for pH determinations. These metals are antimony,[1] tantalum,[2] niobium,[2] tungsten,[3] and molybdenum.[3] The antimony electrode can be used between pH 5 and 10, when air is excluded and precautions are taken to have the stable, cubic form of the oxide. Thus the antimony electrode has rather limited use. In fact, it cannot be used at all in uranyl sulfate solutions where the pH varies from about 1.5 to 3.0.

It has been claimed[2] that the potentials of the tantalum and niobium electrodes show a linear response to pH over a wide range (pH 1 to 13). Since these electrodes are easily polarized, a high-impedance device must be used in measuring the potentials. A series of measurements was performed in sulfuric acid in which the potentials of these electrodes were measured against a saturated calomel electrode as a function of pH and temperature. A vibrating-reed electrometer was used to record the potentials. Although the electrodes did show a rapid response to pH changes, the potential values drifted considerably, and thus the electrodes were unsatisfactory for giving a continuous record of the pH of a solution. The potentials drifted both at room temperature and at 90°C. This same difficulty was observed with the tungsten electrode.

Of the five electrodes mentioned above, the molybdenum electrode seemed to be the most promising. At room temperature and at 90°C, the electrode attained equilibrium very rapidly in sulfuric acid (pH 1 to 2) and in buffered solutions of higher pH. The potential values were fairly stable and did not drift more than a few millivolts over a period of several days. Although more fundamental work must be done with the molybdenum electrode, it was considered desirable to try it at 250°C in uranyl sulfate solution to determine whether it would be suitable for reactor application. It was found that in the complete absence of oxygen, molybdenum will reduce uranyl sulfate solution. However, it is possible that the molybdenum electrode may function in uranyl sulfate solution in the presence of sufficient oxygen to keep the uranium oxidized. These experiments are now in progress and will be reported later. The reference used is the silver-silver sulfate electrode.

Future work will include quantitative experiments in sulfuric acid solutions, buffered solutions of various pH values, and uranyl sulfate solutions in order to determine whether the molybdenum electrode can be used in conjunction with the silver-silver sulfate electrode to measure continuously the pH of solutions at high temperatures.

(1) E J Roberts and F Fenwick, *J Am Chem Soc* **50**, 2125 (1928)

(2) L Jeňšovský, *Collection Czechoslov Chem Communs* **16**, 127 (1951)

(3) H Brintzinger and B Rost, *Z Anal Chem* **120**, 161 (1940)

CHEMISTRY OF CORROSION

G H Cartledge

Studies on Electrode Potentials (R P Yaffe) Further work has been done in the study of the variation of electrode potentials of steel as a function of time, temperature, and previous treatment of the electrode These experiments are part of a program directed toward an understanding of the factors entering into the electrochemical behavior of complex electrode materials All measurements during the past quarter have been made with a vibrating-reed electrometer and a Brown potentiometer, with either a $Ag-Ag_2SO_4$ or a saturated calomel reference electrode To date, experiments have been conducted primarily with electrodes of type 309 or 347

stainless steel rod in an electrolyte of 0 100 *N* H_2SO_4 that was stirred vigorously with free access to air In the usual cycle, the electrolyte was slowly heated from 20 to 85°C and then slowly cooled The temperature of the electrolyte was held constant at each value at which a reading was made until the electrode reached its stable potential at that temperature The results confirm and extend those reported for the previous quarter [4]

A few generalizations may be drawn from the data thus far obtained Figure 25 illustrates some of the various types of behavior that have been observed

[4] G H Cartledge, *Chem Quar Prog Rep Sept 30, 1952*, ORNL-1432 (in press)

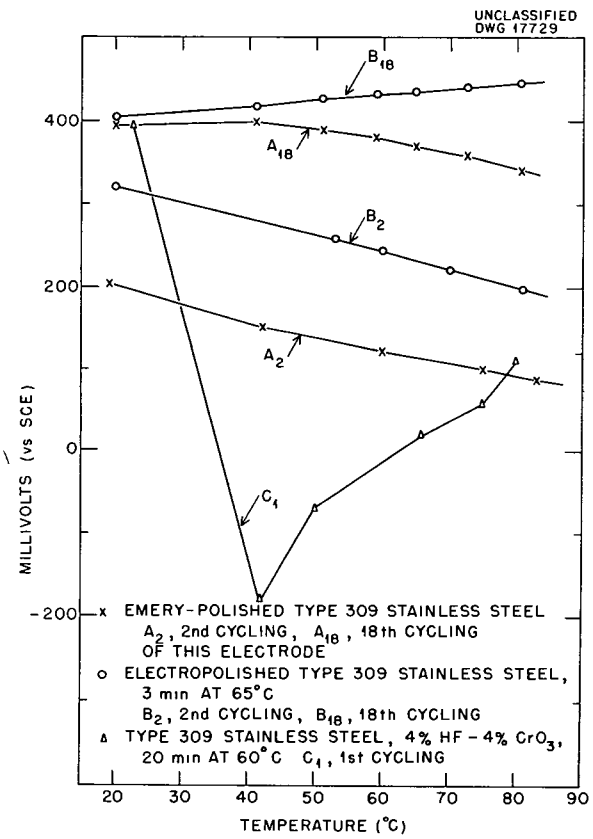

Fig. 25. Variation of Electrode Potential as a Function of Time, Temperature, and Previous Treatment.

In studies on surface treatment, it has been found, under the conditions mentioned above, that some of the conventional passivation procedures produce no measurable potential change, whereas others produce only temporary changes For example, if stainless steel electrodes are treated either with nitric acid or with 4% HF-4% CrO_3 or by flaming, using conventional passivation conditions in each case, in all three treatments, the electrodes attain a temporary nobility (as evidenced by high potentials) that is lost as soon as the temperature of the electrolyte is raised (curve C_1 in Fig 25) Only electropolishing in a phosphoric acid-sulfuric acid bath produces an electrode that remains more noble than an untreated, emery-polished electrode throughout the temperature cycle (curve B_2 vs curve A_2 in Fig 25)

With repeated cyclings, both electropolished and emery-polished electrodes become increasingly noble In these cyclings, hysteresis-type curves represent the behavior of the electrodes on successive heatings and coolings In the early cycles, the electrodes have temperature coefficients of approximately -2 mv/°C, the coefficients change gradually, eventually becoming positive at about +1 mv/°C

The ennobling that gradually results from the repeated temperature cyclings does not produce a visible film The surface condition produced, however, is very sensitive to mechanical disturbance in that light rubbing of the electrode instantaneously causes a considerable decrease in potential Recovery of nobility after the disturbance proceeds rapidly at the higher temperatures used in these experiments

Inhibition of Corrosion by Technetium Compounds (G H Cartledge). Consideration of a possible theory of the action of certain types of corrosion inhibitors led to the expectation that

the pertechnetate ion, TcO_4^-, might have inhibitory properties similar to those of the chromate ion, CrO_4^{--} Exploratory experiments have shown that this is indeed the case and that under certain conditions, at least, effective inhibition is obtained at considerably lower concentrations than are required for protection by chromates.

The experiments have been conducted with electrolytic iron, carbon steel and type 347 stainless steel Carbon steel disks were digested at 100°C in water containing 10 ppm of chloride ion as potassium chloride There was no rust formed in a 2×10^{-3} *f* pertechnetate solution and no weight change, whereas a control sample in chloride solution alone formed much rust and lost 0 9 mg in weight When similar disks were heated for 1 hour at 250°C in water containing 10 ppm of chloride ion, a control specimen lost 0 8 mg, whereas in the same solution containing also 2×10^{-3} *f* potassium pertechnetate, the specimen suffered no weight change (±0 1 mg) The control gave much red brown corrosion product, but the technetium solution remained water white A blue-bronze color appeared on the test piece

Type 347 stainless steel test pieces were heated for 234 hr at 250°C in water containing 2 ppm of chloride ion The specimens were stuck by one corner into a teflon block contained in a platinum-lined bomb The control showed a red-brown rust stain, but the specimen from the technetium solution was only bronze and blue

In uranyl sulfate solution containing 300 g of uranium per liter, one test was made at 235 to 250°C with pins of type 347 stainless steel rotated in fused silica tubes for 46 hours The solutions were largely deaerated and sealed under vacuum. The control pin quickly corroded and lost 1 0 mg (after descaling by rubbing on a paper towel), whereas the pin in technetium showed no change in weight A similar test was run for 96 hr at 176 to 250°C After 74 hr, the technetium tube showed very little corrosion product, in contrast to the heavy red-brown sediment in the control After about 50 hr, however, a flocculent silica precipitate appeared and sometime after 74 hr caused the technetium test to fail The red-brown sediment was found to contain uranium and silica, but only traces of iron The chemical action of silica under these conditions becomes an important factor

Under very actively corroding conditions, such as with carbon steel in a sulfuric acid solution of pH 0 9 and containing 10 ppm of chloride ion, the pertechnetate ion is rapidly reduced to a deposit that hastens solution of the metal With stainless steel under similar conditions, a mat gray surface results and the amount of technetium taken up, as measured by beta activity, correlates qualitatively, at least, with the corrosion rate and electrode potential, as these are determined by the previous history of the metal surface Thus, an electropolished specimen took up only a thousandth as much technetium as a hand-polished specimen given similar digestion at 100°C Autoradiograms showed that the technetium deposited under corrosive conditions seeks the areas known to be most active chemically, for example, scratches

Preliminary results of pile-irradiation studies indicate that, within probable experimental error, potassium pertechnetate is not reduced either in simple aqueous solution or when dissolved with 93%-enriched uranyl sulfate The salts appear to give no precipitate, in the concentration range used, when heated in silica capillary tubes The temperature for the separation of two-liquid phases is considerably raised by the presence of the potassium pertechnetate

A few experiments with potassium perrhenate, $KReO_4$, showed that this compound at 3×10^{-3} *f* does not inhibit corrosion either in evaporation tests or in digestion of carbon steel in water at 100°C

Further work is being directed toward a more thorough evaluation of technetium inhibition under reactor conditions and also to a fundamental study of the detailed action of the material in corrosion [5]

RADIATION OF UO_2F_2 AND UO_2SO_4 SOLUTIONS

F. H. Sweeton W. C. Yee

Experiment H5, which has now been completed, differed from the previously reported experiment H2 primarily in that UO_2F_2 was substituted for UO_2SO_4. In addition, the later test contained 0.03 *M* CuF_2 instead of 0.01 *M* $CuSO_4$. In both cases, 2.5 ml of solution (room temperature) was added to 5.0-cm^3 bombs constructed of type 347 stainless steel. Sufficient O_2 in the form of H_2O_2 was added to give a partial pressure of about 900 psi at 250°C. In the fluoride test, the bomb was etched with HF solution before the test but was not pretreated with chromic acid, as was the sulfate bomb. Both solutions contained 40 g of uranium (93% enriched) per liter. The tests were made in a flux of approximately 3.5×10^{12} neutrons/cm^2·sec, which gave a power density of 6 kw/liter. Both irradiations were carried out at 250°C, however, during the fourth and fifth weeks of the fluoride test, the temperature was raised to 260°C in order to control the total pressure. The fluoride test was run for nine weeks, and the total uranium burnup was calculated to be about 1.0%. The oxygen partial pressure during the fluoride irradiation was about 1100 psi at the start and 500 psi at the end. The oxygen partial pressure at the end of the test was produced by the remaining excess oxygen plus the oxygen produced by the decomposition of the water.

The amount of excess oxygen remaining each week was determined in the same manner as described in the previous report. The quantity remaining has been converted to average corrosion over the surface of the bomb wetted by the solution. The results of both the fluoride and sulfate tests are shown in Fig. 26. The sulfate solution data are those given in the previous report except for a correction for an error in calculation that amounts to about 20% for each of the points. The average corrosion rate over the nine-week period is 3.5 mpy. An out-of-reactor control test indicated a corrosion rate of approximately 0.9 mpy over a six-day period. Thus neutron irradiation appears to make UO_2F_2 solutions, as well as UO_2SO_4 solutions, more corrosive to type 347 stainless steel. The fluoride solution appears to have essentially the same initial rate of corrosion as the sulfate solution, but a more increased rate later.

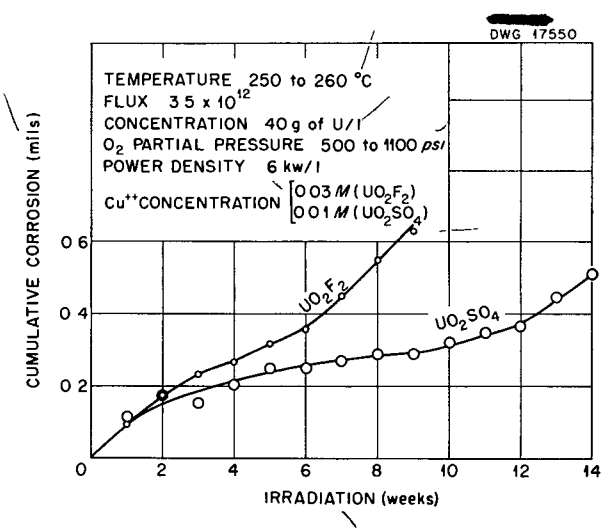

Fig. 26. Corrosion of Type 347 Stainless Steel by UO_2SO_4 Under Neutron Irradiation. Experiments H2 and H5.

[5] The assistance of J W Boyle, A R Brosi, G D Gibson, J S Gill, E K Hennessee, W L Marshall, H W Wright, and R P Yaffe in connection with certain phases of the experiments is gratefully acknowledged

The UO_2F_2 solution, like the UO_2SO_4 solution, appeared to gradually lose uranium as a precipitate. Pressure data recorded immediately after a periodical lowering of the temperature to 210°C were analyzed and used to calculate the uranium in solution by making use of the known *G* value. The results are shown in Fig. 27, where the calculated fraction of uranium still in solution is plotted against the loss in partial pressure of excess oxygen. Since the data appear to fall on a straight line, there is indication that the loss of uranium is directly related to the corrosion process. The slope of the line drawn through these points corresponds to the precipitation of 1 mole of uranium for each mole of nickel oxidized and gives circumstantial support to the belief that the oxidized nickel converts an equivalent amount of UO_2F_2 to UO_3, which precipitates.

The analysis of the solution after the irradiation showed that about 20% of the uranium was still in solution, which is a reasonable check with that indicated by Fig. 27. Only about 30% of the copper originally added was found in solution after completion of the irradiation. The oxygen-absorption data indicated that 23 mg of nickel should have been oxidized, but only about 15% of this was found in the solution.

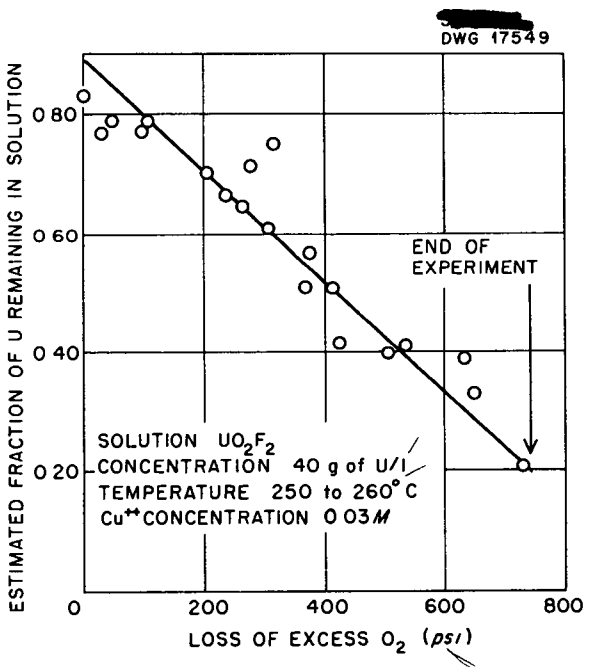

Fig. 27. Uranium Precipitation as Calculated from Apparent *G* Value. Experiment H5.

Effect of Low Oxygen Pressure on Corrosion of Type 347 Stainless Steel in Radiation. In a recent experiment (H7), a uranium sulfate solution containing 40 g of uranium per liter and 0.01 *M* $CuSO_4$ was irradiated in a stainless steel bomb at 250°C. The excess oxygen present in the bomb was much less than that in experiment H2, consequently, the oxygen partial pressure during irradiation was only about one-third of that in the earlier experiment. The resulting corrosion was significantly less during the first week but then increased to significantly more for the remaining week and a half of the test. This experiment will be reported in detail after the solution has been analyzed.

RADIATION CHEMISTRY OF AQUEOUS REACTOR SOLUTIONS

J. W. Boyle

Effect of pH on Gas Production It has been shown[6] that acidity has an effect on G_{H_2} for a uranyl sulfate solution containing 105 g of uranium per liter and for a uranyl fluoride solution containing 377 g of uranium per liter. The amount of gas produced per unit energy input was decreased by an increase in acidity.

In the work reported here, the acidity has been varied from pH 0.60 to 3.48 by adding either H_2SO_4 or NaOH to a UO_2SO_4 solution containing approximately 40 g of 93.2%-enriched uranium per liter. Eight ampoules

[6] J. W. Boyle, W. F. Kieffer, C. J. Hochanadel, T. J. Sworski, and J. A. Ghormley, *Radiation Chemistry of Aqueous Reactor Solutions*, ORNL CF-52-8-103

were irradiated at 120°C for 3 min each at a power density of about 1 kw/liter. All the gas produced (99.7% or better) was identified as hydrogen, oxygen, and condensable gas (CO_2). The G_{H_2} value for the unaltered (pH) UO_2SO_4 solution agreed exactly with previously found values.[6] The results are presented in Fig. 28.

No acid effect was found in the pH range of 1.4 to 3.5, but a lowering in the G_{H_2} value of about 3% was observed in going from pH 1.41 to 0.60. The studies of the effect of pH will be extended to solutions of greater uranium concentrations in which acidity appears to have a more pronounced effect.

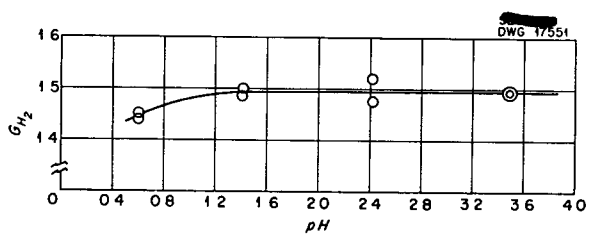

Fig. 28. Effect of pH on G_{H_2} for UO_2SO_4 Solution. 40 g of U/l, 93.2% U^{235}.

MECHANISM OF THE HYDROGEN-OXYGEN RECOMBINATION REACTION IN SOLUTIONS

H. F. McDuffie L. F. Woo

During the past quarter, attention has been focused upon the mechanism of the homogeneous recombination reaction catalyzed by dissolved copper salts. Previous work[7] with copper sulfate dissolved in uranyl sulfate solutions has indicated that the reaction

1. is first order in dissolved copper from 0.005 *M* to at least 0.05 *M*,
2. is first order in hydrogen and independent of oxygen pressure, at least from a 2 1 to a 1 1 ratio of hydrogen to oxygen,
3. is effective in recombining hydrogen and oxygen formed *in situ* from fissioning solutions,
4. is responsive to geometry and diffusion in a way that permits inference of the rate of the reaction in the solution phase from the measurement of the pressure changes in the associated gas phase,
5. presumably involves a slow rate-controlling reaction of dissolved hydrogen with cupric copper (in a 1 1 ratio), followed by a very rapid oxidative regeneration of the cupric copper with the simultaneous formation of water.
6. has a rate constant that can be expressed as $k_{Cu} = [Cu]^1 \times 5.9 \times 10^{13}$ $exp\ (-24{,}000/RT)\ hr^{-1}$.

The particular items concerning the mechanism of the reaction to be discussed in this report include the significance of the frequency factor and the effects of added sulfate-containing solutes.

Frequency Factor. For bimolecular reactions between neutral molecules (or presumably between a neutral molecule and an ion if there are no substantial changes in hydration), there are two values that may be considered normal for the frequency factor 10^{11} and 10^7. The first value corresponds to a reaction every time the molecules come within a distance of the order of a molecular diameter of each other, the second value requires that in the activated complex the two molecules are essentially bonded to each other.[8] When the frequency factor in the expression for the rate constant for copper (presented above) is divided by 60 to express the constant in appropriate units (min^{-1} instead of hr^{-1}), it becomes approximately 10×10^{11}. This is considered very good agreement for the case in which there is a reaction every time the copper ion and hydrogen

(7) H. F. McDuffie *et al.*, *HRP Quar. Prog. Rep. March 15, 1952*, ORNL-1280, p. 161-172.

(8) G. K. Rollefson, *J. Phys. Chem.* **56**, 976 (1952).

molecule approach each other in the solution (if they have the required energy), that is, there is no evidence here that a highly specific orientation of the reacting species is necessary.

Effect of Added Solutes By using the technique for determining k_{Cu} described earlier,[7] values have been determined at 250°C for solutions 0.00080 *M* in $CuSO_4$ and containing various amounts of added sodium sulfate, sulfuric acid, sodium bisulfate, and potassium sulfate. These values are presented in Table 20 and are also shown in Fig. 29.

It seems probable that both sulfate ions and hydrogen ions may be involved in the reaction, possibly in opposite ways. It is planned to attempt to separate and elucidate these effects by using the perchloric acid-lithium perchlorate system, if this system is stable under the experimental conditions. The competitive effects of copper vs. stronger sulfate complexing agents, for example, zirconium, will be considered as a possible indication of the relative complexing power of various cations at high temperatures. The effect of changes in the total ionic strength will be determined to gain information as to the charge type of the reaction. Since one of the reactants (hydrogen) is neutral, it is expected that changes in ionic strength will not materially affect the recombination rate constants.

TABLE 20. EFFECT OF ADDED SOLUTES ON HYDROGEN-OXYGEN RECOMBINATION RATE OVER 0 00080 *M* $CuSO_4$* AT 250°C

EXPERIMENT NUMBER	SOLUTE ADDED	MOLARITY AT ROOM TEMPERATURE	pH AT ROOM TEMPERATURE	$k_{250°C} \times 10^{-2}$
B-18	None		5 13	67
B-24	Na_2SO_4	0 00050	5 38	36
B-25	Na_2SO_4	0 00100	5 42	16
B-26	Na_2SO_4	0 00150	5 38	8
B-23	Na_2SO_4	0 00200	5 44	7 6
B-22	Na_2SO_4	0 0040	5 45	6 4
B-21	Na_2SO_4	0 0060	5 44	6 2
B-19	Na_2SO_4	0 0100	5 44	5 2
B-20	Na_2SO_4	0 100	5 68	4 0
B-47	H_2SO_4	0 00040	3 1	110
B-33	H_2SO_4	0 0010	2 7	210
B-34	H_2SO_4	0 0020	2 43	200
B-35	H_2SO_4	0 0030	2 25	190
B-40	$NaHSO_4$	0 0010		125
B-41	$NaHSO_4$	0 0020		140
B-36	K_2SO_4	0 0010		25
B-37	K_2SO_4	0 0020		17
B-38	K_2SO_4	0 0030		14

*0 0010 *M* at room temperature

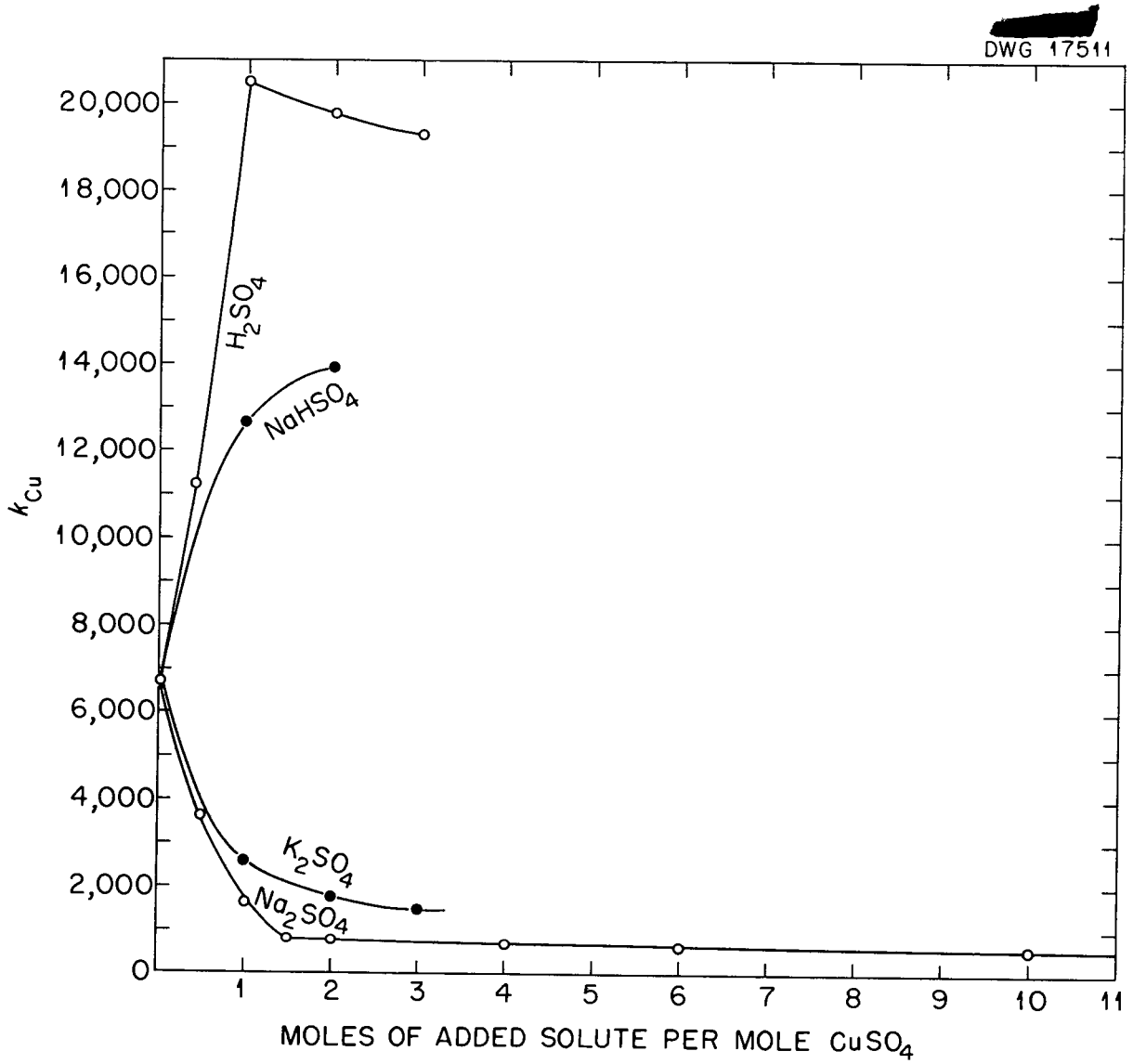

Fig. 29. Effect of Added Solutes on Rate of H_2-O_2 Recombination at 250°C Over 0.00080 *M* $CuSO_4$ (0.0010 *M* at 25°C).

CATALYTIC DECOMPOSITION OF HYDROGEN PEROXIDE IN URANYL SULFATE SOLUTIONS

M. D. Silverman

Several series of experiments have been conducted in the study of the catalytic decomposition of hydrogen peroxide in uranyl sulfate solutions since the last report. More detailed studies of the decomposition of hydrogen peroxide at 100°C in uranyl sulfate solutions have revealed that iron added as iron(III) is a better catalyst than iron(II), by a factor of approximately 1.5. However, promoter action by cupric ion is slightly more effective with iron(II) than with iron(III). Furthermore, it has been found that copper(II), in a concentration of 6 to 10 ppm, is sufficient for promoter action. In all previous

work, a copper concentration of 793 ppm had been used.

Another potential corrosion catalyst, manganese(II), was investigated, and its catalytic properties were found to be negligible in these systems.

A safe power level for operation of the HRE at 100°C, indicated as approximately 400 kw in a previous HRP quarterly report, is based on a steady-state concentration in the reactor of 15 ppm of both iron and ruthenium. It is doubtful whether the ruthenium will ever reach such a concentration in solution because hydrolysis is extremely rapid at this temperature and at the pH of the reactor solution. However, it is probable that the iron concentration will exceed 15 ppm. Promoter action by added copper(II) would increase the permissible power level to approximately 600 kw.

SOLUBILITY OF UO_3 IN AQUEOUS UO_2SO_4 AND UO_2F_2

E. V. Jones W. L. Marshall
J. S. Gill

In previous reports on the solubility of UO_3 in aqueous UO_2SO_4 and UO_2F_2 at 175°C[9] and at 250°C,[9,10] it was pointed out that the behavior of the sulfate system in the low-concentration region was uncertain.[9] The question as to whether the equilibrium ratio, U to SO_4, drops below 1.00 in this region is still unanswered, partly because of analytical difficulties for very low concentrations of sulfate. Efforts are being made to resolve these difficulties.

In the previous reports it was stated that, "In most of the experiments on the fluoride system at 250°C, corrosion of the titanium filter bombs and some reduction of uranium was noted, but this attack was not evident at 175°C."[9] This statement must now be revised as follows The corrosion of the titanium filter bombs and some reduction of uranium have been found in the sulfate system also and in the fluoride system at 175°C, as well as at 250°C. However, at 175°C this reduction of uranium, which occurred in two or three days in the filter bombs with titanium-plated iron stirrers operated by solenoid, had not occurred even in ten or twelve days in titanium filter bombs that were "rocked" in heated aluminum cylinders without stirrers. A black deposit on one side of a stirrer from a filter bomb that had been placed in a slightly inclined position suggested that the corrosion and reduction of uranium might be due to the rubbing of the stirrer against the side of the bomb. Snugly fitted teflon caps were put over the ends of the stirrers, and eleven runs at 250°C and three at 175°C in UO_2SO_4 solutions have shown no reduction of uranium.

Studies are being made of the solubilities of UO_3 in aqueous UO_2F_2 at 25 and 100°C, but the data will be presented in a later report.

Studies are also being made on the equilibration time for UO_3 in 1.25 *M* UO_2SO_4 and in 1.25 *M* UO_2F_2 at 25°C. Preparations are being made for similar studies at 100°C.

OXIDATION STATES OF FISSION PRODUCTS IN REACTORS

D. W. Sherwood

A study of the chemical states of iodine in environments related to those likely to prevail in homogeneous reactors has been started. Apparatus has been built, and a search of the applicable literature is being made. The immediate objective is the determination of the rates of oxidation and reduction of the several oxidation states of iodine.

(9) E V Jones, J S Gill, W L Marshall, and C H Secoy, *HRP Quar Prog Rep Oct 1, 1952*, ORNL-1424, p 105-108

(10) J S Gill, E V Jones, and W L Marshall, *HRP Quar Prog Rep July 1, 1952*, ORNL-1318, p 144